Spaceborne radar and lidar at ECMWF

EUMETSAT/ECMWF NWP-SAF Satellite Data Assimilation training course
March 2026

Mark Fielding (mark.fielding@ecmwf.int)

Thanks to colleagues from:
ECMWF, ESA and
EarthCARE DISC

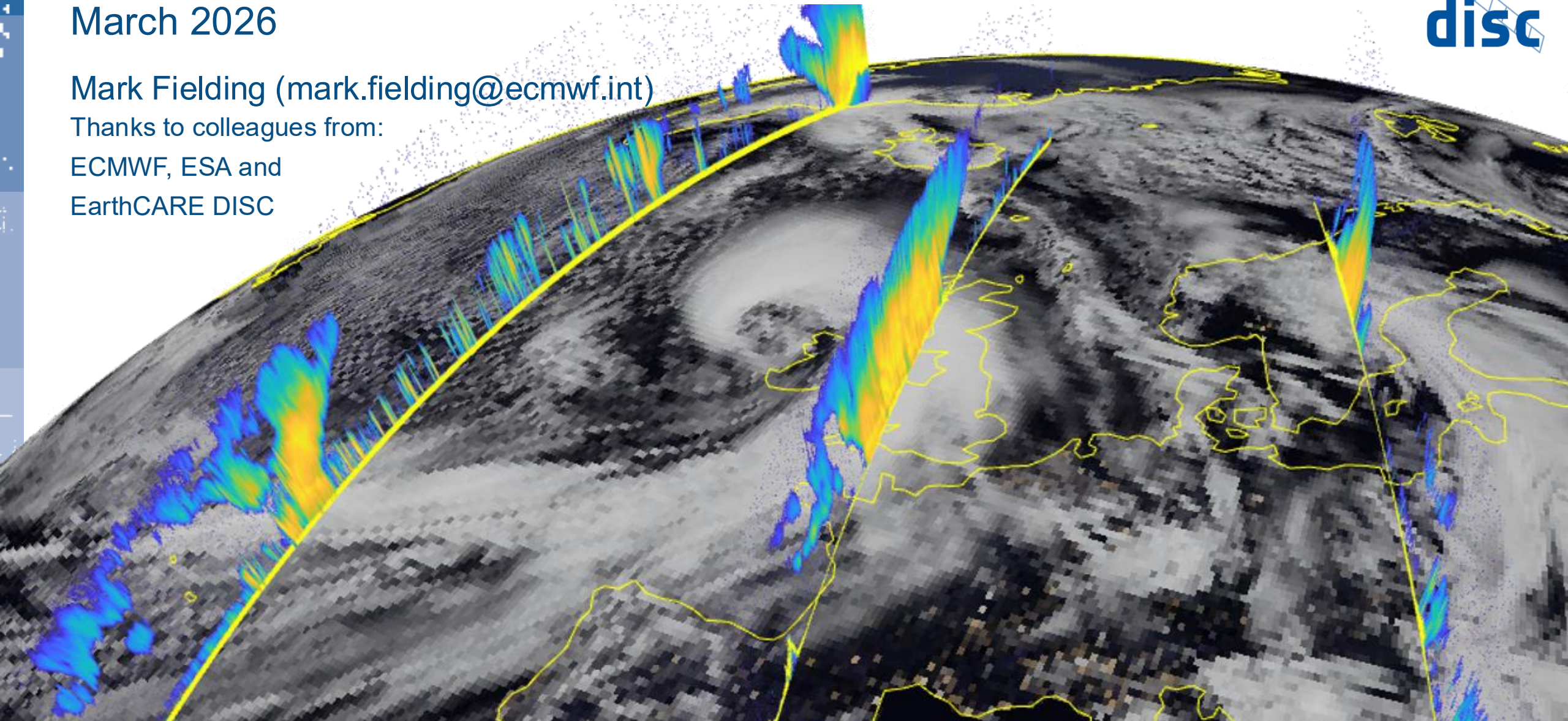

Active sensors provide vertically-resolved measurements of cloud and precipitation

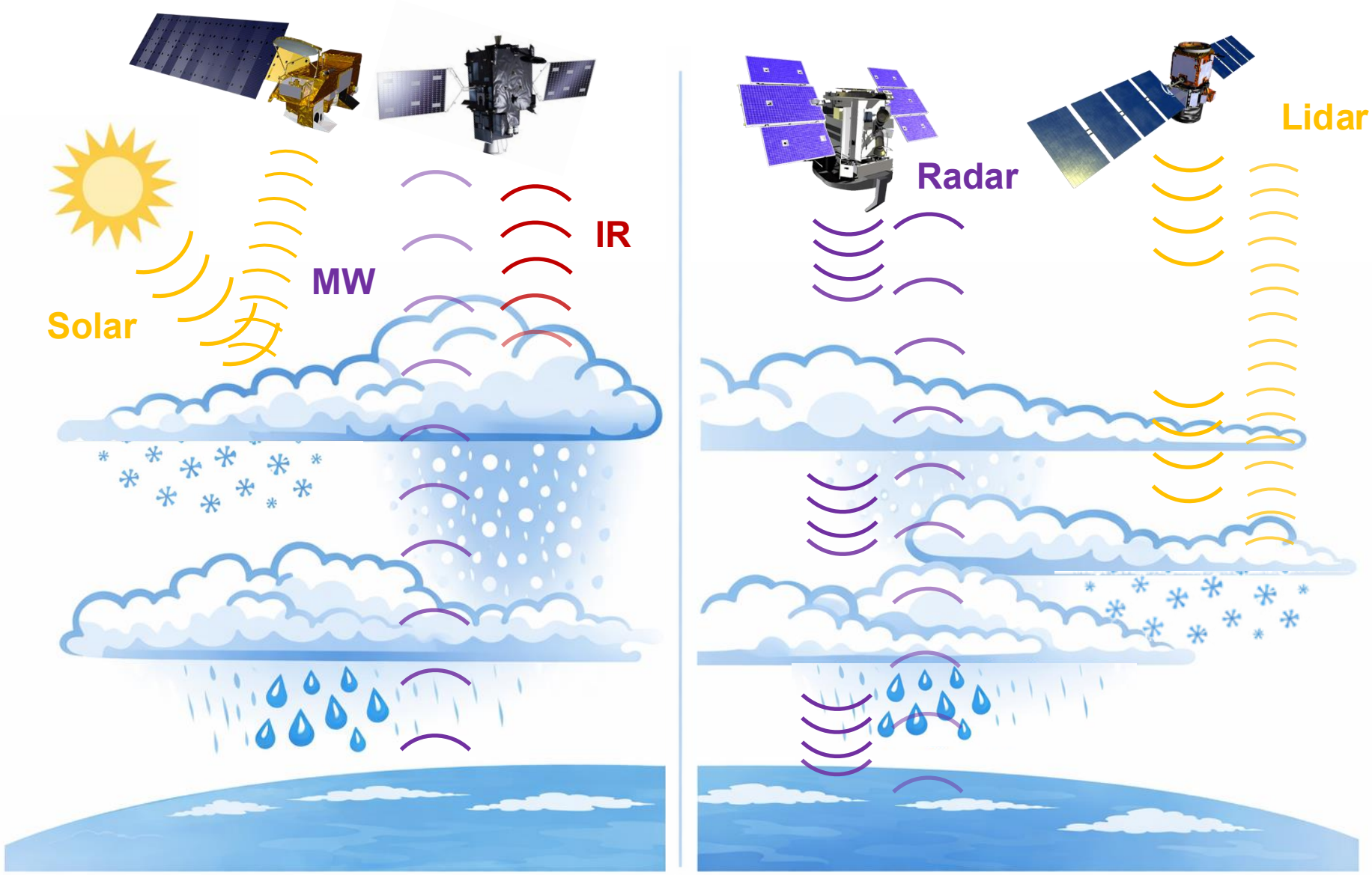

Brief history of spaceborne radar and lidar

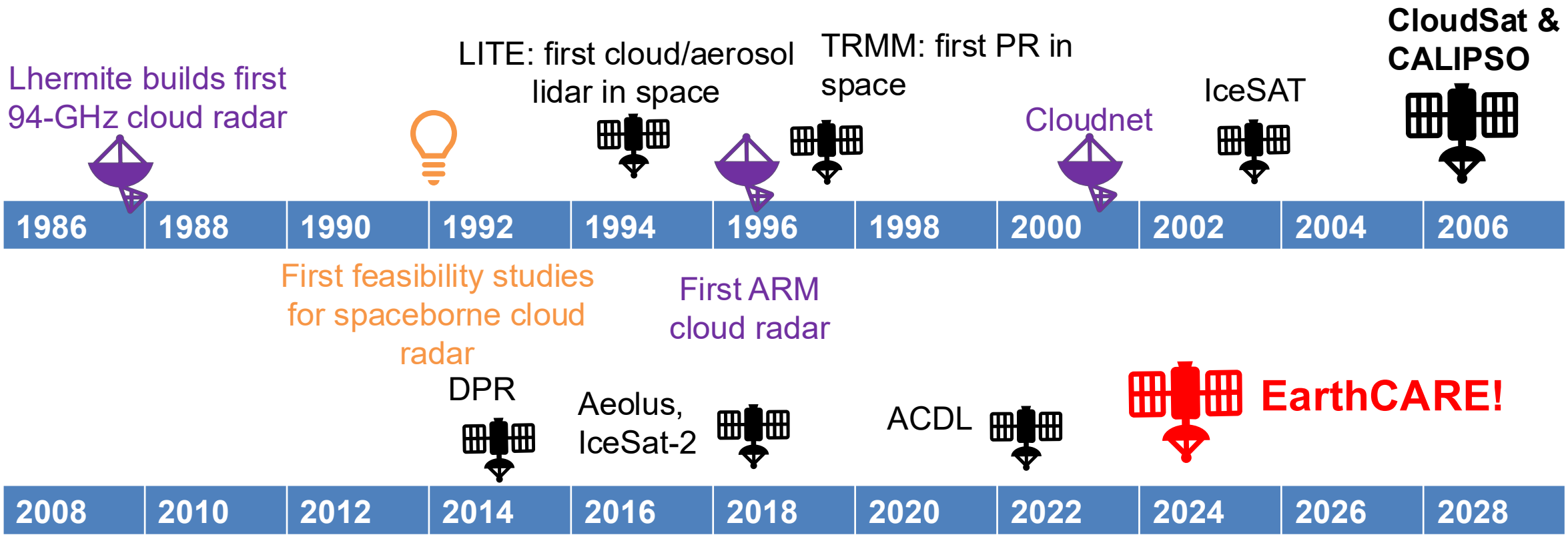

“Lidar curtain” of space-borne lidar (CALIOP on CALIPSO (532 nm)), attenuated backscatter: βT^2

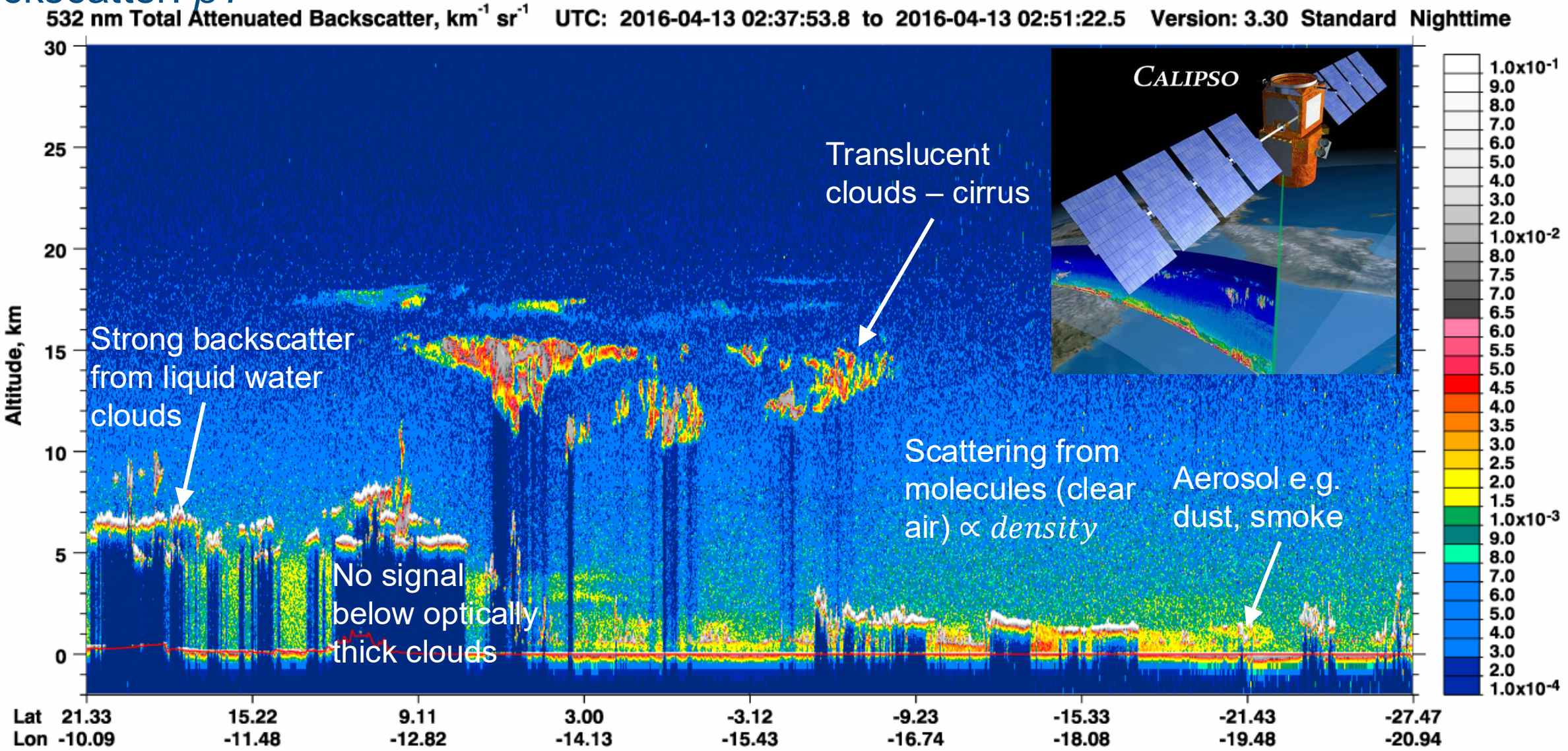

A very successful NASA mission lasting from 2006 to 2023!

Radar reflectivity from CloudSAT (W-band radar)

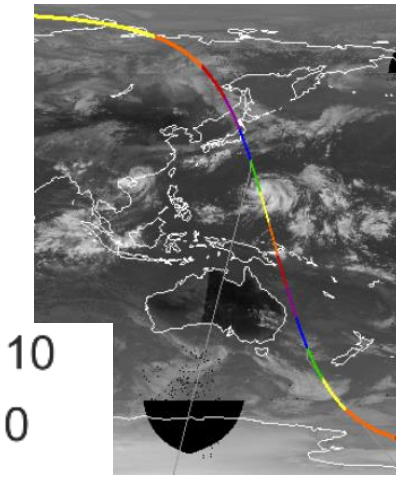

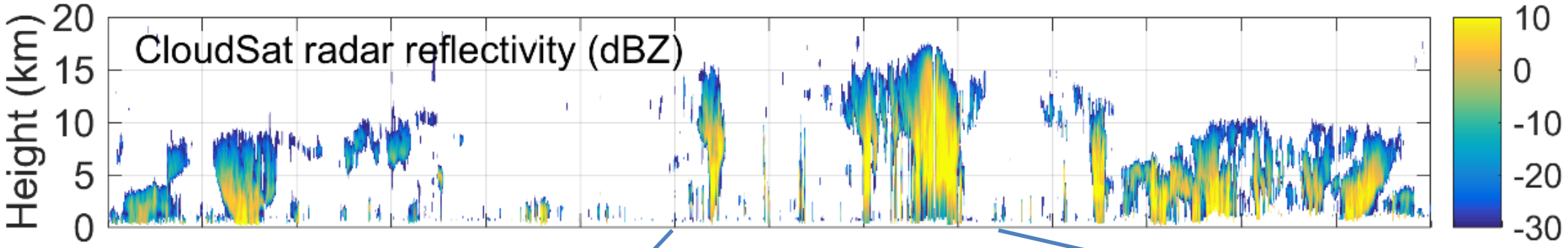

Typhoon Choi-wan
(Sept. 15th 2009)

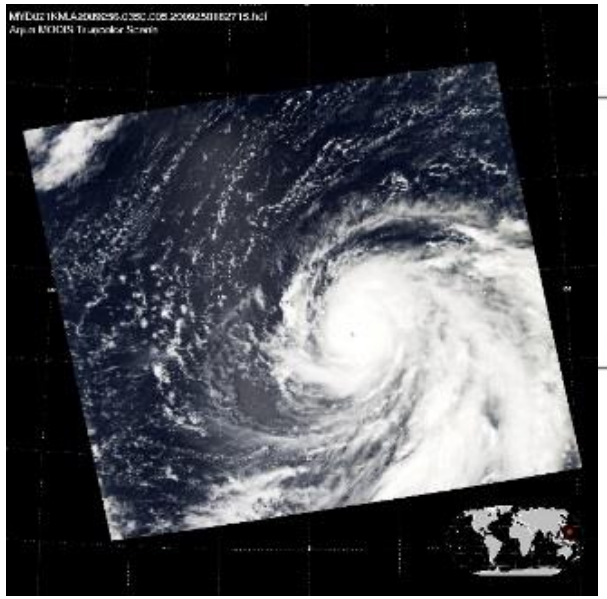

Larger ice particles

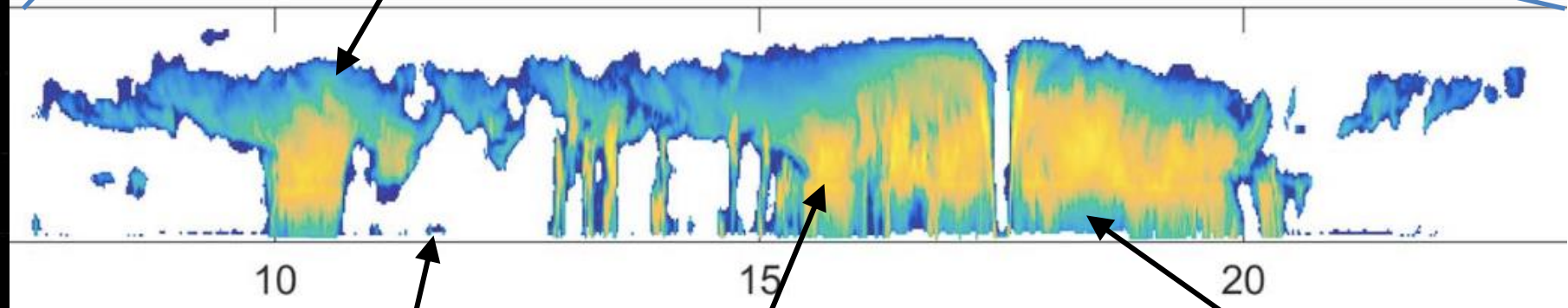

Drizzling boundary-layer cloud

Melting layer

Attenuation in strong precipitation

Radar-lidar synergy leaves clouds ‘no-where to hide’

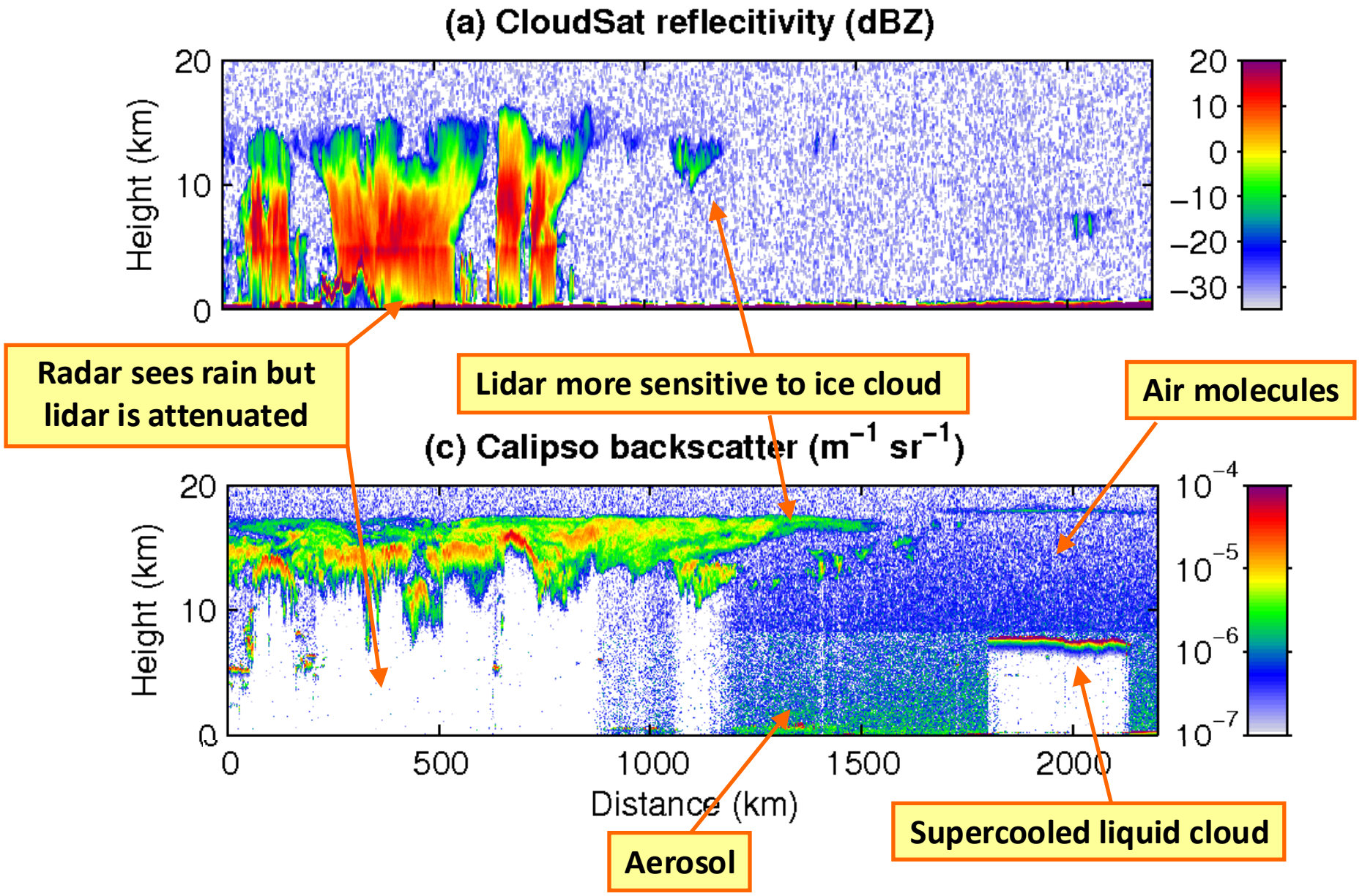

Aeolus satellite mission

- **E**uropean **S**pace **A**gency "*Earth Explorer*" mission to measure wind profiles globally
  - Greek mythology: "Keeper of the Winds"

- Payload: **D**oppler **W**ind **L**idar, ALADIN: **A**tmospheric **LA**ser **D**oppler **IN**strument
- **Technology demonstration mission**; 3-years
- Status of mission:
  - Launched on **22 August 2018**
  - **First wind lidar in space** and first European lidar in space
  - Measured winds from **3 September 2018 until 5 July 2023**. Exceeded nominal mission lifetime; deorbited on 28 July 2023 (lack of fuel!)

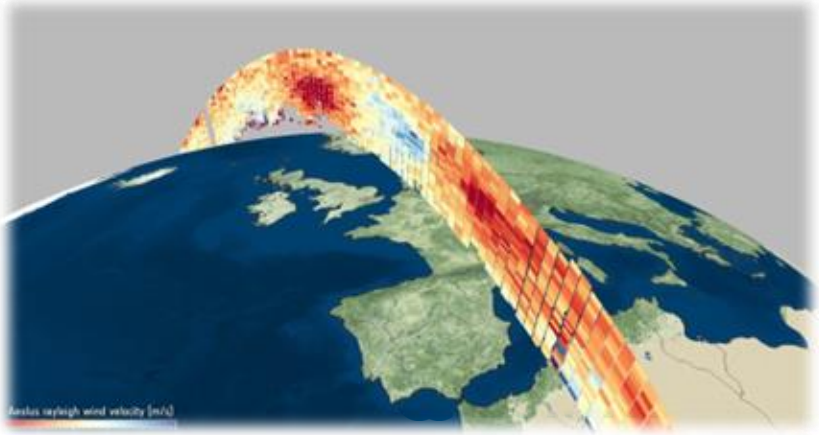

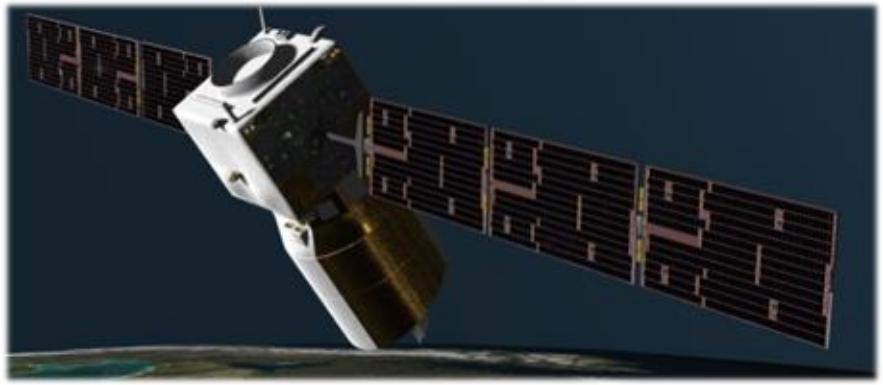

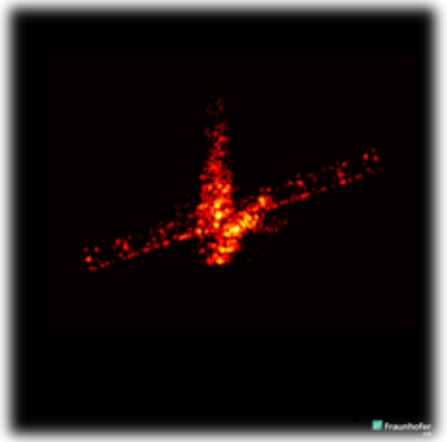

Aeolus Level-2B **horizontal line-of-sight (HLOS) winds provide good sampling through jet streams**

120 m/s polar front jet stream
9 Feb 2020; near record-breaking

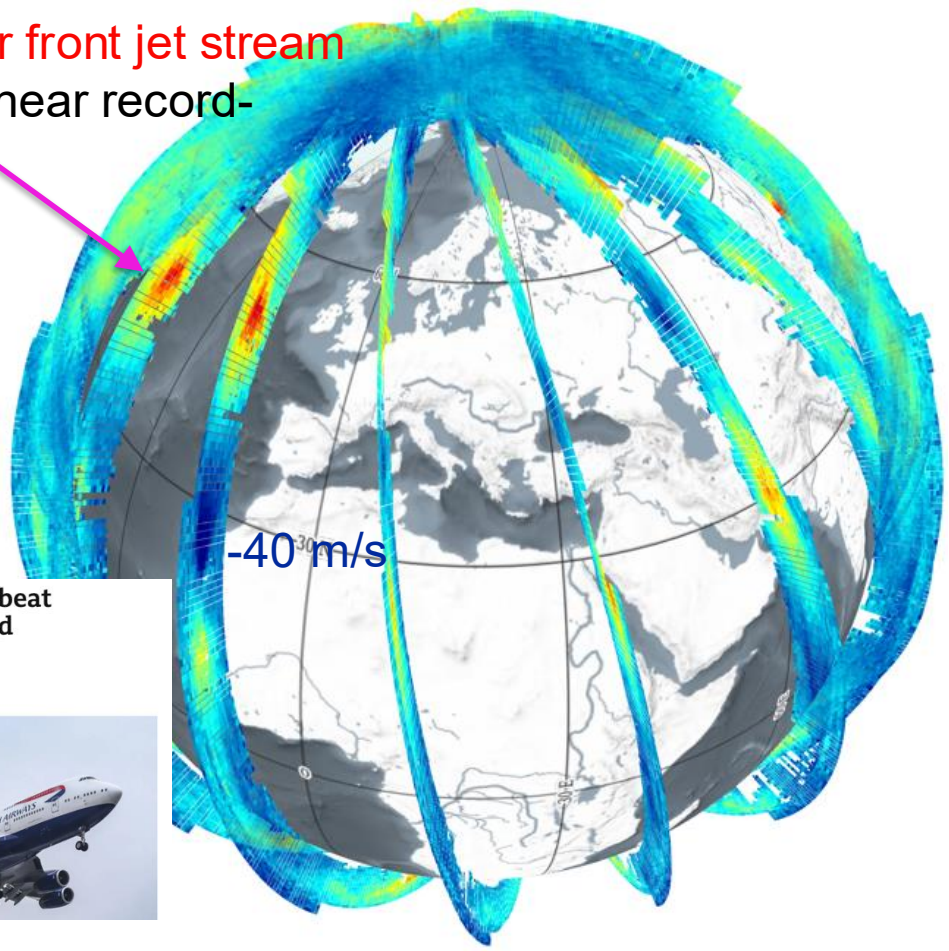

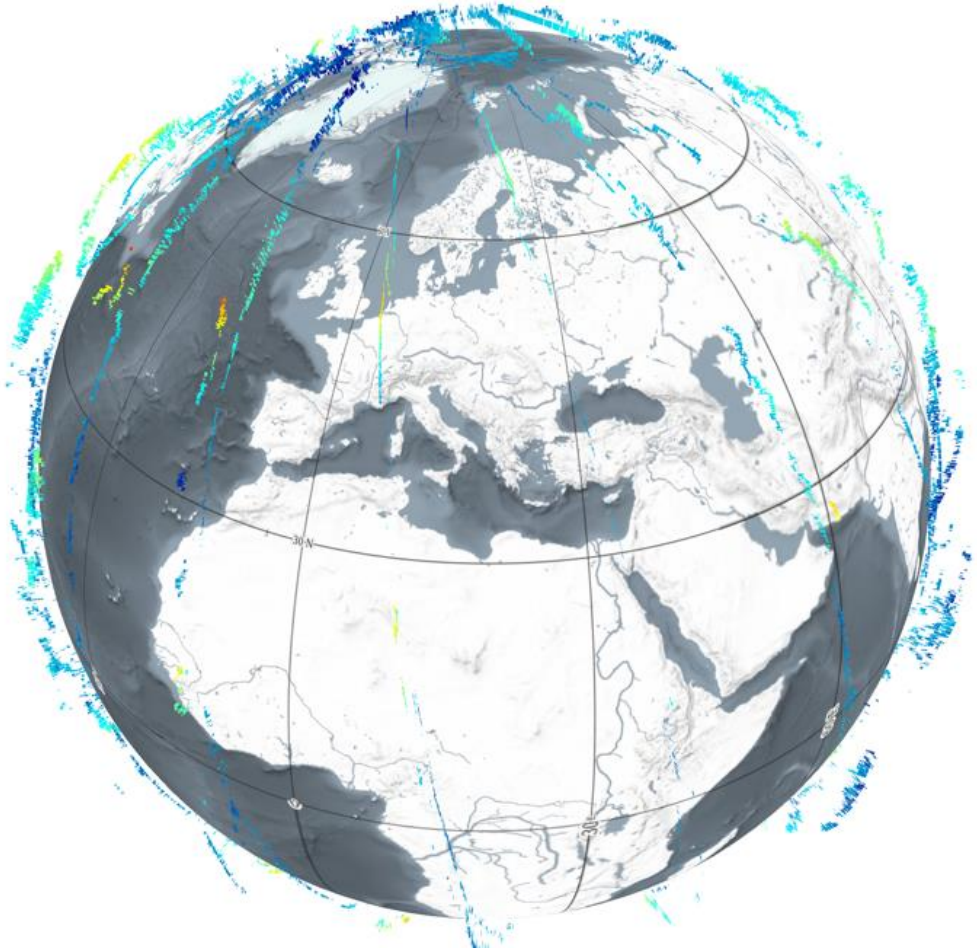

Rayleigh-clear HLOS winds

Mie-cloudy HLOS winds

Independent wind and radiance observations confirm improvements from assimilating Aeolus

Fit to vector wind from aircraft, radiosondes and radar wind profilers

tropics

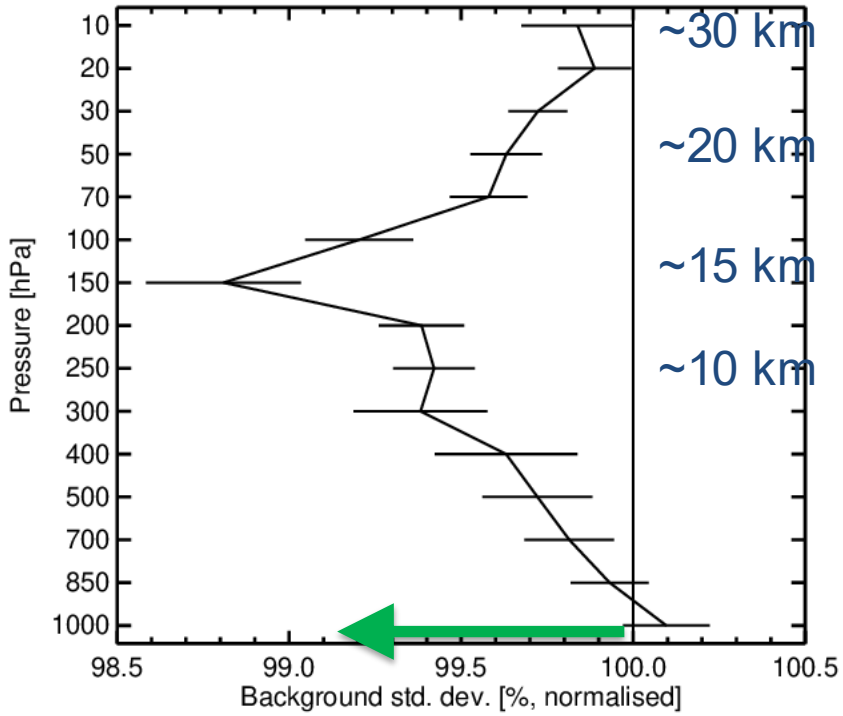

Positive impact in mid-troposphere to lower stratosphere. Largest impact on **wind in upper troposphere and lower stratosphere in tropics**

Global, ATMS (microwave radiances)

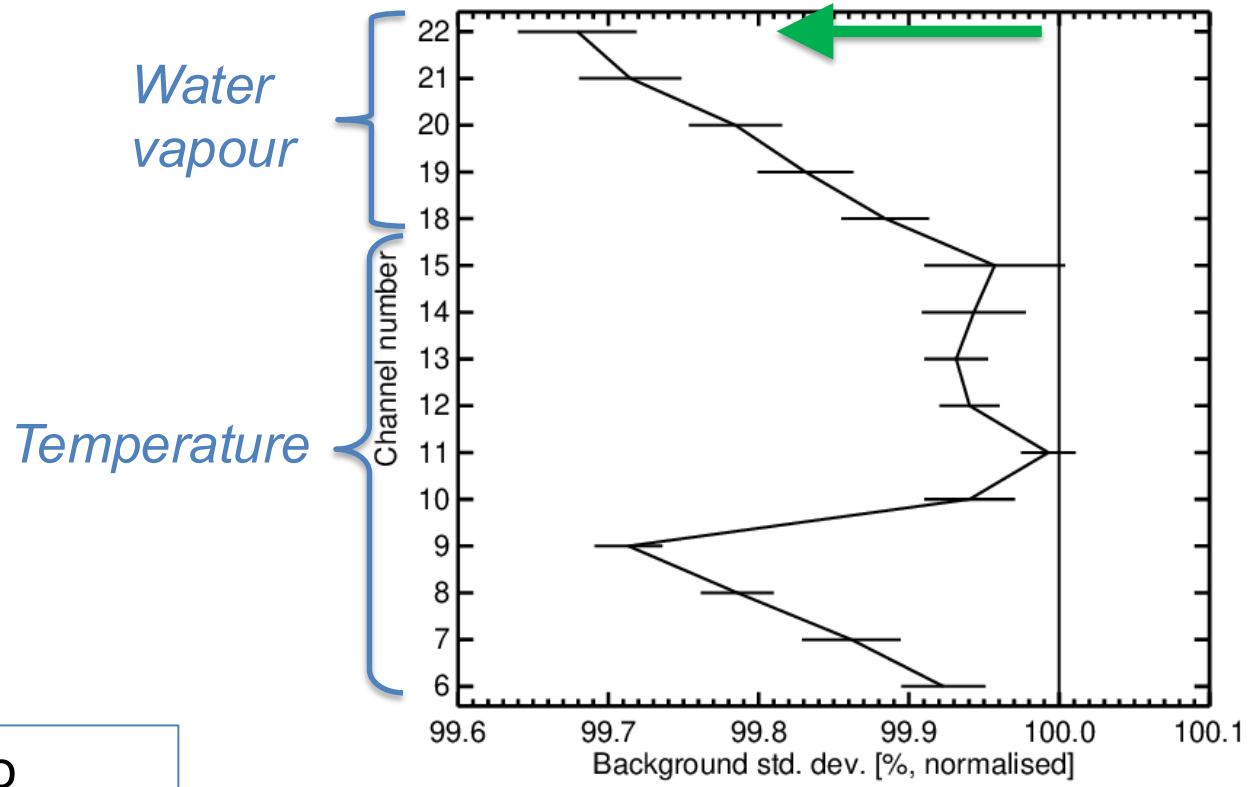

Positive impact on **temperature** and **humidity.** Strongest in **upper troposphere/lower stratosphere**

ECMWF

The Earth Cloud, Aerosol and Radiation Explorer (EarthCARE)

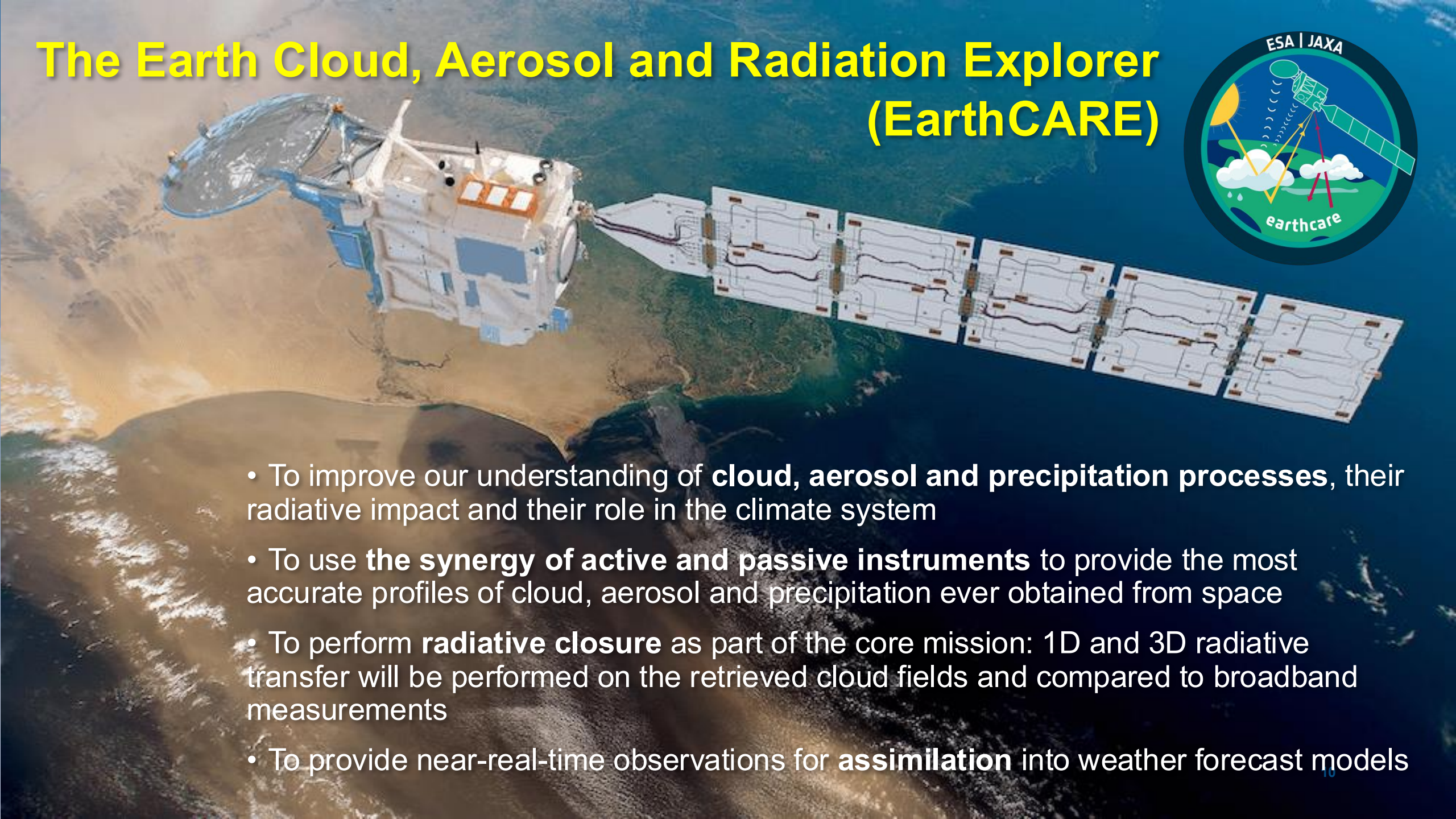

- To improve our understanding of **cloud, aerosol and precipitation processes**, their radiative impact and their role in the climate system
- To use **the synergy of active and passive instruments** to provide the most accurate profiles of cloud, aerosol and precipitation ever obtained from space
- To perform **radiative closure** as part of the core mission: 1D and 3D radiative transfer will be performed on the retrieved cloud fields and compared to broadband measurements
- To provide near-real-time observations for **assimilation** into weather forecast models

EarthCARE: key facts

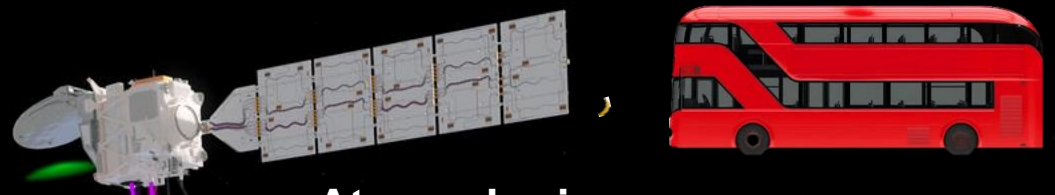

Cloud profiling radar (CPR)

First Doppler cloud radar in space

Launched May 2024

Atmospheric lidar (ATLID)

First "high spectral resolution" cloud & aerosol lidar with freely available data in space!

Multi-spectral imager (MSI)

Provides wider context, optical depth constraint and pretty pictures

Broadband radiometer (BBR)

Provides broadband fluxes for radiative closure

Mission lifetime: 10 years+

New measurements from radar and lidar

Robin Hogan (ECMWF)

Radar reflectivity

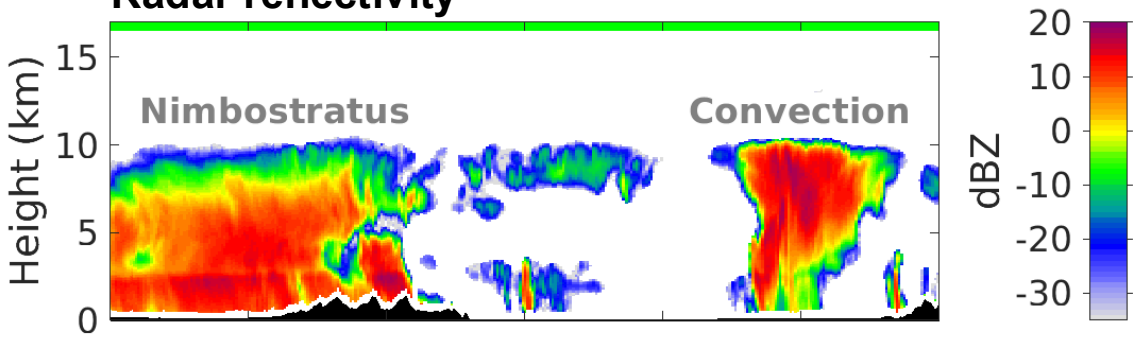

Radar Doppler velocity

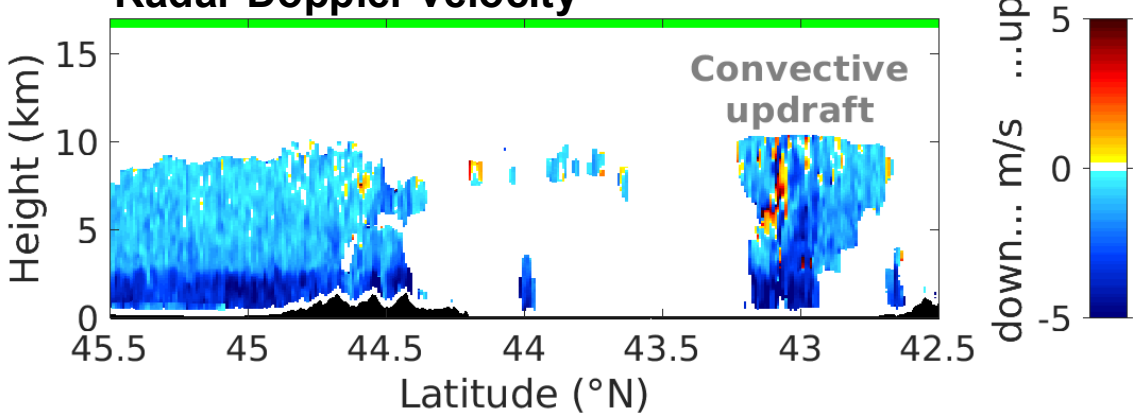

- **Radar Doppler velocity** provides rain and snow fall speed from which we can infer drop size and rimed fraction
- We can also measure the strength and width of convective updrafts

Lidar particle backscatter

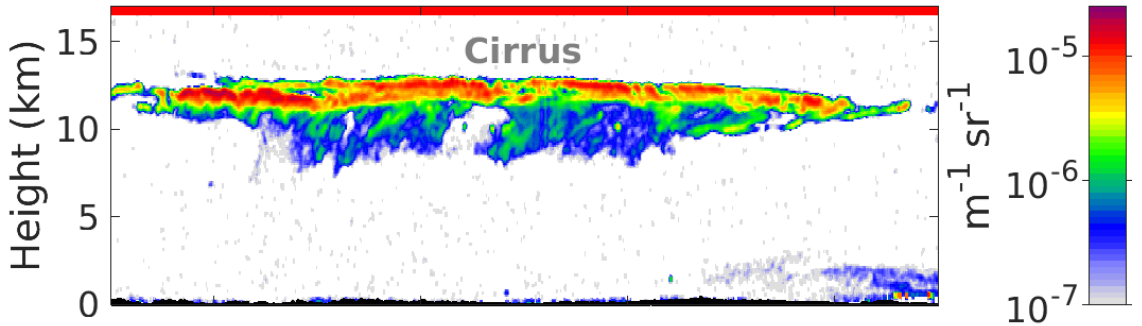

Lidar air backscatter

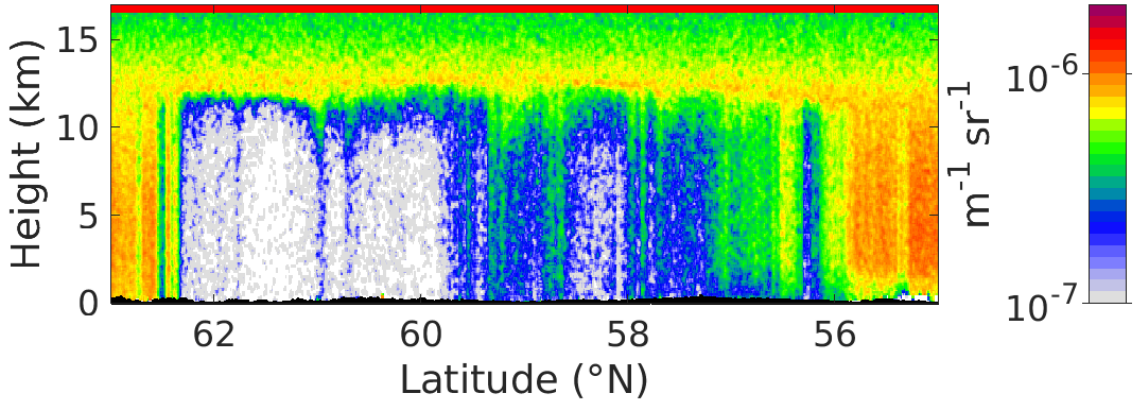

- **High spectral resolution lidar** separately measures backscatter of particles (clouds & aerosols) and air (Rayleigh scattering)
- Can unambiguously calculate the important profile of extinction coefficient from how much the air backscatter is attenuated

ECMWF

EarthCARE data coverage and availability

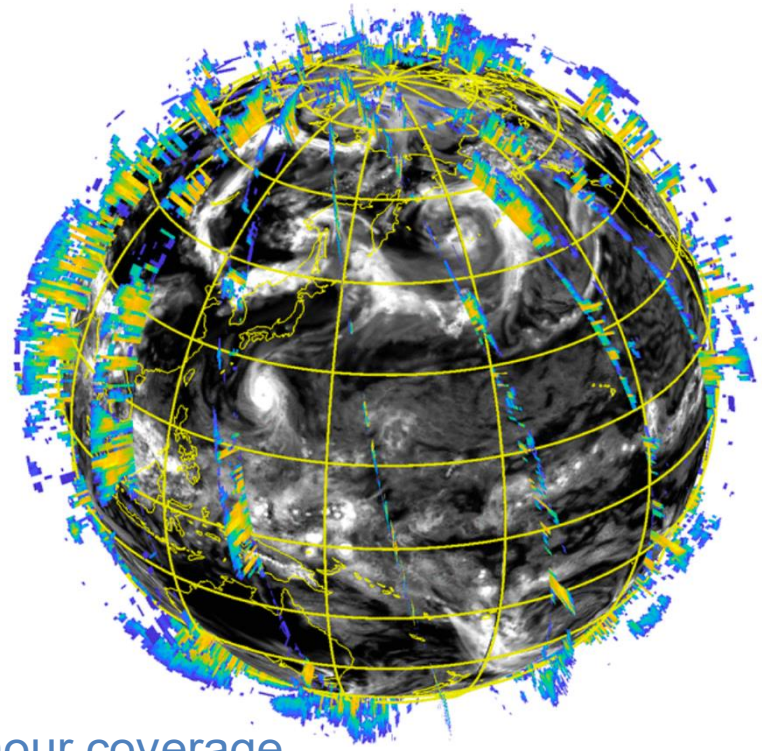

12-hour coverage

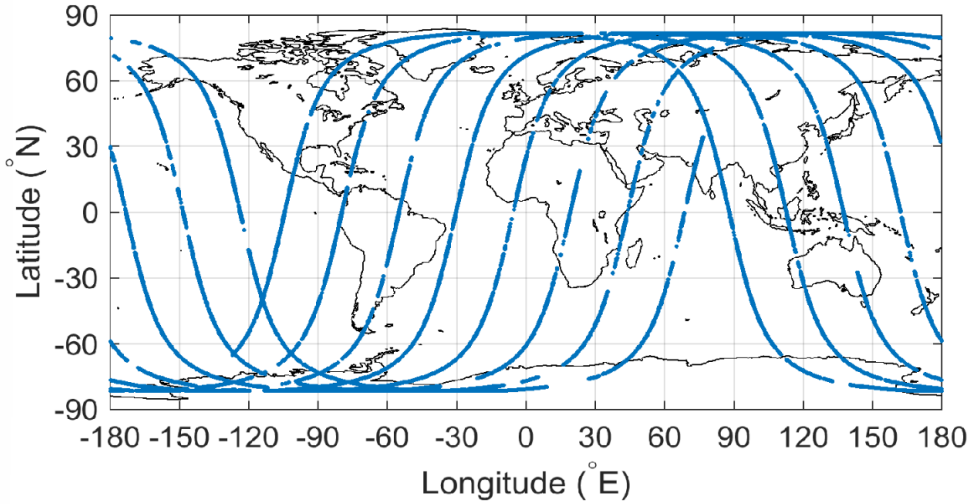

- **Satellite:**
  - **Sun-synchronous, early morning- afternoon** (02/14 Local Solar Time) near **polar orbit**
- **Instrument characteristics:**
  - CPR, 94 GHz Doppler radar, sensitivity -36 dBZ. 500m vertical resolution, 1 km horizontal resolution.
  - ATLID 355 nm HSRL lidar, three channels, 24 range-bins; 30-60 m vertical resolution; 30 m footprint:
    - **"Mie" cloud** and **aerosol** backscatter ("cloudy")
    - **"Rayleigh" molecular** backscatter ("clear")
    - "**Cross-polar Mie**", measures depolarization
  - MSI visible near-Infrared imager ~500 km swath.
  - BBR broadband radiometer (3 views)
- **Availability:**
  - Near-realtime, L1 and L2 products arrive with mean ~120 min delay

Applications for EarthCARE in NWP

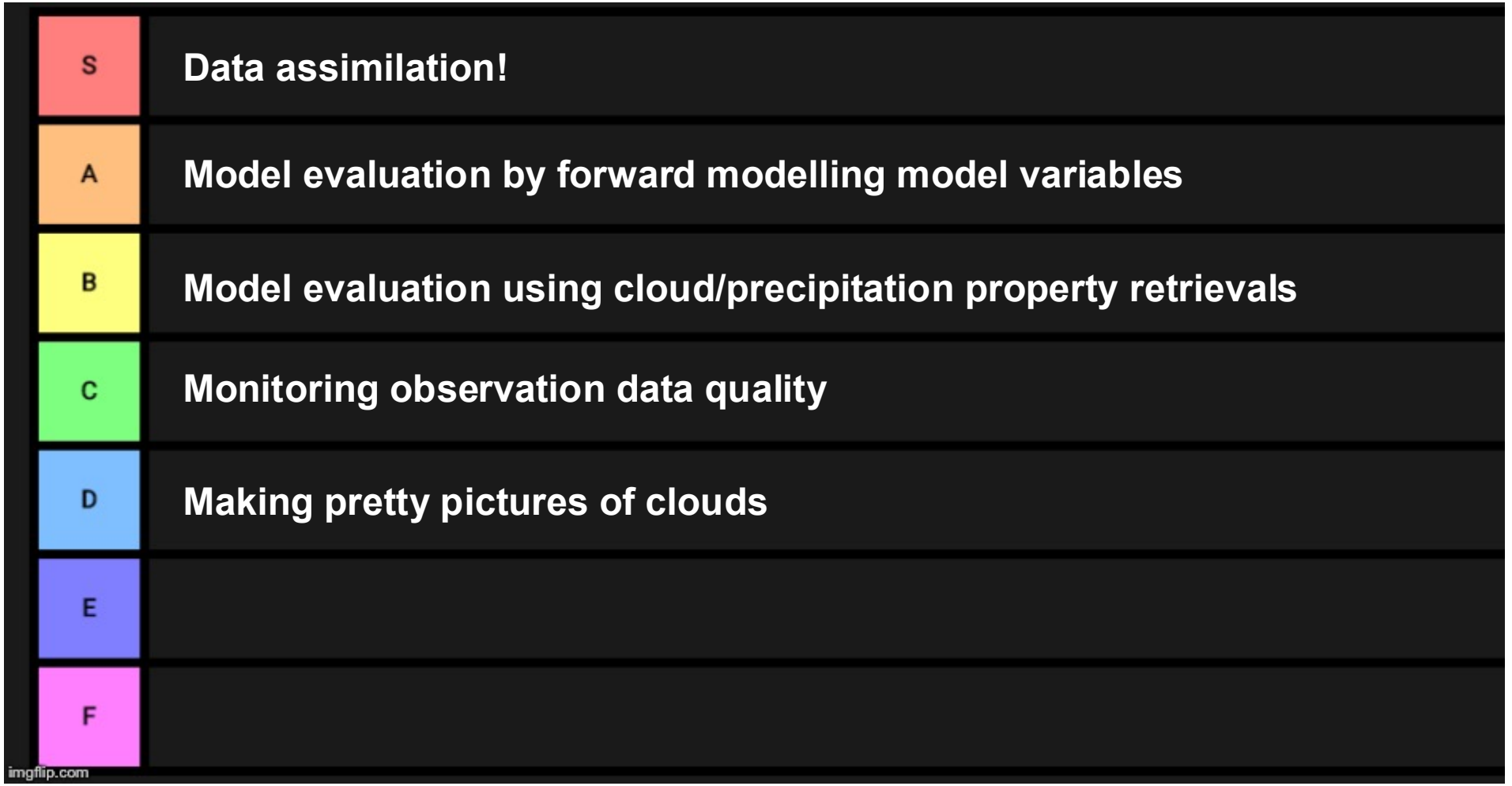

EarthCARE observations can advance global NWP forecasts by:

1. Reducing regime-dependent systematic errors
   - Clouds affect radiation, dynamics, precipitation prediction
   - Need to increase the realism, detailed representation of physical processes

2. Constraining higher resolution models – convective storms/high impact weather
   - resolving smaller scale motions (km-scale, convective permitting/resolving)
   - details of the microphysics becomes more important (macrophysics less important)

3. Improvements to model initial conditions (data assimilation)
   - cloudy areas are often meteorologically sensitive areas (reduce error growth)
   - better analyses, better forecasts, more accurate cloud microphysics means more data can be used in the assimilation
   - Direct observation prediction forecasts, and training data for AI/ML

Requirements for 4D-Var assimilation of radar and lidar observations

- Need to be able to compute cost function and its gradient

Penalty for departure from background

Observation errors

$$J(\boldsymbol{x}) = \frac{1}{2}\left(\boldsymbol{x} - \boldsymbol{x}^{\mathrm{b}}\right)^{T} \widetilde{\mathbf{B}}^{-1} \left(\boldsymbol{x} - \boldsymbol{x}^{\mathrm{b}}\right) + \frac{1}{2}\boldsymbol{d}^{T} \widetilde{\mathbf{R}}^{-1} \boldsymbol{d}$$

Cost function

Penalty for departure from observations

Observation *Model equivalent*

$$\boldsymbol{d} = \boldsymbol{y} - \boldsymbol{b} - H(\boldsymbol{x})$$

Radar reflectivity
Mie backscatter
Doppler velocity
Lidar extinction
Rayleigh backscatter

Observation operator

+ observation pre-processing

Forward modelling radar and lidar observations

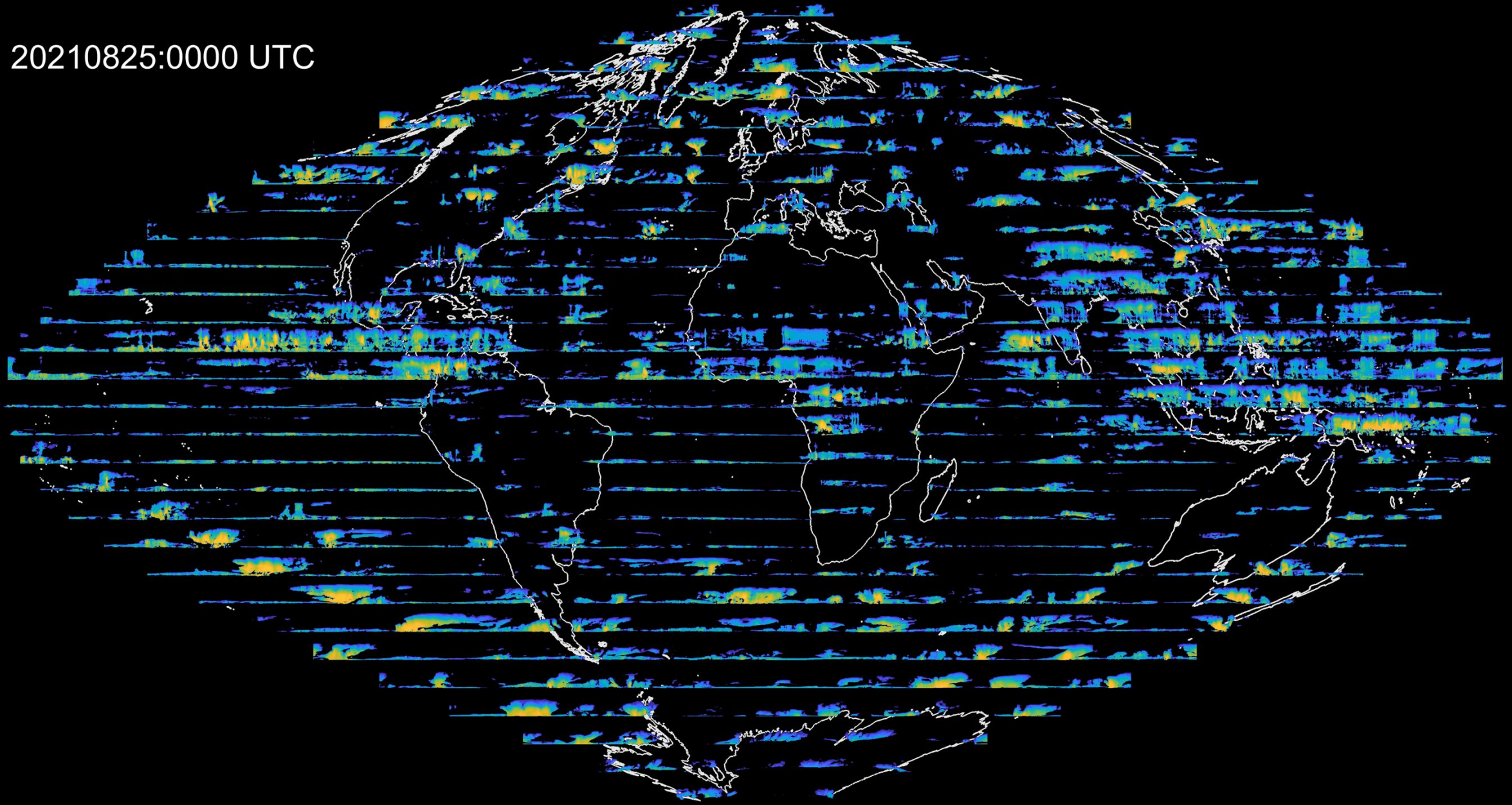

Model space

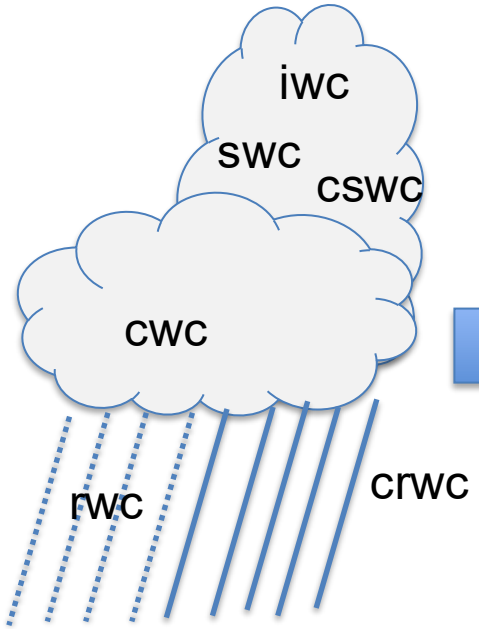

+cc, pfra

Microphysical

Scale invariant

Particle habit

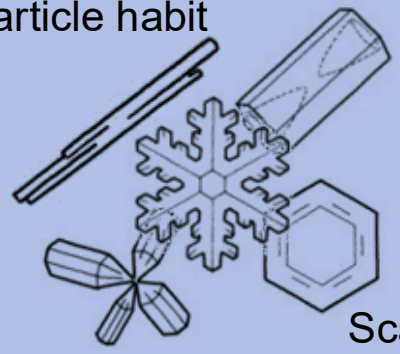

Scattering properties

Particle size and density

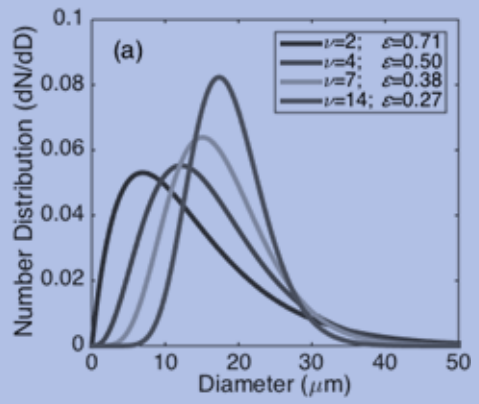

Particle size distribution

Macrophysical

Scale dependent

Cloud overlap

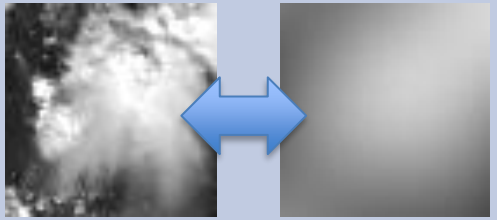

Subgrid scale condensate variability

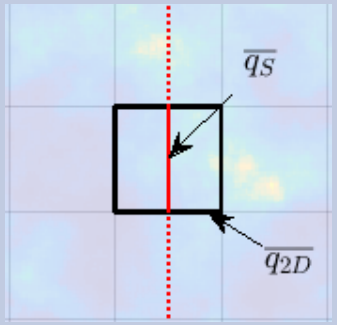

Representativity

Radiative transfer

Observation space

Radar reflectivity

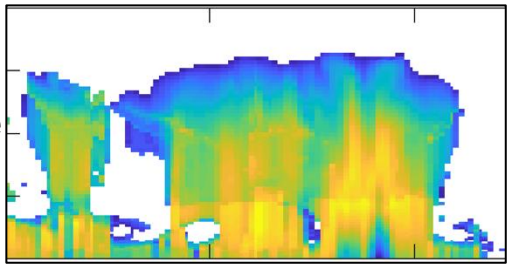

Lidar backscatter

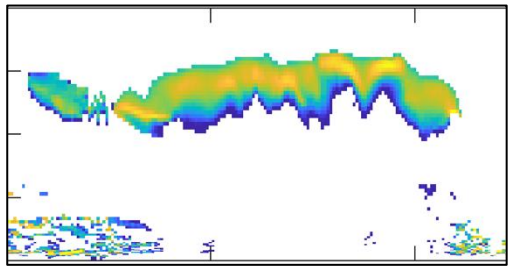

What are the components of an active observation operator for cloud/precip?

Computing attenuated radar reflectivity (and lidar backscatter)

- Unattenuated reflectivity is computed off-line by integrating scattering properties over particle size distribution (PSD) and stored in LUT.
- Attenuated radar reflectivity at each level is computed by multiplying the unattenuated reflectivity by the transmission from the satellite to the level.

$$Z_l^a = Z_l e^{-2\tau_l} \frac{1 - e^{-2\Delta h_l \alpha_l}}{2\Delta h_l \alpha_l},$$

$$Z = \sum_{j=1}^{N} F^j Z^j, \qquad \alpha = \alpha^{\text{gas}} + \sum_{j=1}^{N} F^j \alpha^{\text{cloud},j}.$$

Microphysical assumptions in ZmVar forward model

Hydrometeor	Habit	Scattering model		PSD	Effective density (g/cm^3) $\rho_e(D) = aD^b$
		Radar	Lidar		
Liquid cloud	Sphere	Mie	Mie	$N(r) = \frac{N_t}{\sqrt{2\pi}(\ln\sigma_g)r} e^{-\frac{\ln^2(r/r_g)}{2(\ln\sigma_g)^2}}$ (Miles et al., 2000)	$a = 1$, $b = 0$
Ice cloud	Aggregates	SSRGA Hogan et al. (2017)	Baran (2004)	Field et al. (2007) (N_0, D_0 from Delanoë and Hogan, 2008)	$a = 0.0026$, $b = -1.42$
Stratiform Rain	Sphere	Mie	Mie	$N(D) = N_0 \exp(-\lambda D)$, $N_0 = x_1 \lambda^{x_2}$ (Abel and Boutle, 2012)	$a = 1$, $b = 0$
Convective Rain	Sphere	Mie	Mie	$N(D) = \frac{0.03 N_L D_0^4 \Lambda^{\mu+4}}{\Gamma(\mu+4)} D^\mu e^{-\Lambda D}$ (Illingworth and Blackman, 2002)	$a = 1$, $b = 0$
Stratiform Snow	Aggregates	SSRGA Hogan et al. (2017)	Baran (2004)	Field et al. (2007) (N_0, D_0 from Delanoë and Hogan, 2008)	$a = 0.0026$, $b = -1.42$
Convective Snow	Sphere	Mie	Mie	Field et al. (2007)	$a = 0.0026$, $b = -1.42$

Visualising the ZmVar look-up tables

Larger particle sizes

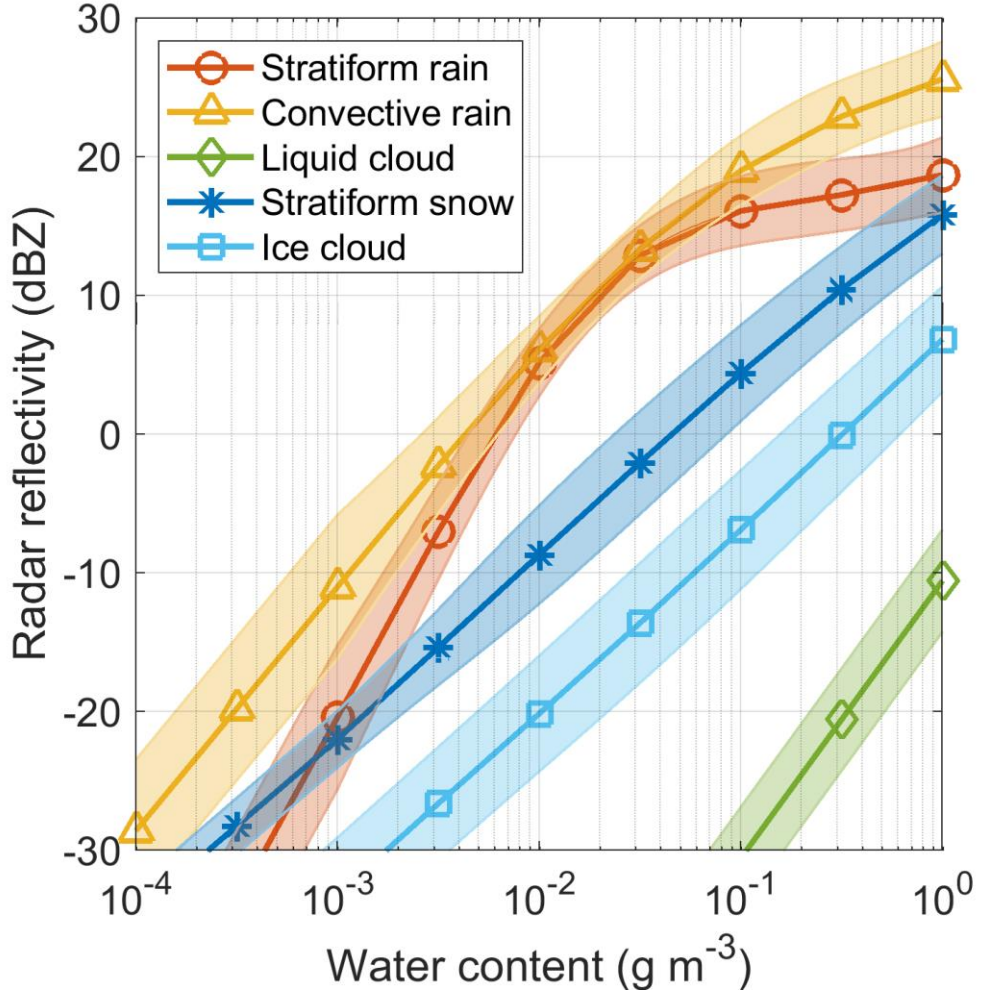

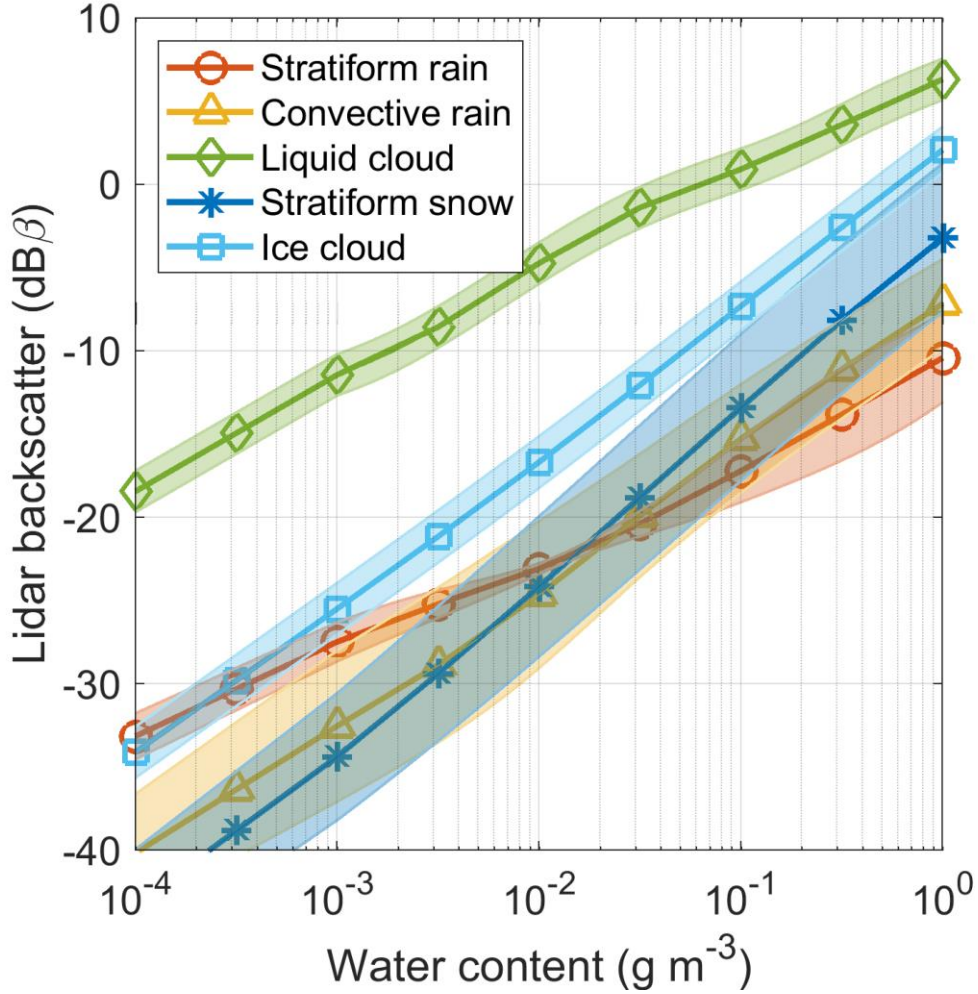

Larger particle sizes

Observation operator for Doppler velocity

Model air motion

$$V_D = w + v_d$$

Doppler velocity

Reflectivity-weighted fall speed

$$v_d = -\frac{\int_0^\infty n(D)\eta(D)v(D)dD}{\int_0^\infty n(D)\eta(D)dD}$$

$$v(D) = c_x D^{d_x}\left(\frac{\rho_0}{\rho}\right)^{0.5}$$

Hydrometeor	c_x	d_x
Rain	386.8	0.67
Snow	16.8	0.527

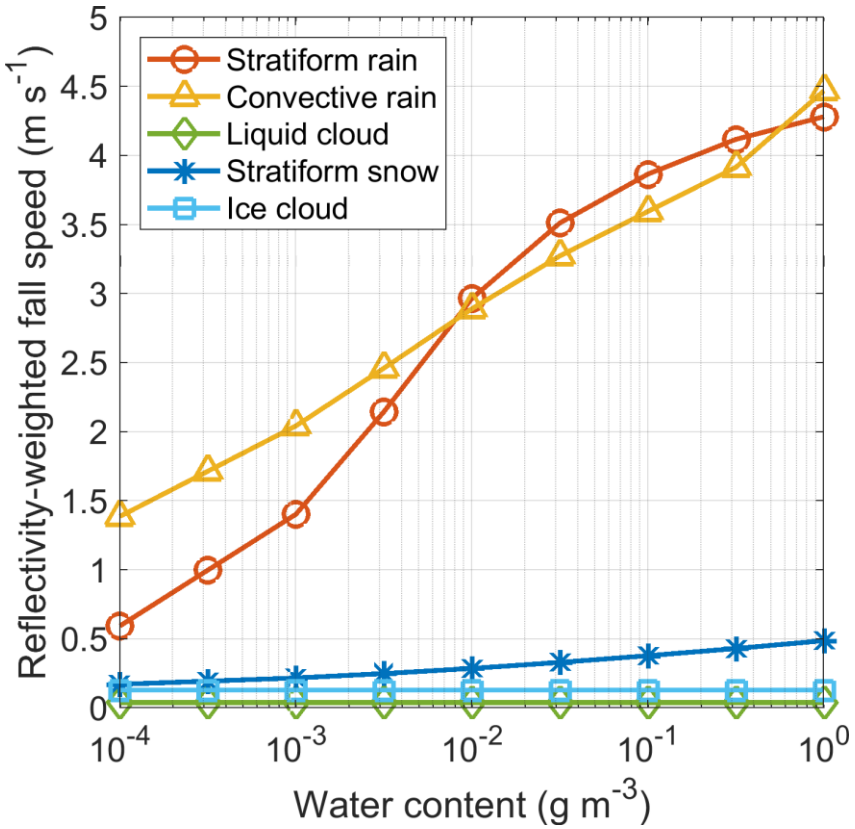

- Assumptions on hydrometeor fall speed follow current IFS cloud physics (ice 0.13 m s^{-1}, snow 1 m s^{-1} variable fall speed for rain), with option for variable snow fall speed.

Representing subgrid variability

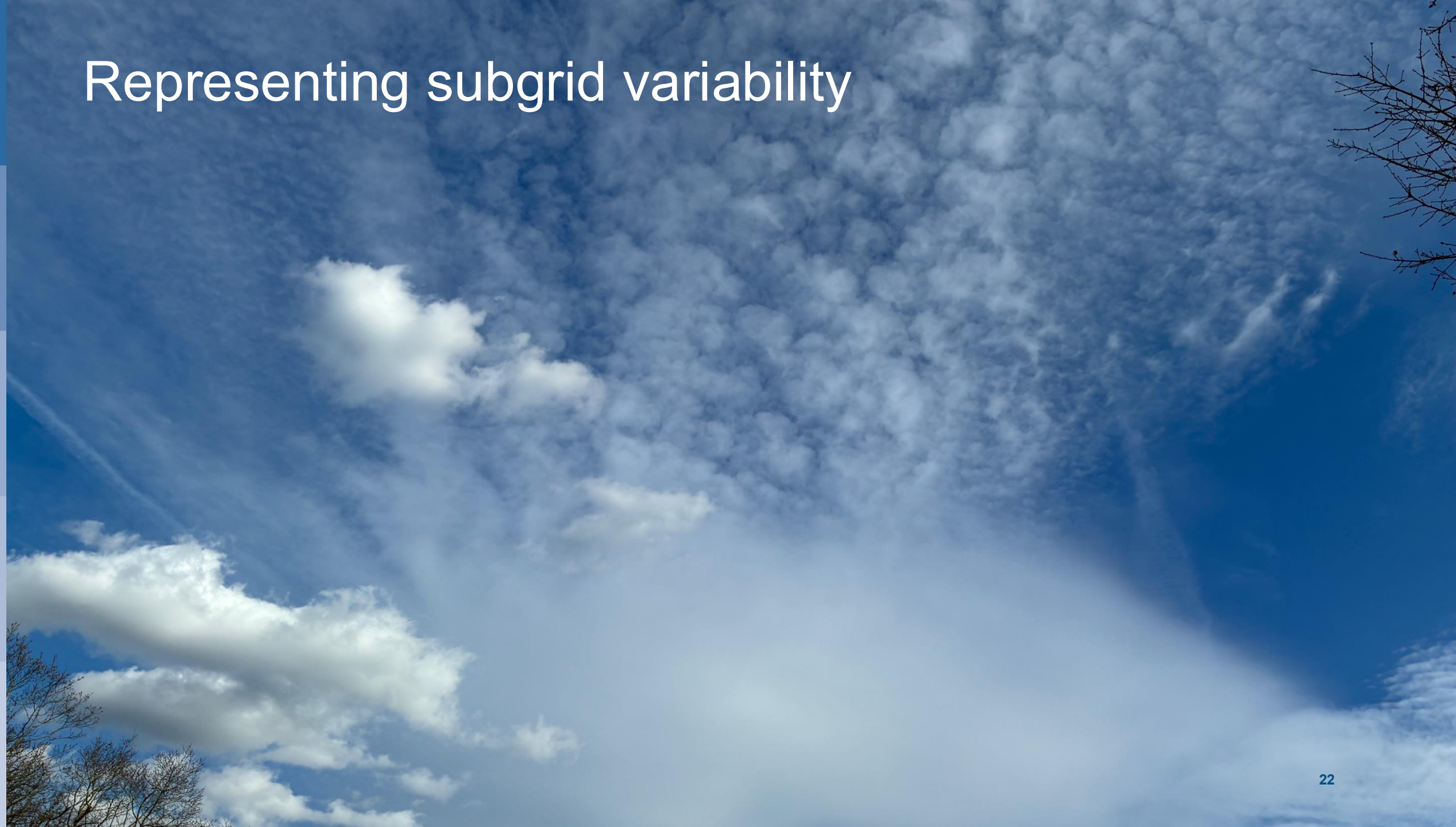

Any non-linear process acting on a grid-box mean variable is likely to be biased

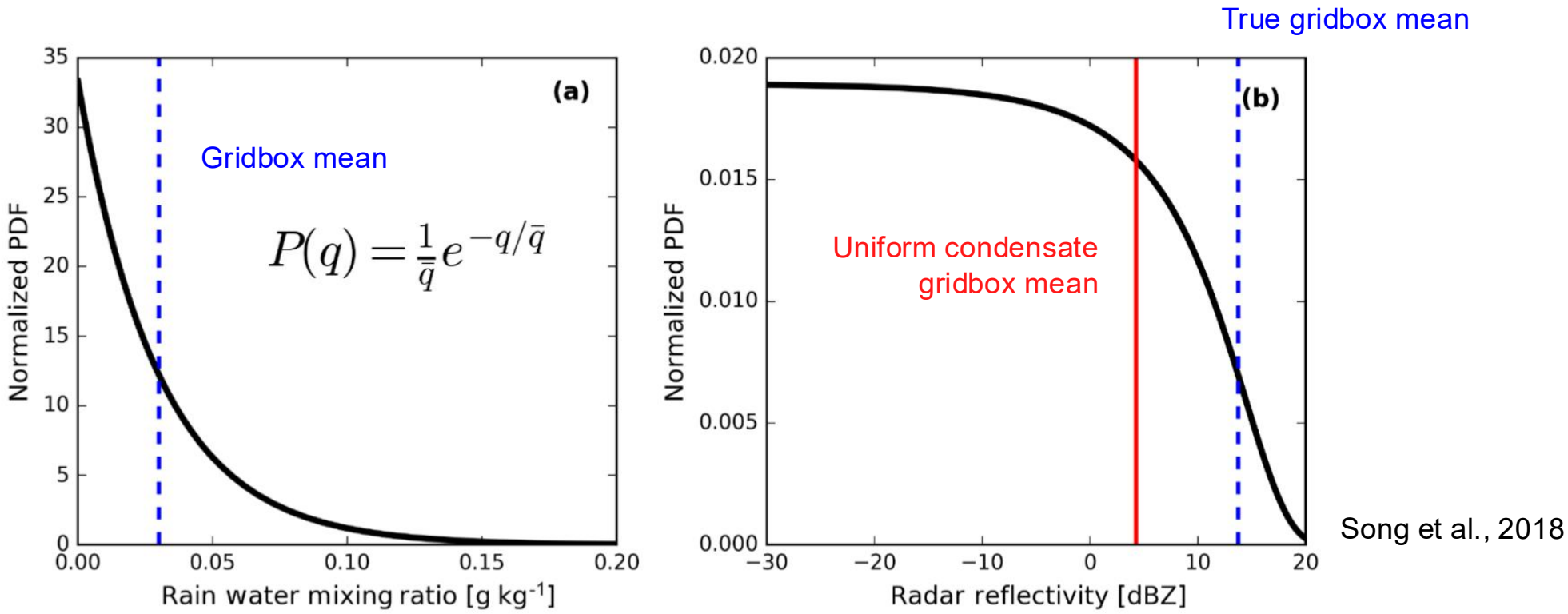

Song et al., 2018

- For simple equations, expressions for the bias can be found analytically by integrating over sub-grid variability distributions.
- Effect of sub-grid variability on radiative transfer is more complex and depends on cloud overlap and vertical correlation assumptions.

ECMWF

Song, H., et al,: The importance of considering sub-grid cloud variability when using satellite observations to evaluate the cloud and precipitation simulations in climate models, Geosci. Model Dev., 11, 3147–3158, 2018.

Multi-column approach

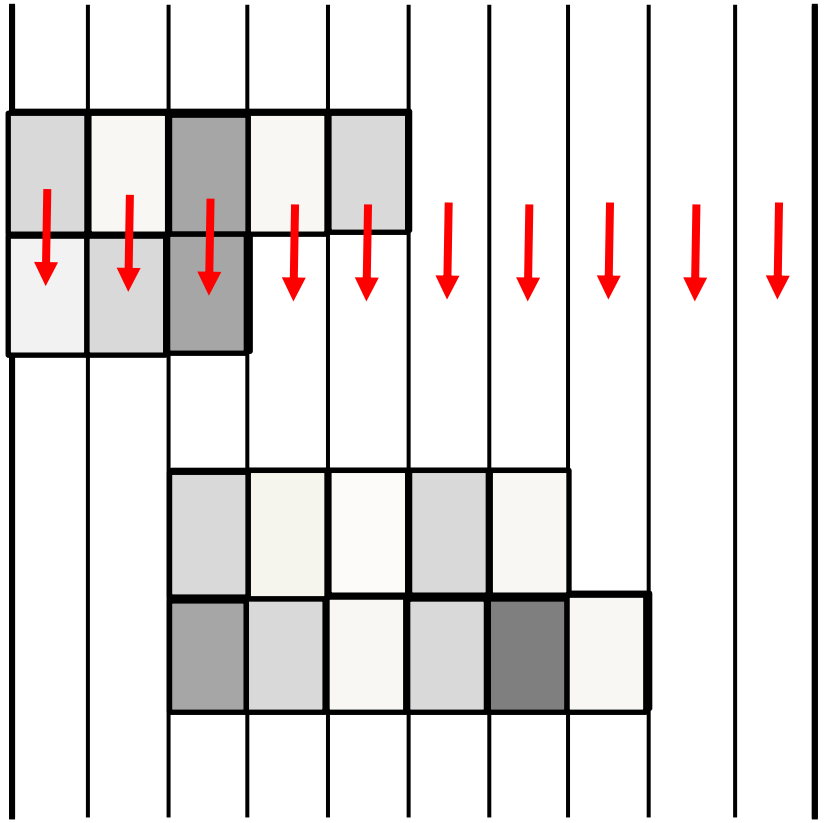

- Multi-column approach (analogous to McICA RT; *Barker et al., 2002, Pincus et al., 2003*) is *status quo* for solving radar/lidar equation at grid-box scales (e.g., COSP/COSP2; *Bodas-Salcedo et al., 2011*).

METHOD

1. Divide model gridbox into N subcolumns and populate subcolumns into cloudy or clear according to model cloud fraction and assumed overlap.
2. Randomly scale optical depth in each subcolumn drawn from assumed condensate variability (e.g., gamma distribution with specified fractional standard deviation (FSD).
3. Solve radiative transfer in each column independently.
4. Average columns of reflectivities/backscatter to compute grid-box mean at each layer.

Multi-column approach is flexible, but expensive

Advantages

- Intuitive.
- Straight-forward to apply to different solvers.
- Flexible to overlap and sub-grid variability assumptions.

Disadvantages

- Costly, particularly if representation of large variability (large FSD) required.
- Use of random cloud generator makes it difficult to differentiate (requirement for 4D-VAR assimilation).

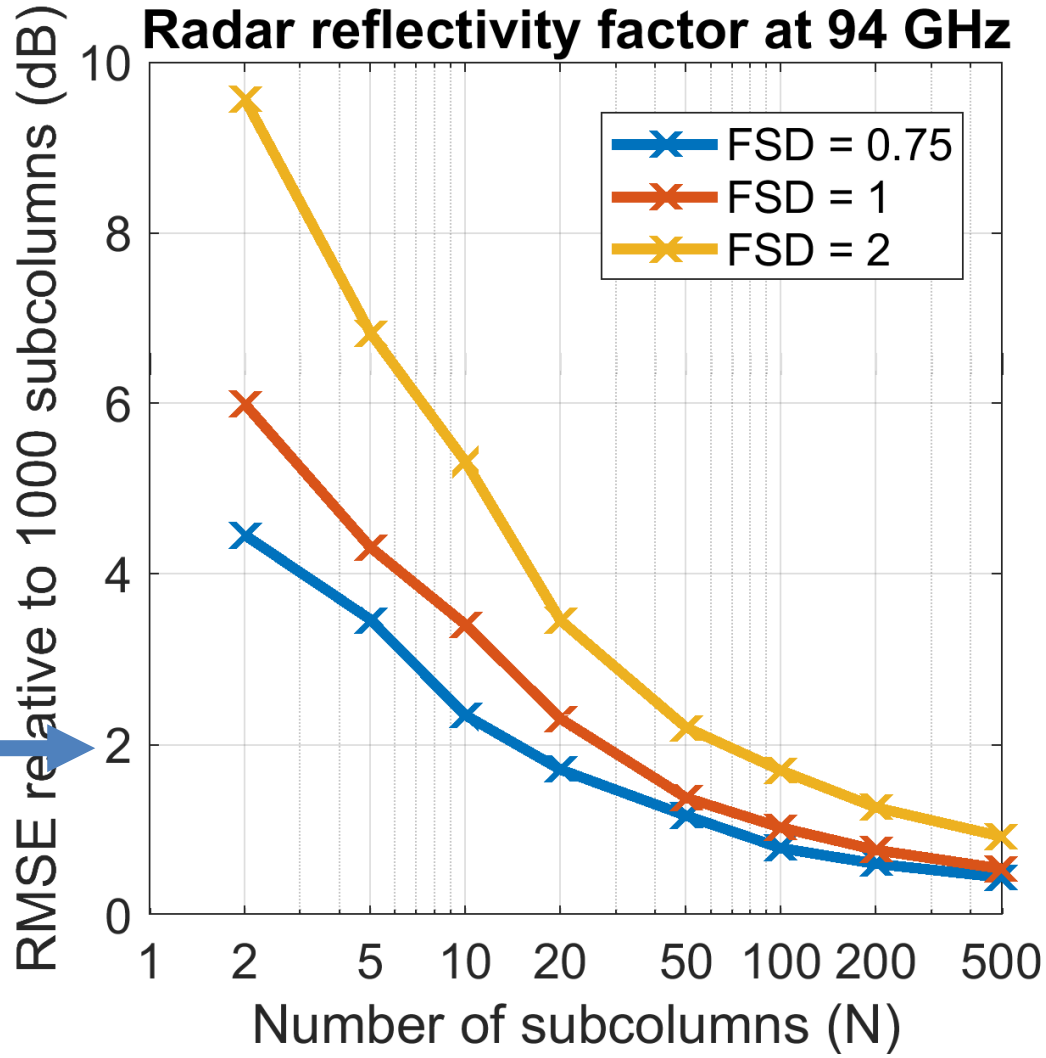

Triple-column approach

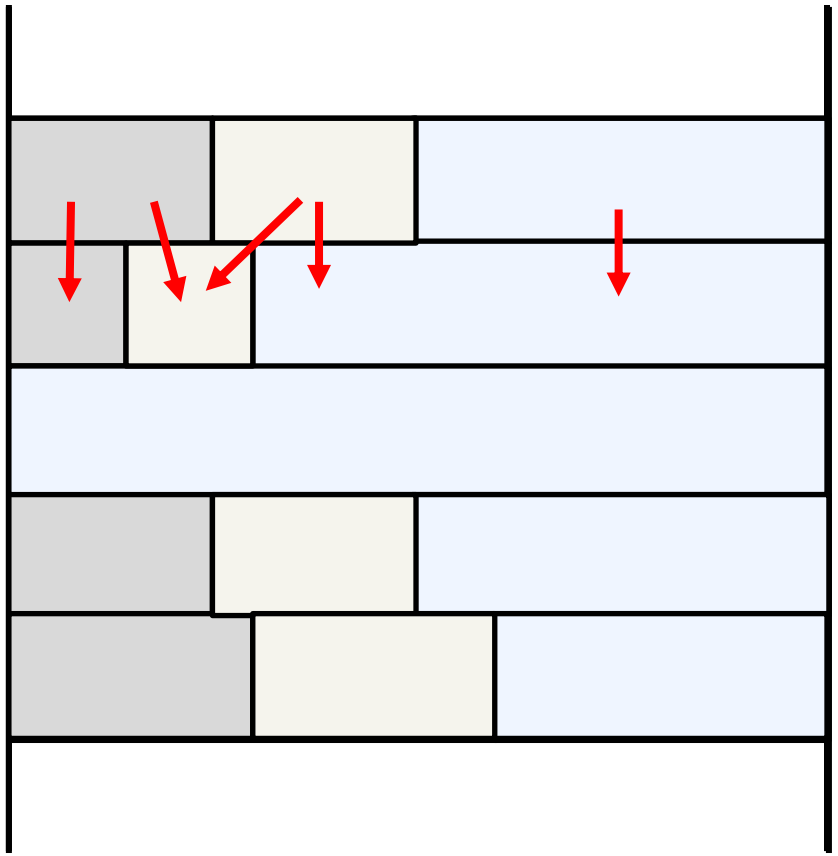

- Triple-column approach (analogous to Tripleclouds RT for fluxes; *Shonk and Hogan, 2008*) provides noise-free, differentiable handling of sub-grid variability (*Fielding et al., 2022, in prep*).

METHOD

1. Divide model gridbox into 3 *sections* according to cloud fraction (one clear, two cloudy)
2. Scale optical depth in cloudy sections according to assumed condensate variability (For FSD<1, 1 ± FSD; see Shonk and Hogan 2008; Hogan et al., 2019)
3. Working down from top of atmosphere (for satellite sensors), pass transmission of signal between each layer according to a 3x3 overlap matrix.
4. Total grid-box mean reflectivity/backscatter is sum of transmissions in each section multiplied by unattenuated reflectivity/backscatter.

Validation of triple-column method against multi-column approach for radar

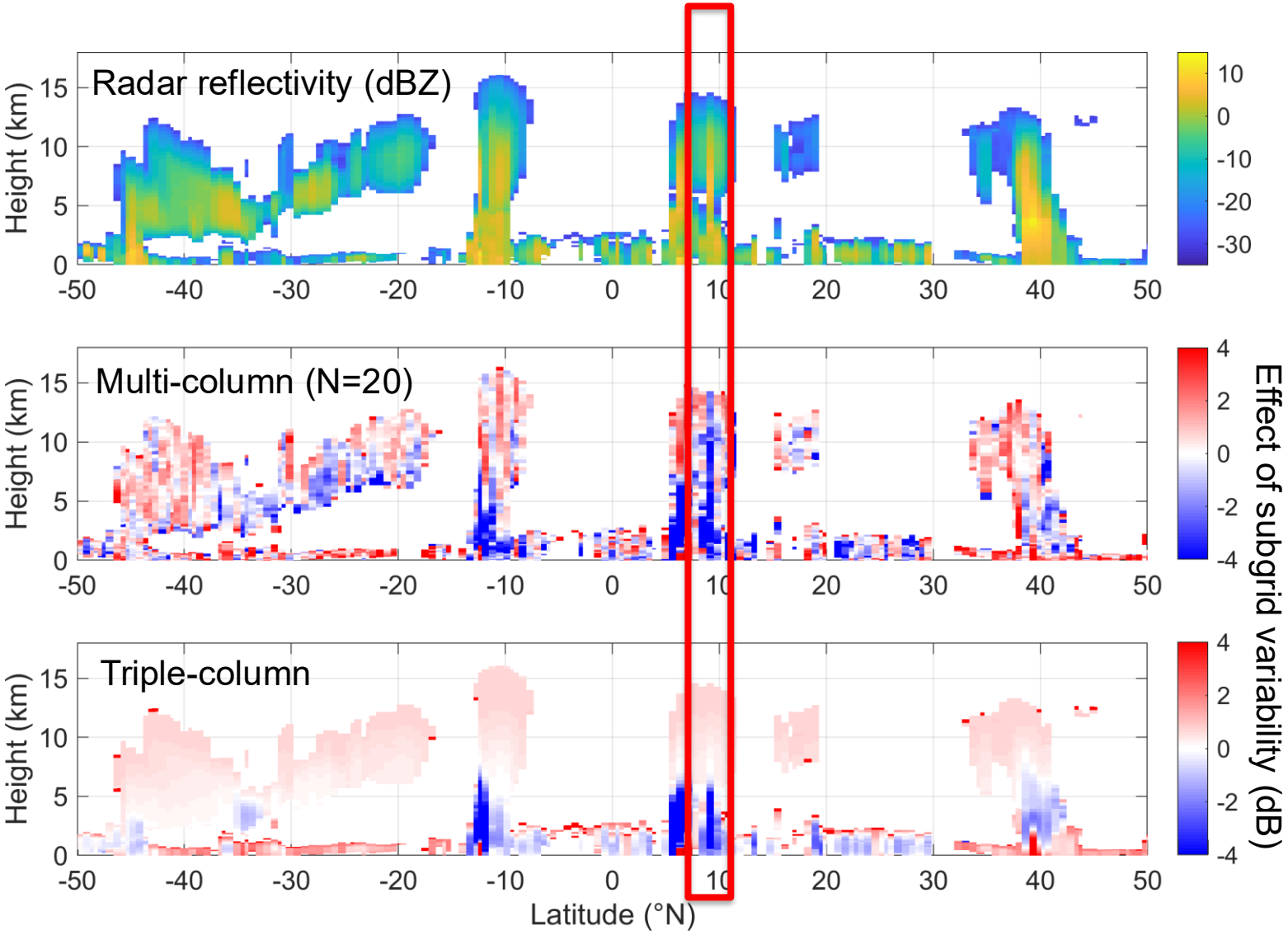

- Triple-column provides noise-free computation of radar reflectivity.
- In general, sub-grid variability increases (decreases) radar reflectivity in weakly (strongly) attenuating regions.

Example for deep convective profile

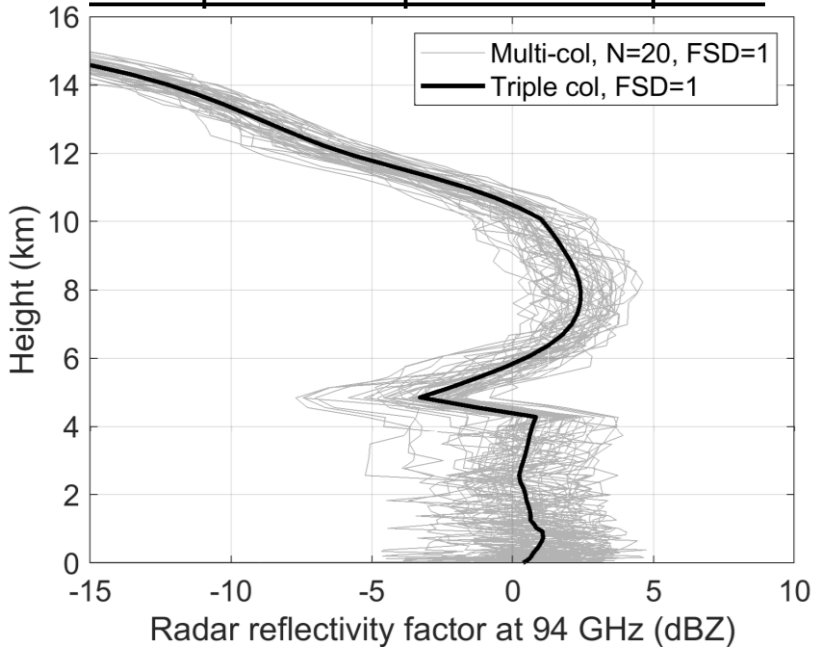

Validation of triple-column method against multi-column approach for radar

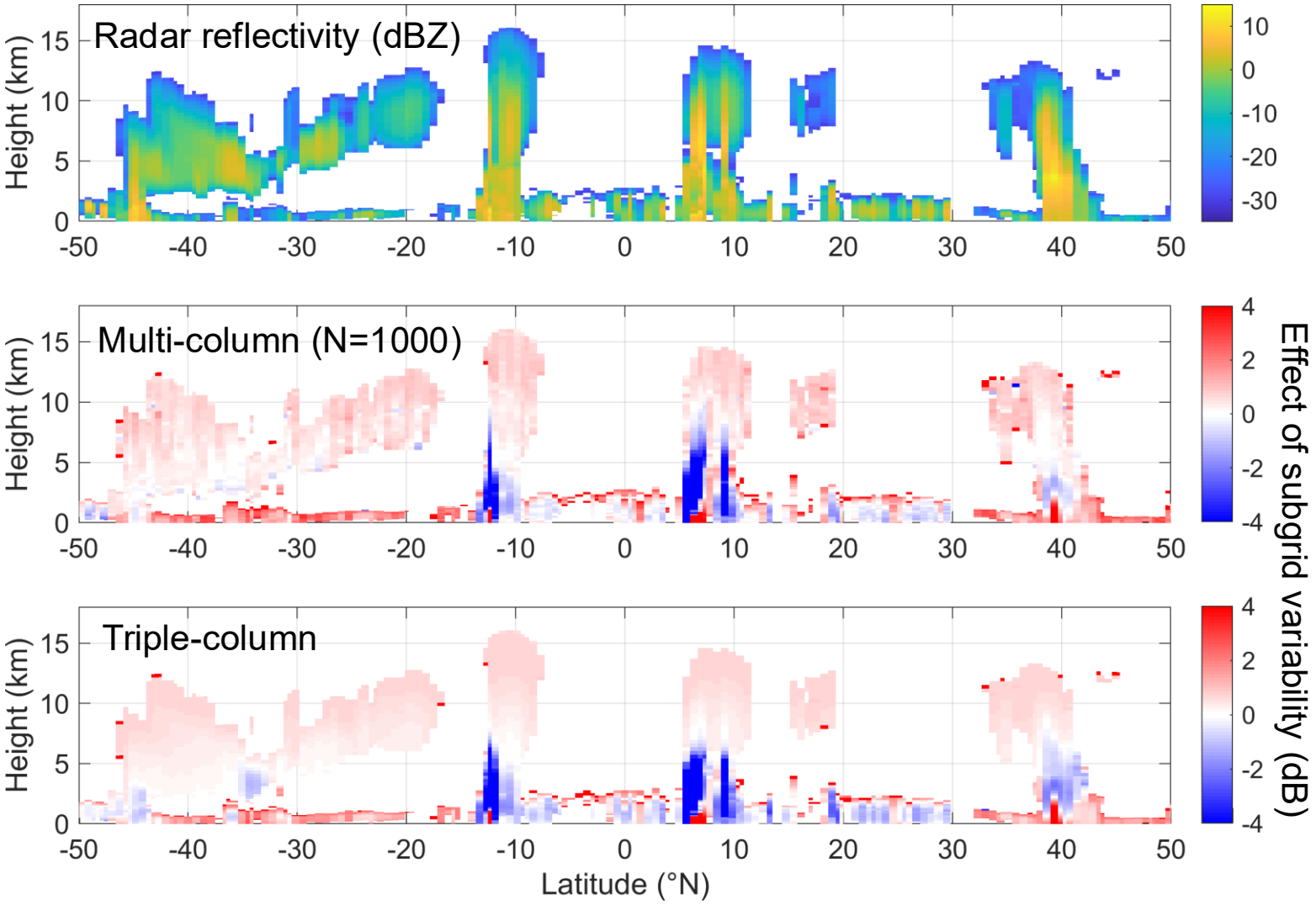

- Triple-column provides noise-free computation of radar reflectivity.
- In general, sub-grid variability increases (decreases) radar reflectivity in weakly (strongly) attenuating regions.

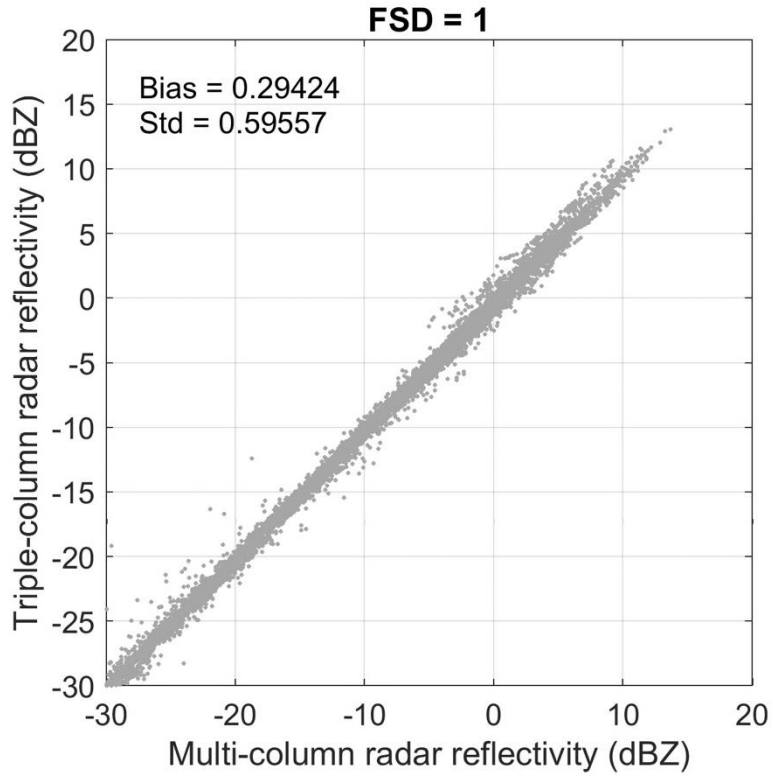

Validation of triple-column method against multi-column approach for lidar

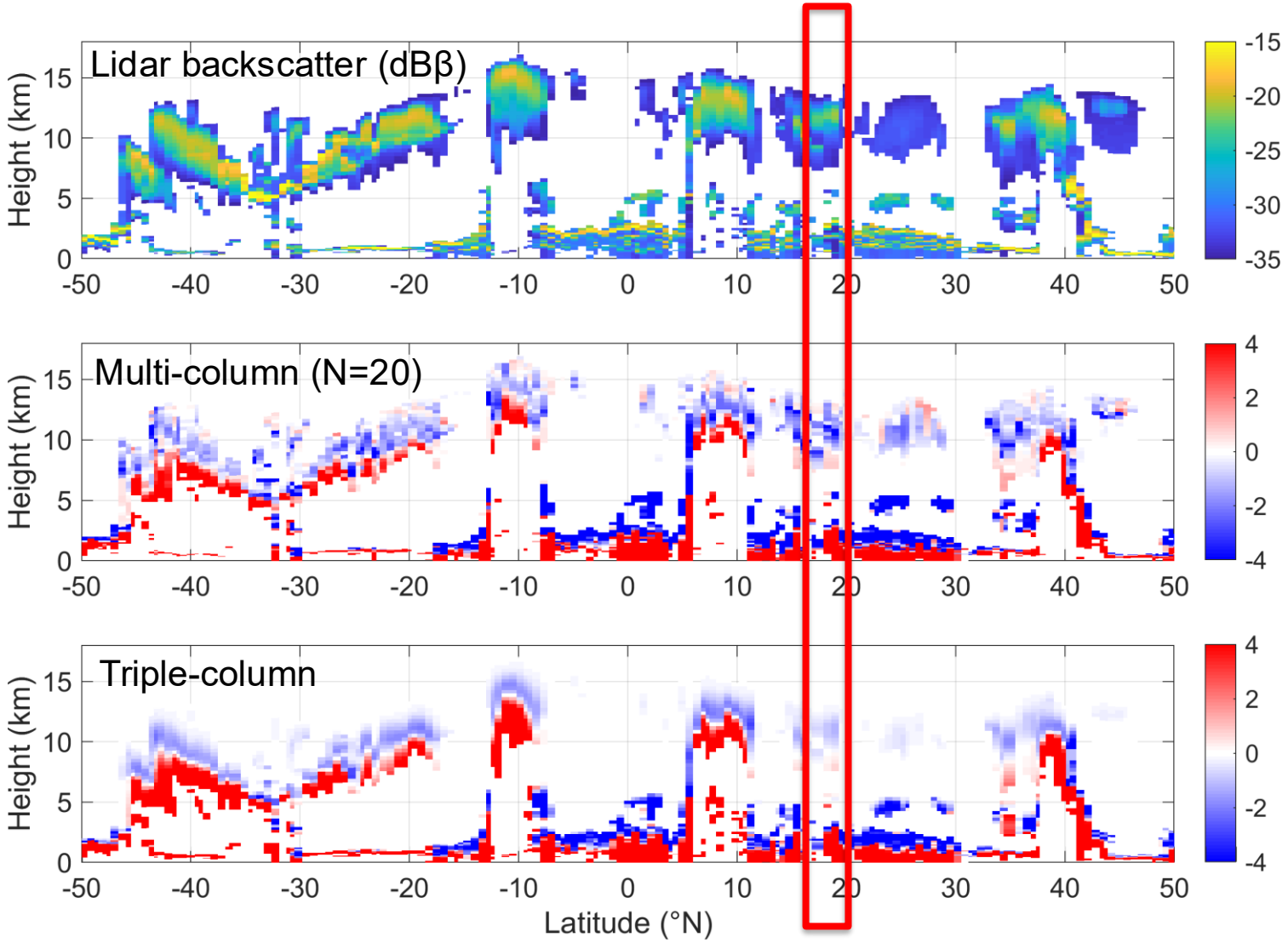

- Triple-column provides noise-free computation of lidar backscatter.
- In general, sub-grid variability allows lidar signal to penetrate further into clouds; more boundary layer clouds are visible

Example for multi cloud-layer profile

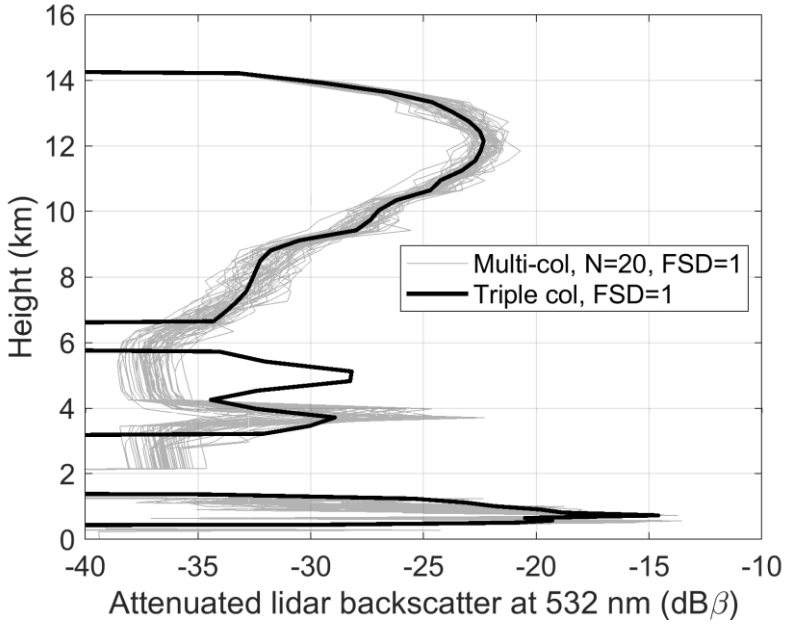

An observation error inventory approach

- Observation errors are a crucial component of a data assimilation system as, coupled with the background error, control the weight each obs. is given.
- Often assumed to have no correlation & used for tuning data assim. system
- Can be estimated directly or inferred through a statistical evaluation of FG departures and/or analysis increments

- Selected approach – defining the observation error explicitly based on physical understanding because:
  - Owing to the profiling nature of the observations, the true obs. error likely to be highly situation dependent
  - At the time EarthCARE becoming operational, no availability of long history of observations to generate a climatological obs. error covariance matrix

- Under the hypothesis of uncorrelated errors, obs. error is defined as a combination of instrument error, obs. operator error and representativity error:

ECMWF

$$\sigma^2_{obs} = \sigma^2_{ins} + \sigma^2_{oper} + \sigma^2_{rep}$$

Example of PSD uncertainty via Monte Carlo methods

$$Z' = Z\exp(-2\tau) \Rightarrow \ln(Z') = \ln(Z) - 2\tau$$

$$\Delta Z'_{dB} = 4.343\sqrt{(\Delta \ln Z)^2 + 4(\Delta\tau)^2}$$

Uncertainty in backscatter

Uncertainty in attenuation

Hydrometeor type	Parameter and mean value	Perturbation (%)
Cloud liquid	$N_t = 100\,\mathrm{cm}^{-3}$	20
	$\sigma_g = 0.3$	20
Cloud ice	$a = 0.0094$	10
	$b = -0.87$	10
Rain LS	$x_1 = 0.22$	20
	$x_2 = 2.2$	0
Snow LS	$a = 0.0026$	10
	$b = -1.42$	10
Rain conv.	$N_L = 0.08\,\mathrm{cm}^{-4}$	50
	$\mu = 5.0$	30
Snow conv.	$a = 0.0026$	10
	$b = -1.42$	10

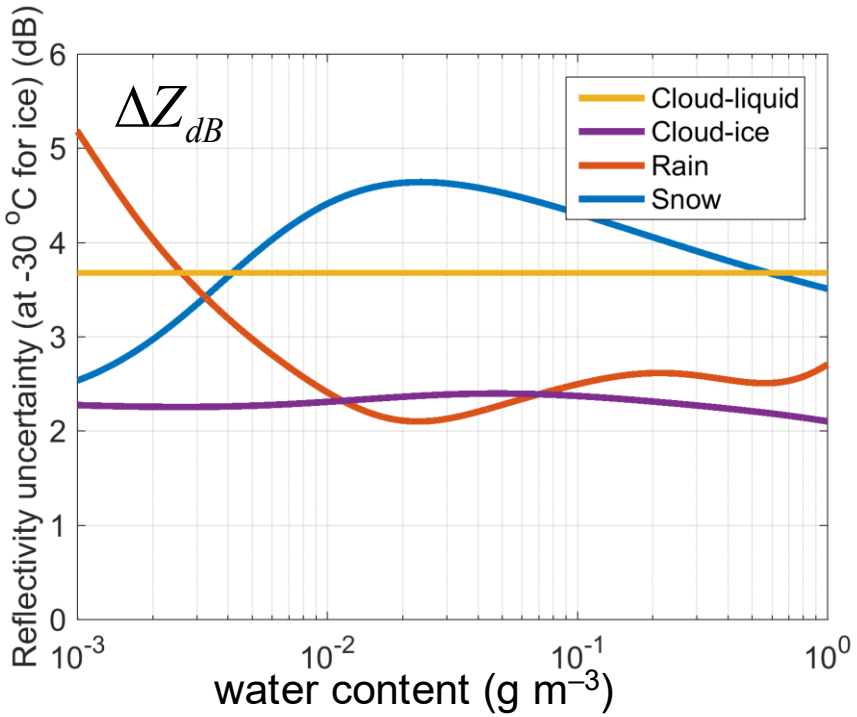

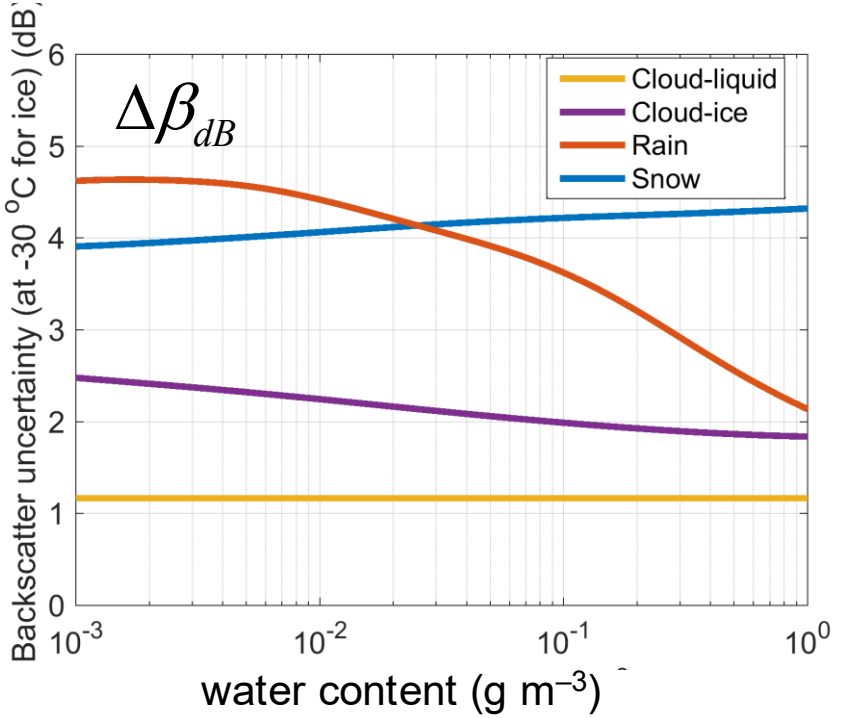

Representativity error

- Representativity error is the expected error due to mismatch between the model and the observational spatial and/or temporal scales.
- Use ‘sampling approach’ based upon the assumption that:
  - the local variability of measurements along the satellite track is representative of the gridbox variability
  - the spatial variability can be approximated using a climatological correlation

$$\sigma_{RE}^2 = E\left[(\bar{q}_s - \bar{q}_{2D})^2\right]$$

$$\sigma_{RE}^2 = \sigma_q^2 \left(\alpha_{[2D,2D]} + \alpha_{[s,s]} - 2\alpha_{[s,2D]}\right)$$

Variance of measured variable within gridbox

Scaling factor

$$\alpha_{[2D,2D]} = \frac{1}{A_{2D}^2}\int_{A_{2D}}\int_{A_{2D}} \rho(\|\mathbf{x_1} - \mathbf{x_2}\|)d\mathbf{x_1}d\mathbf{x_2}$$

$$\alpha_{[s,s]} = \frac{1}{A_s^2}\int_{A_s}\int_{A_s} \rho(\|\mathbf{x_1} - \mathbf{x_2}\|)d\mathbf{x_1}d\mathbf{x_2}$$

$$\alpha_{[s,2D]} = \frac{1}{A_s A_{2D}}\int_{A_s}\int_{A_{2D}} \rho(\|\mathbf{x_1} - \mathbf{x_2}\|)d\mathbf{x_1}d\mathbf{x_2}$$

Correlation of measured variable within gridbox

A_s – area of superob, A_{2D} – area of gridbox

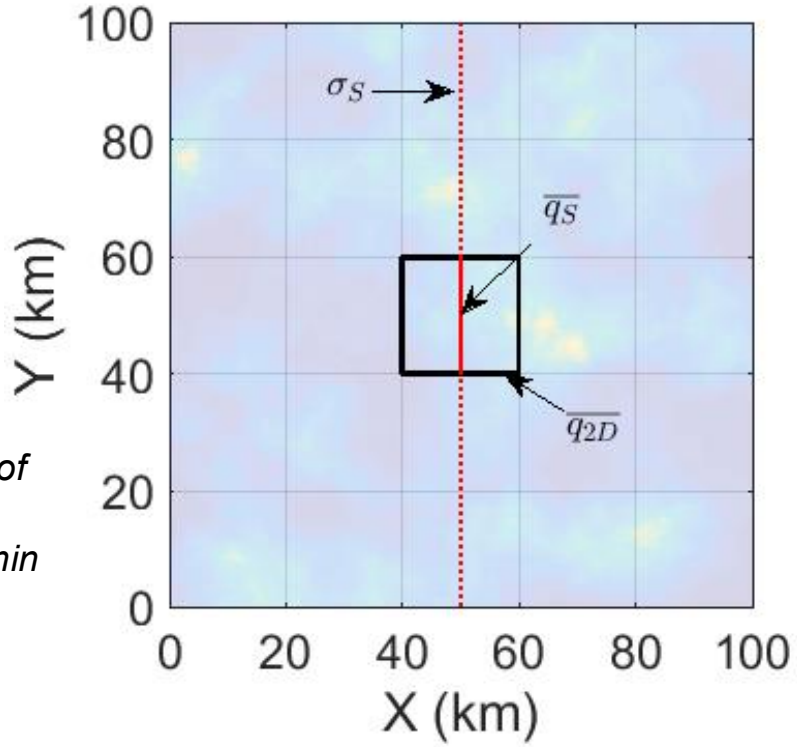

Error components for radar

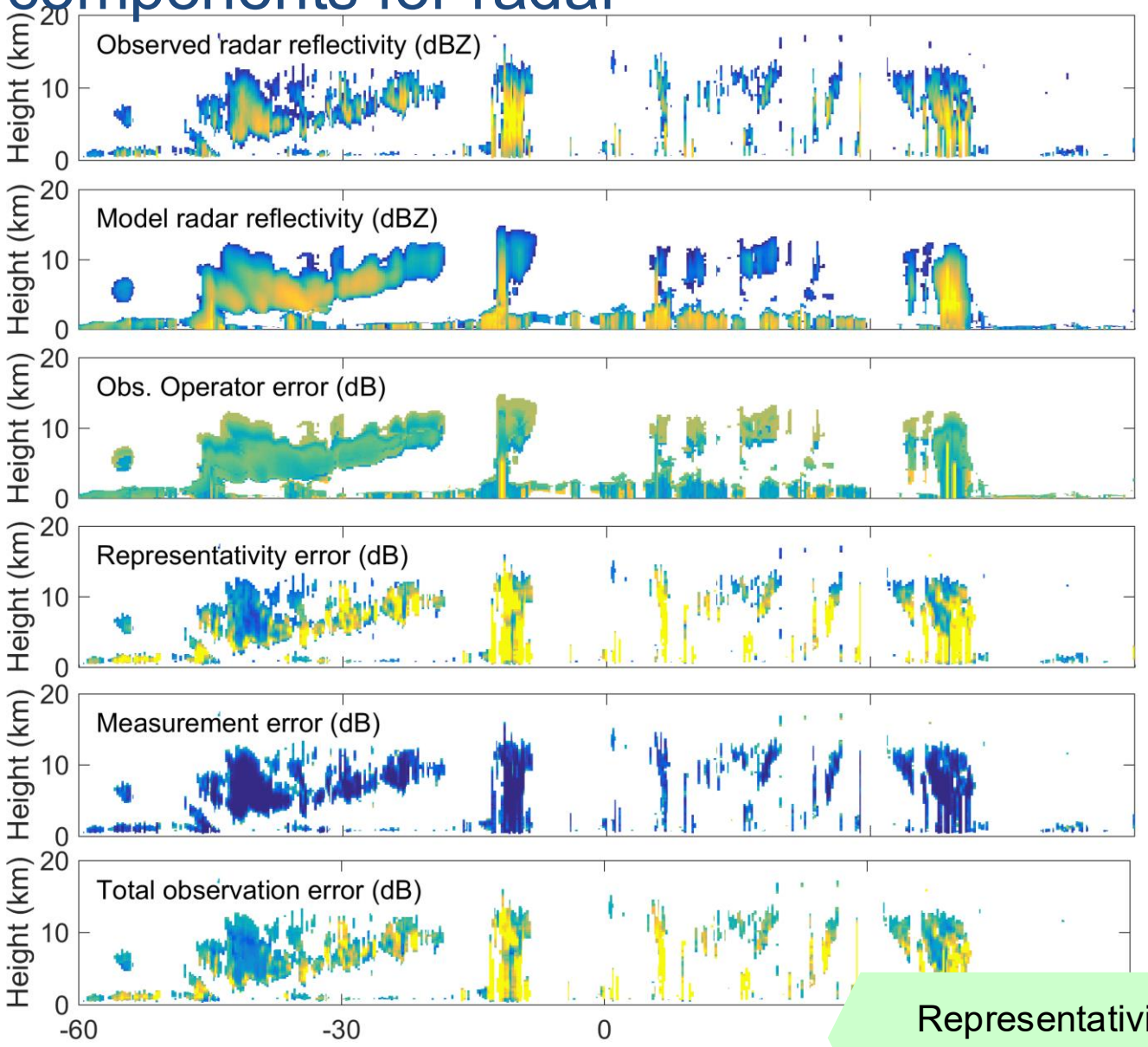

Cloudsat

FG

Obs. operator error

Repres. error

Ins. error

Total error

Representativity error dominates total error

Error components for lidar

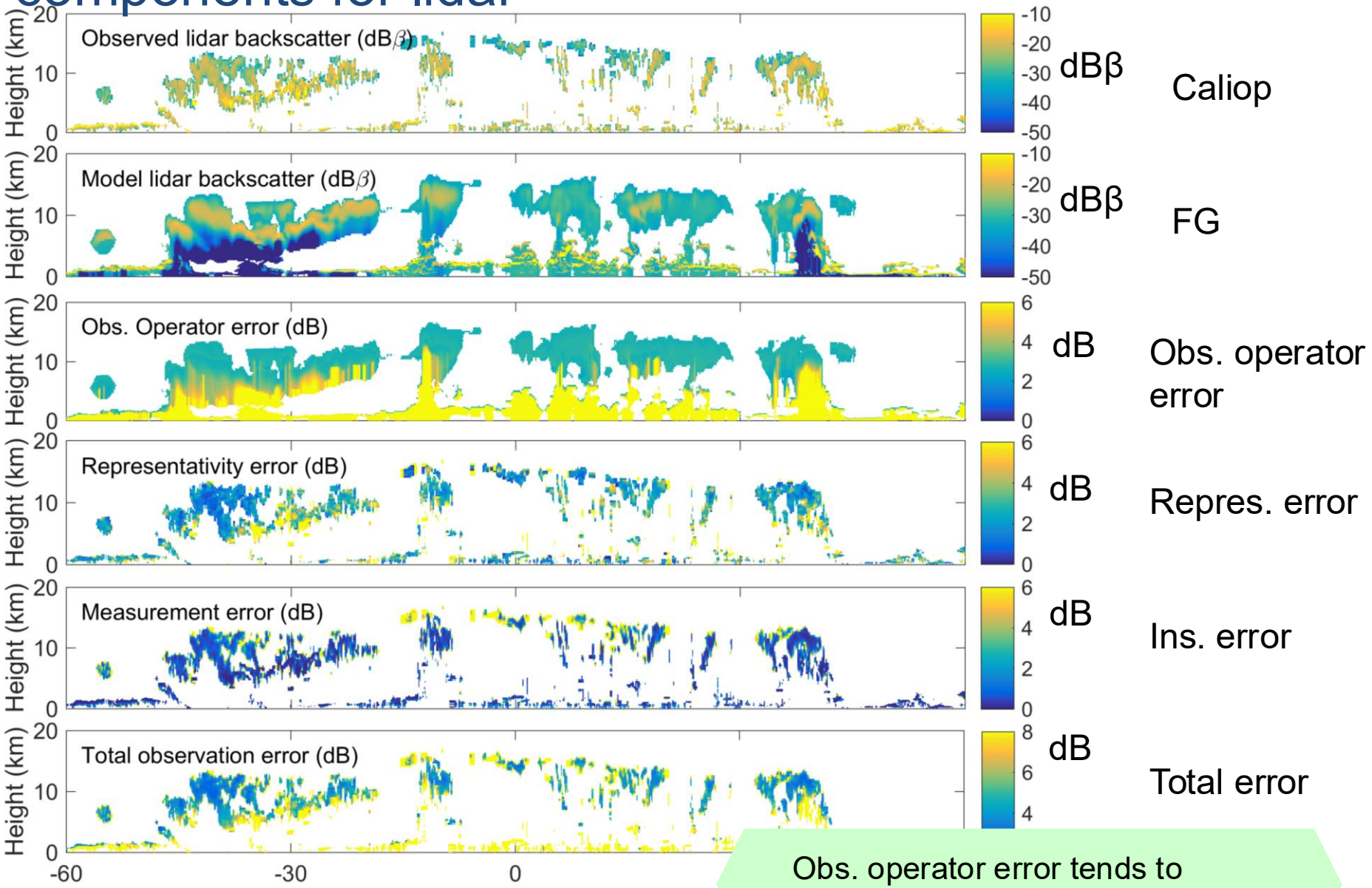

Obs. operator error tends to dominate total error

Assimilation of cloud radar and lidar observations from

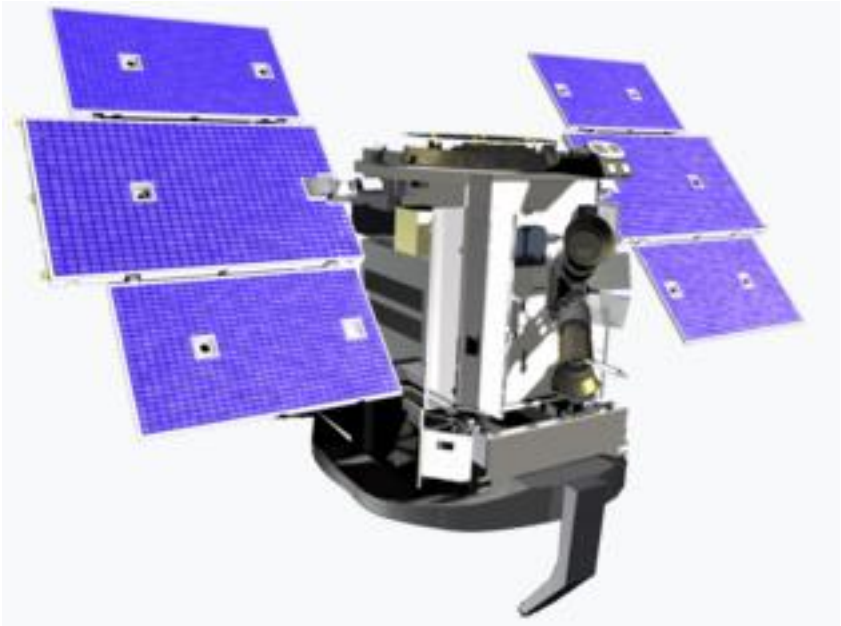

CloudSat

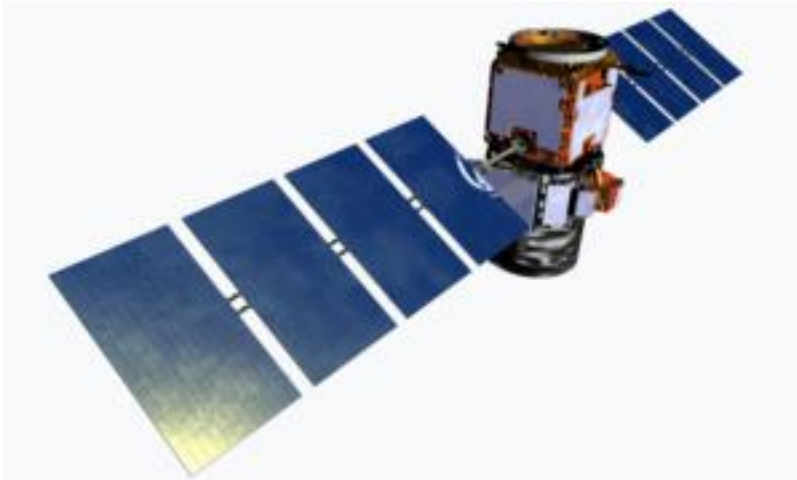

CALIPSO

Experimental setup

- 4D-Var experimentation using a horizontal resolution of TCo639 spectral truncation (corresponding to ~ 18 km on a cubic octahedral grid) and 137 vertical levels:
  - ASO: 1 August 2007 – 31 October 2007
  - DJF: 1 December 2007 – 29 February 2008
  - FMA: 1 February 2008 – 31 April 2008
  - JJA: 1 July 2008 – 31 August 2008
  - COMBI: 11-month period between 1 August 2007 – 31 August 2008
- Observations of cloud radar reflectivity (at 94 GHz, CloudSat) and cloud lidar backscatter (at 532 nm, CALIPSO) horizontally averaged to TCo159 (~70 km grid) except FMA, averaged to TL255 (~72 km grid)
- Observation errors follow 'inventory approach' (*Fielding and Stiller, 2019*), with 2x scaling
- Bias correction based on climatology of FG departures using model temperature and latitude as indicators.
- Comprehensive quality control and screening applied to observations (see *Fielding & Janisková, 2020*)

Fielding, M. D., and O. Stiller, 2019:. Characterizing the representativity error of cloud profiling observations for data assimilation. JGR, 124, 4086– 4103.

Fielding, M. D. and M. Janisková, 2020: Direct 4D-Var assimilation of space-borne cloud radar reflectivity and lidar backscatter. Part I: Observation operator and implementation. Quarterly Journal of the Royal Meteorological Society, 146(733), 3877–3899.

Impact on analysis – wind observations

Radiosonde - Global

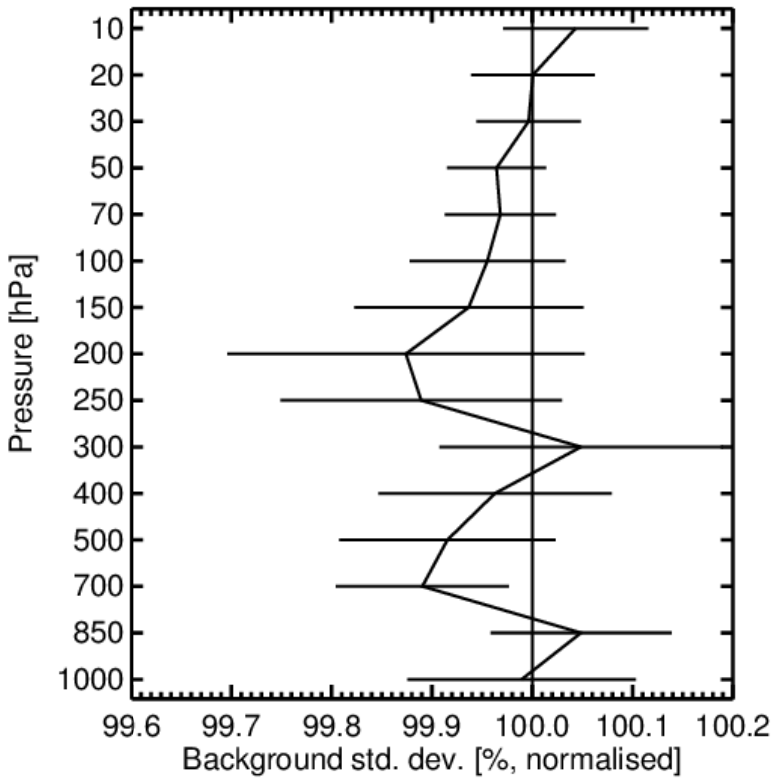

SATOB - Global

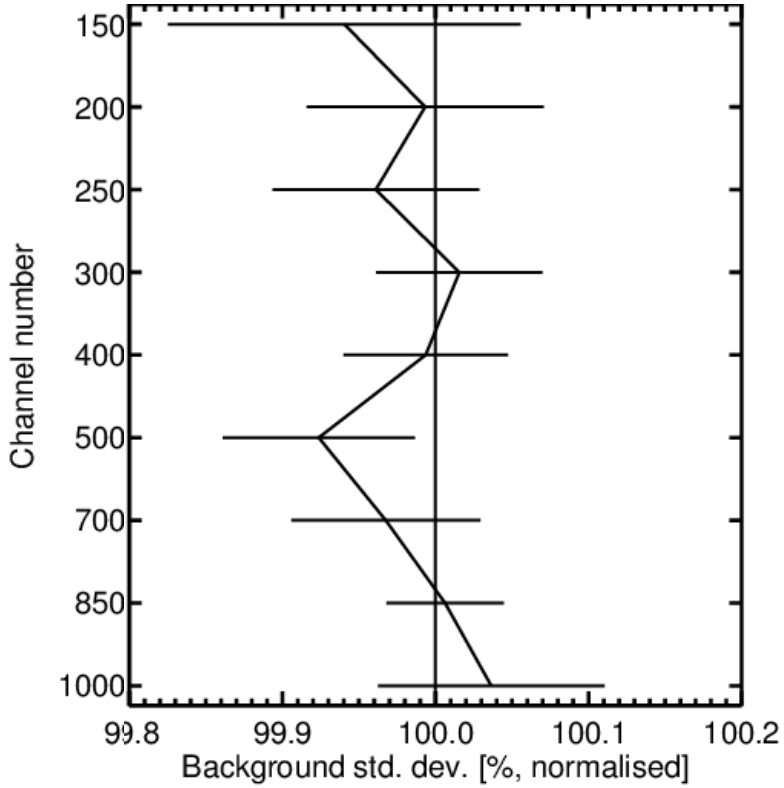

- Wind observations mostly positive, but generally not at 95% significance
- However, both radiosonde and SATOB (motion vector) observations agree on significant positive impact at 500 hPa

11-month combined period: 1 August 2007 – 31 August 2008

Impact on analysis – temperature and humidity

AMSUA - Global

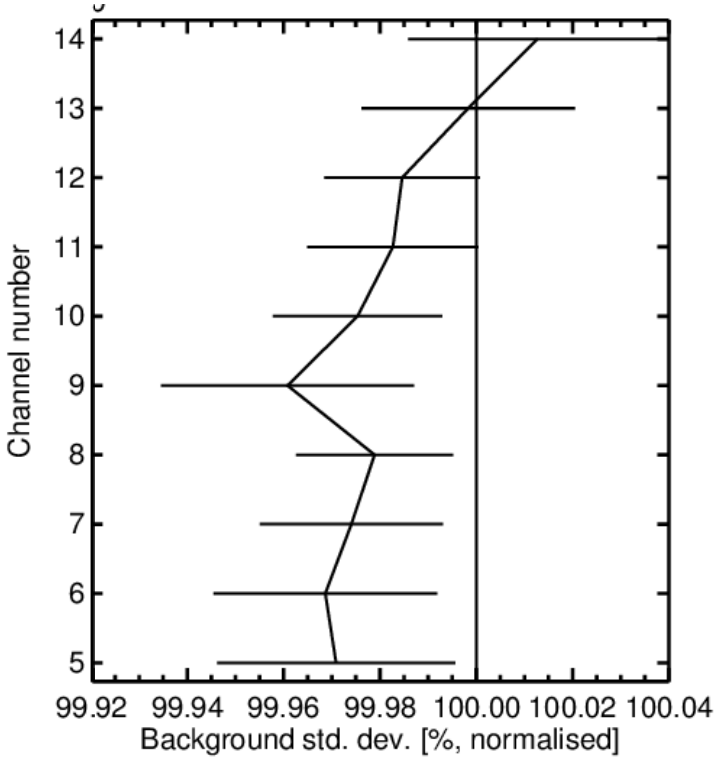

HIRS - Global

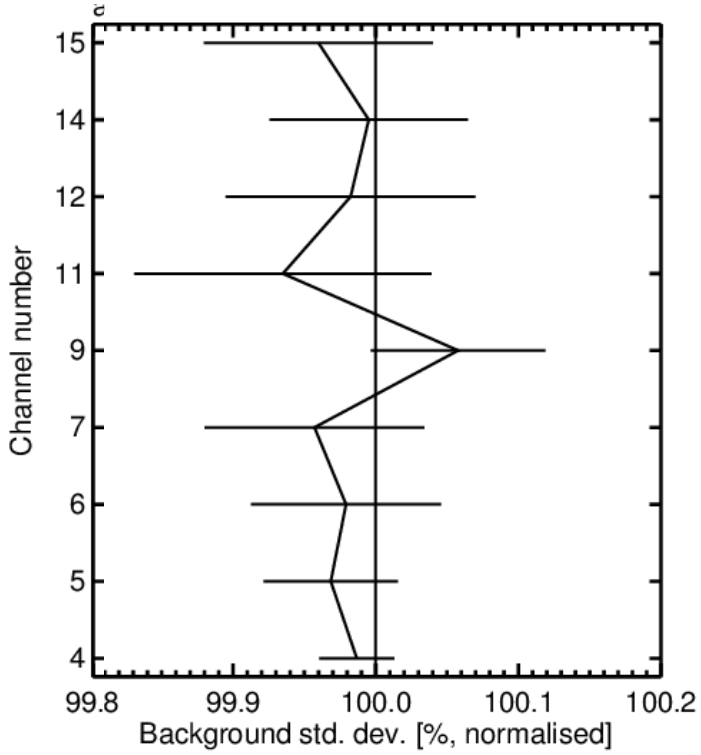

- Promising FG departure fits to AMSU-A channels (both tropospheric (i.e. channel 6) and lower stratosphere (9 and 10).
- Greatest positive impact in HIRS are in upper-tropospheric water vapour channels (11 and 12).

Improved fit to other assimilated observations

11-month combined period: 1 August 2007 – 31 August 2008

Impact on forecast – change in global average forecast skill

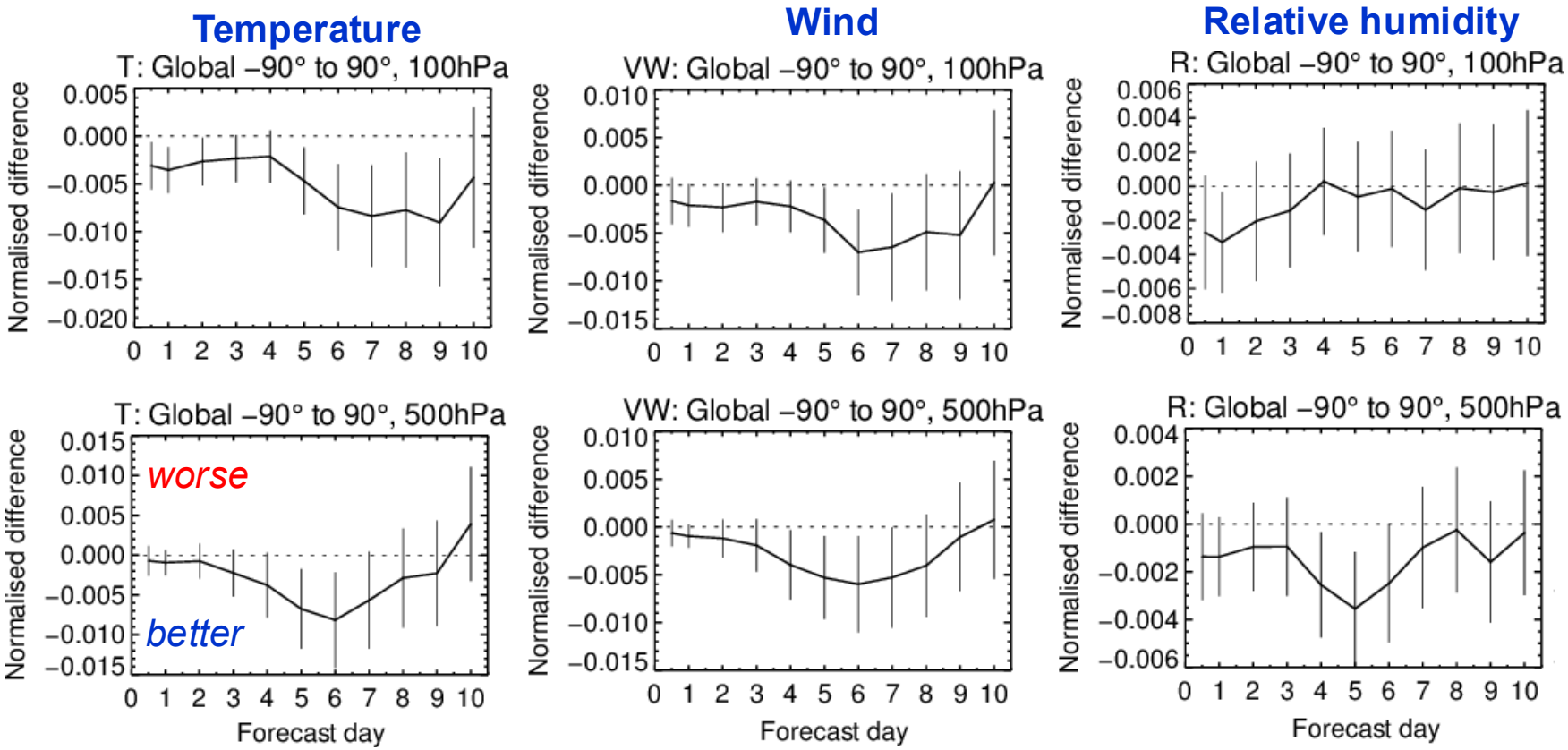

Forecast error reduction grows with forecast lead time

Shorter lived improvements in humidity?

- Assimilation of CloudSat radar reflectivity and CALIPSO lidar backscatter significantly improves temperature and winds in medium-range!

11-month combined period: 1 August 2007 – 31 August 2008

Impact on forecast – zonal means

- Some significant impacts in short-term forecast skill for Southern Ocean
- Longer-term significant impacts in extra-tropics on days 4-6, between 0.5 – 2 % improvements
- Mainly short-term improvements in upper-level tropics

➡ ***Improvements to medium-range FC skills***

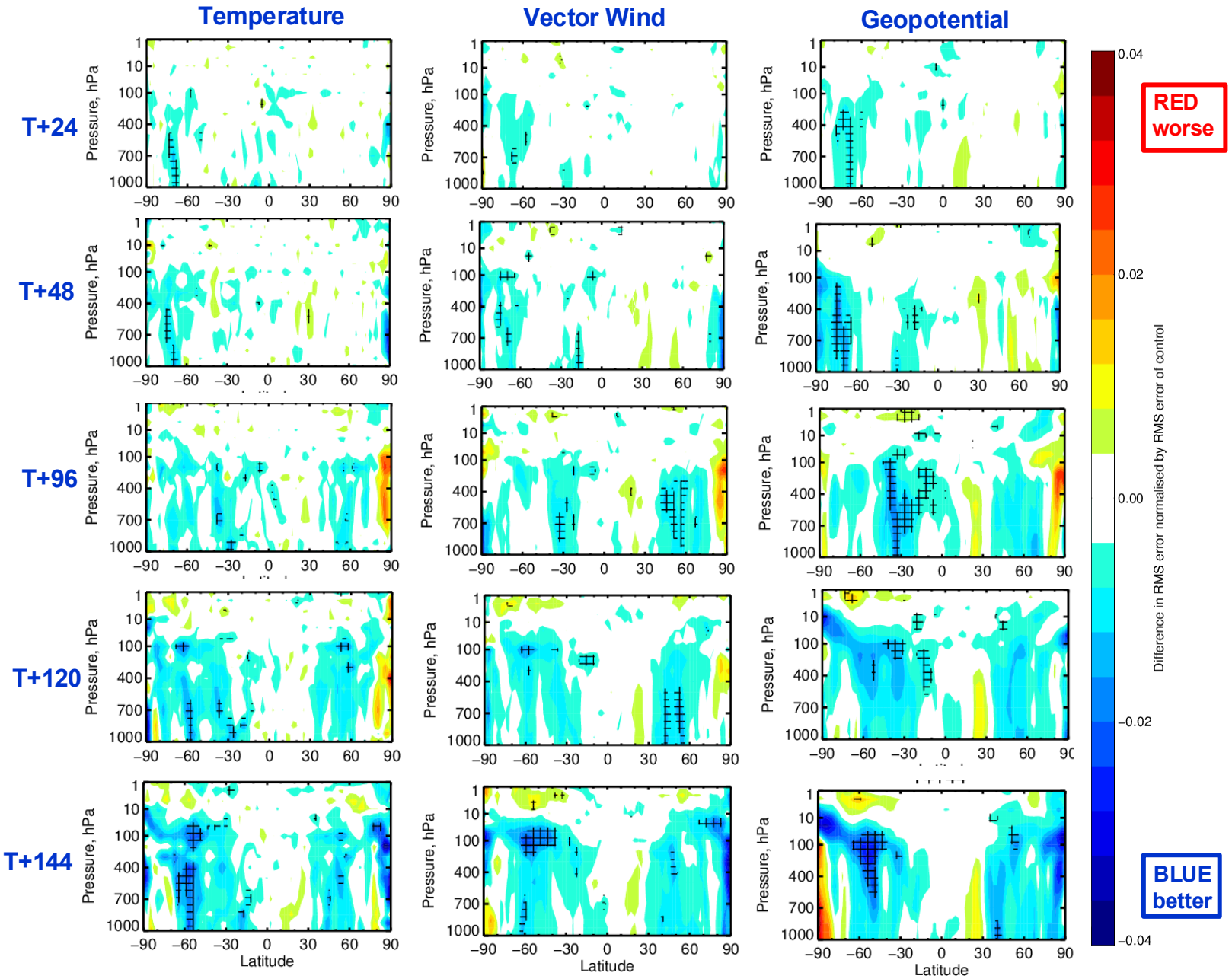

11-month combined period: 1 August 2007 – 31 August 2008

How does the impact of assimilating CloudSat and CALIPSO change over time?

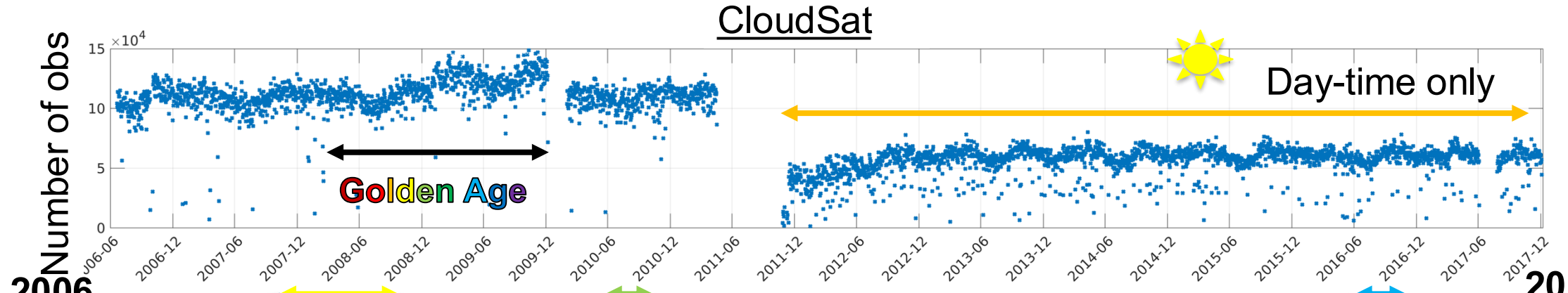

2006 — **2008** — **2010** — **2016** — **2018**

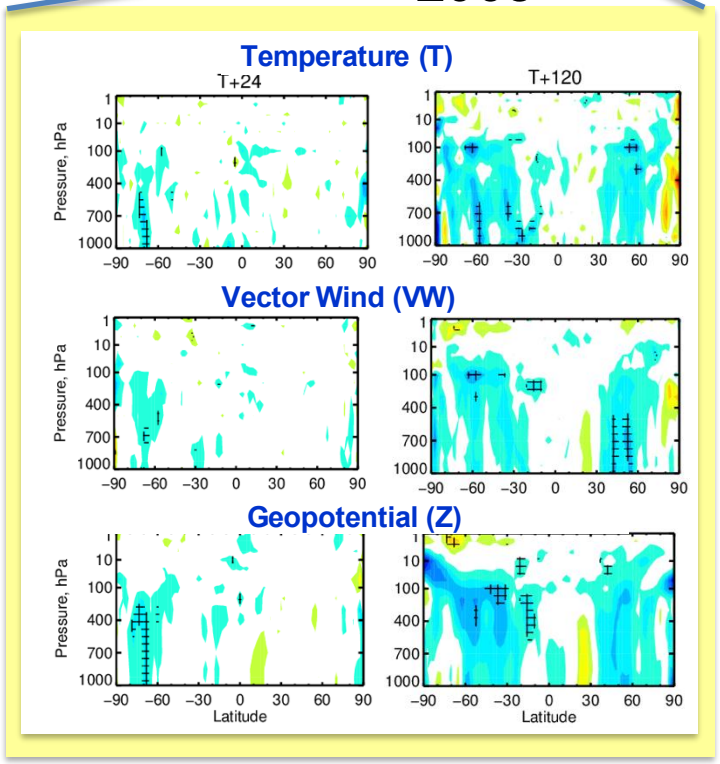

11-month period

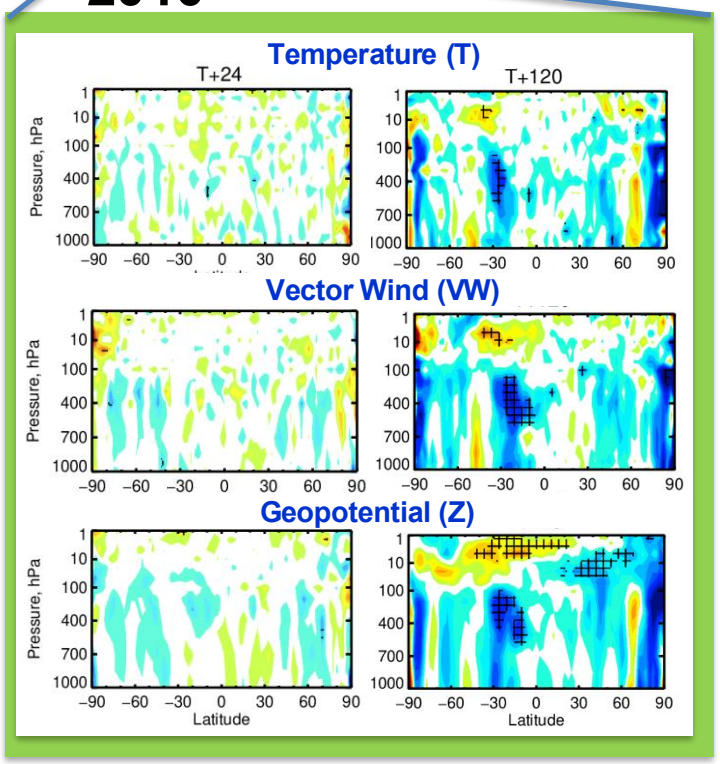

3-month period

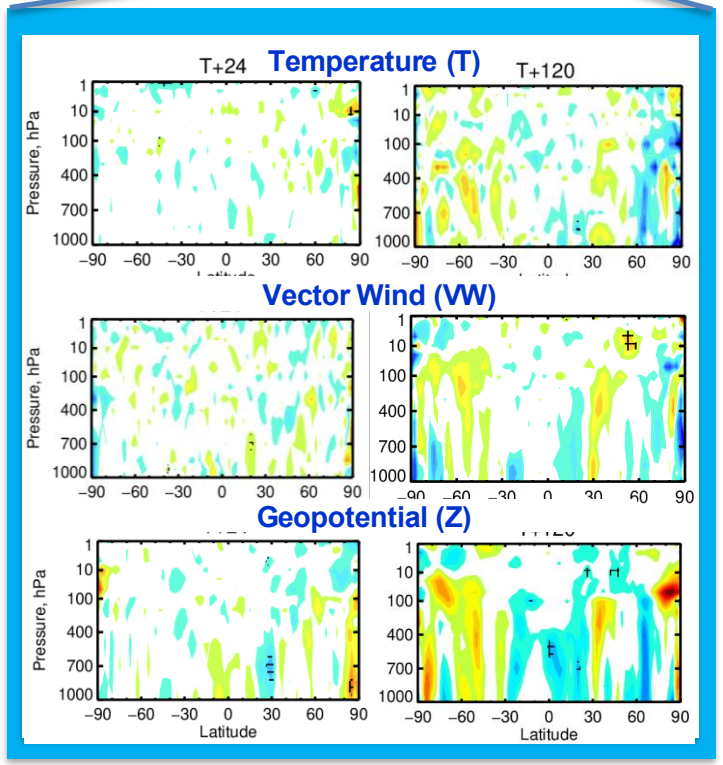

3-month period

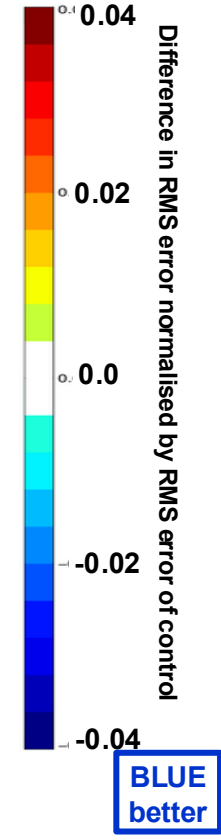

Fielding, M. D., 2023

EarthCARE launch!
29 May 2024
Vandenberg, California,

esa

First operational monitoring! 03 February 2026 – 0300 UTC

- Operational monitoring of EarthCARE activated for 06bc
- Storm Leonardo first sampled at 03:03 UTC

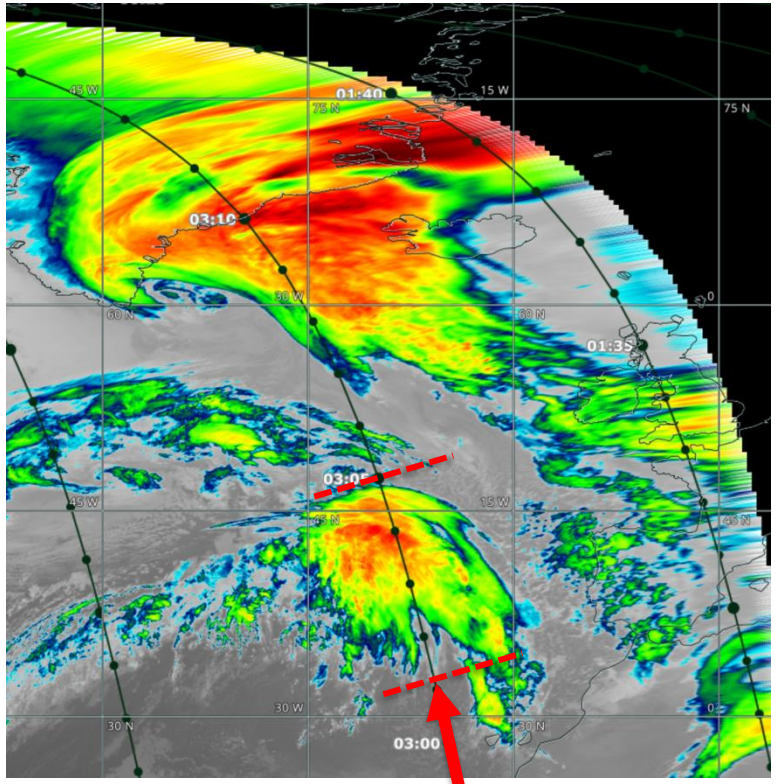

GOES-E IR

Too much precipitating ice

Strongest precipitation further North

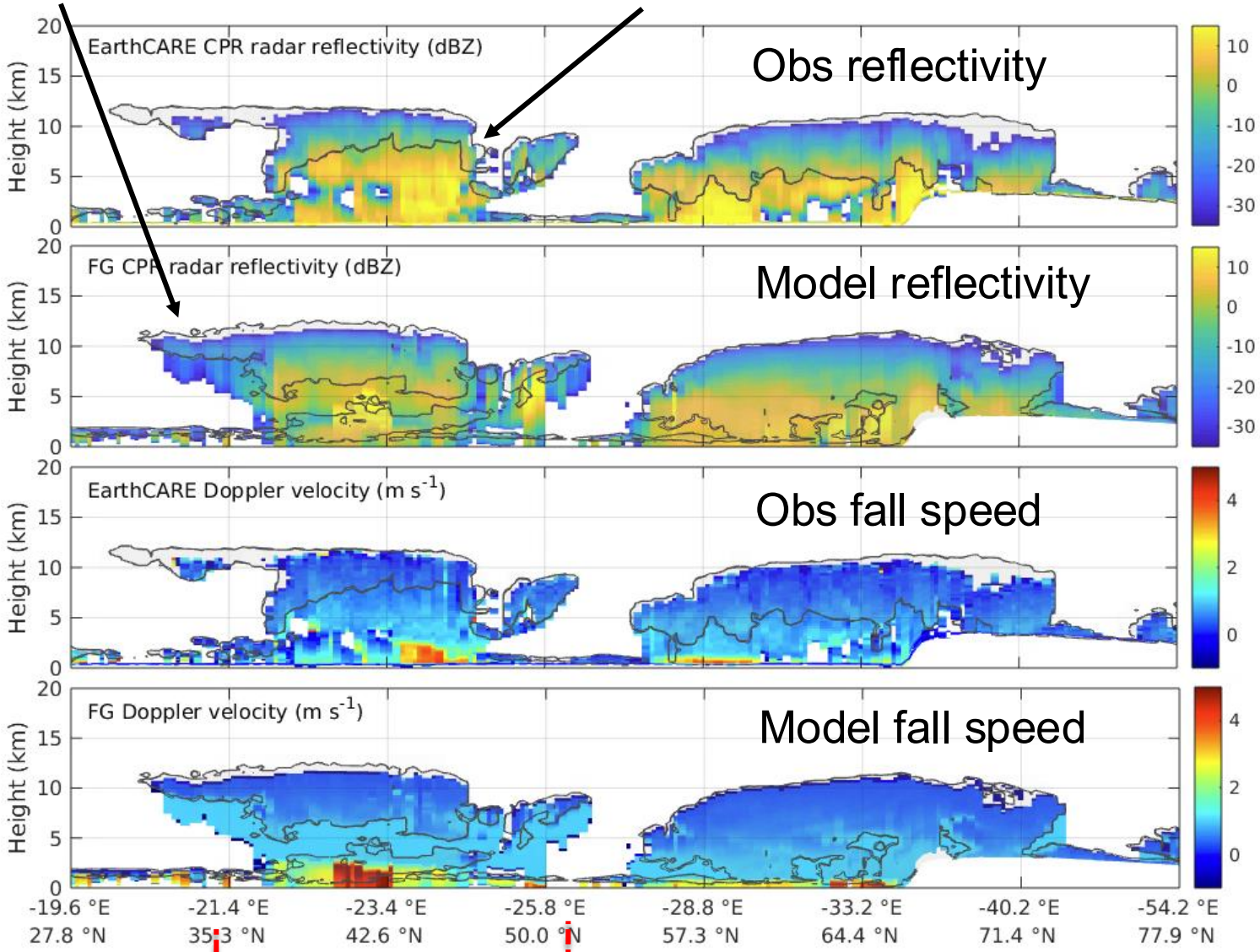

4D-Var observing system experiment setup

- Integrated Forecast System (IFS) CY49R1 4D-Var experimentation with forecasts using TCo639 grid (~18 km) for 5-month period between 01 December 2024 – 06 April 2025.
- Assimilate CPR L1B radar reflectivity and/or ATLID L2 extinction (at 355 nm) superobbed to (O320-> ~38 km) and model vertical levels, in addition to current observing system.
- Verification of **analysis** skill evaluated by comparing:
  - analysis to independent observations (e.g., EarthCARE BBR fluxes).
- Verification of **forecast** skill evaluated by comparing:
  - Short-term forecast fits to other observations in observing system (background departures)
  - Forecasts of model variables (e.g., T, RH, winds) against own analysis at variety of lead times.
  - L3 gridded observational products (e.g., CERES TOA radiative fluxes), to model variables at different lead times.

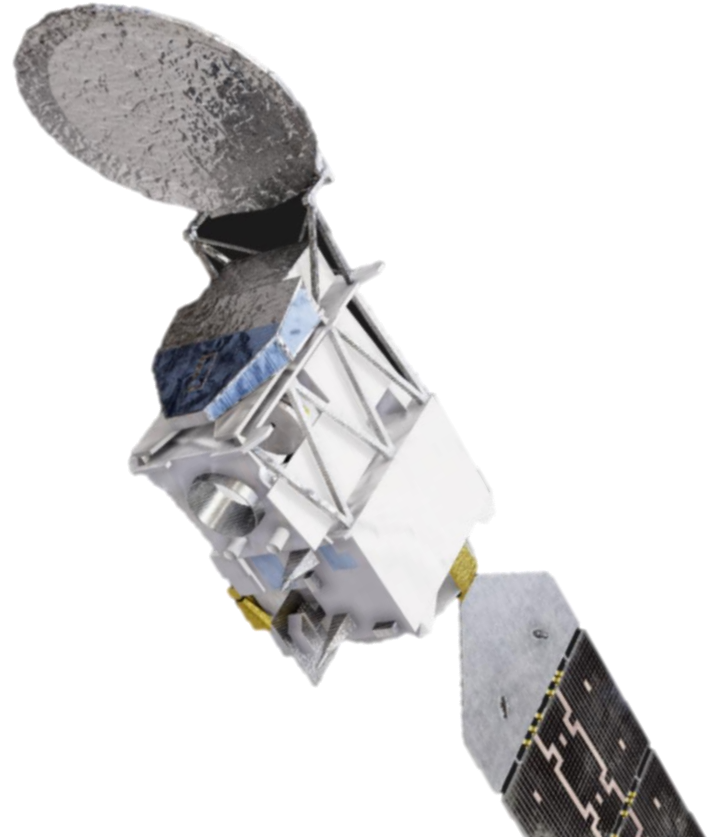

Verification against conventional observations – CPR only

- Assimilating radar reflectivity improves short-term forecasts (background departures) of wind and humidity

Profiler and radiosonde **Wind**

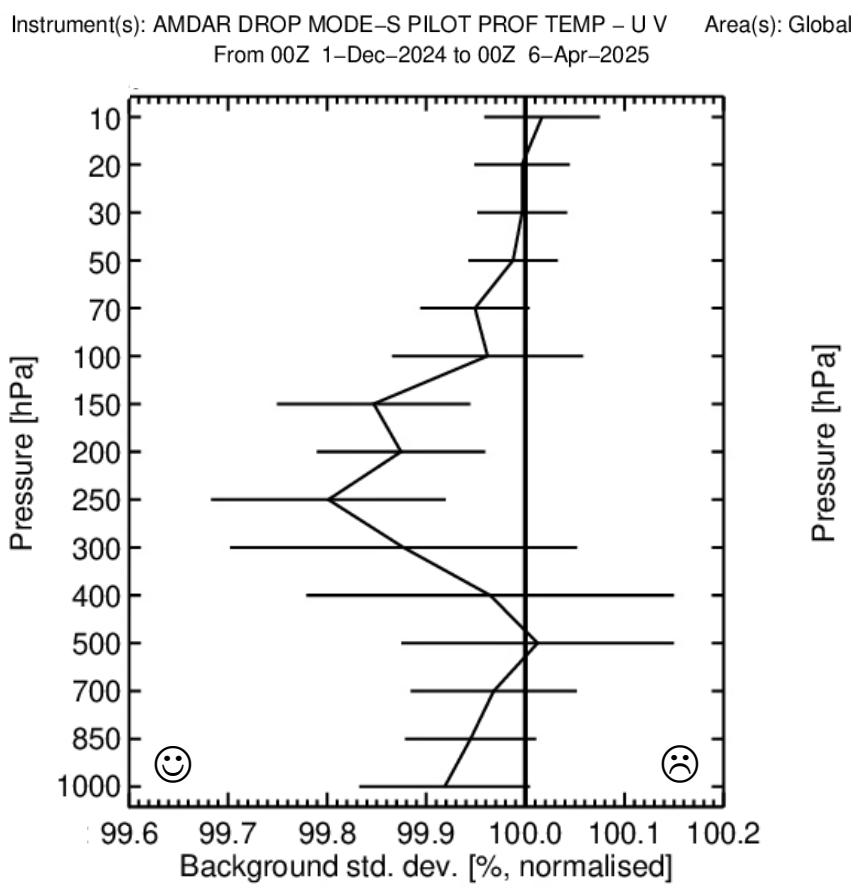

Radiosonde **Temperature**

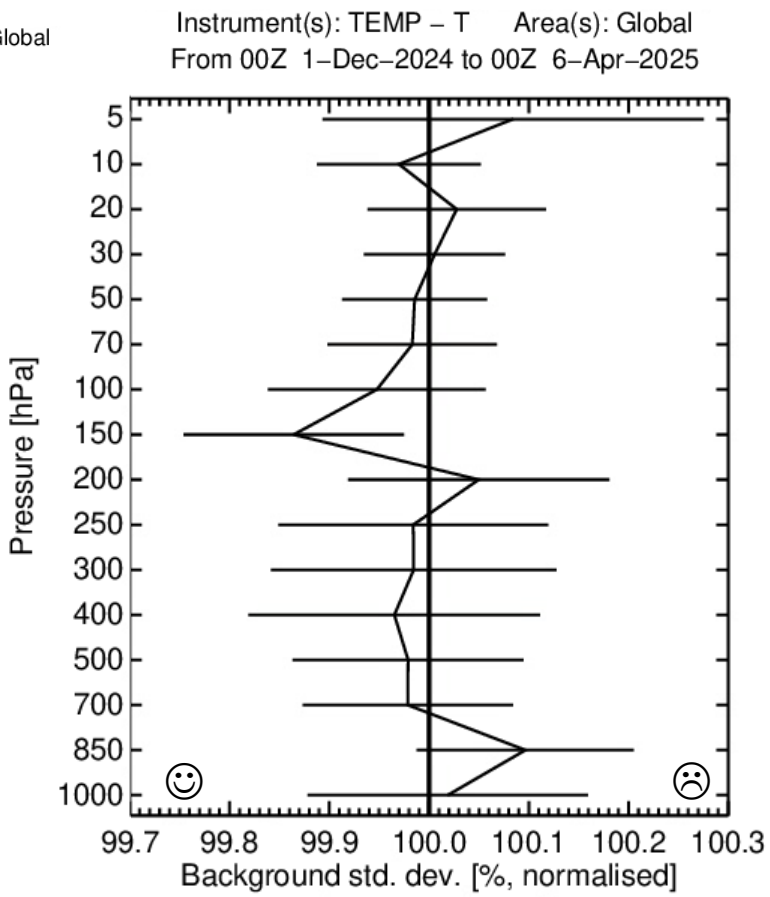

Radiosonde **Humidity**

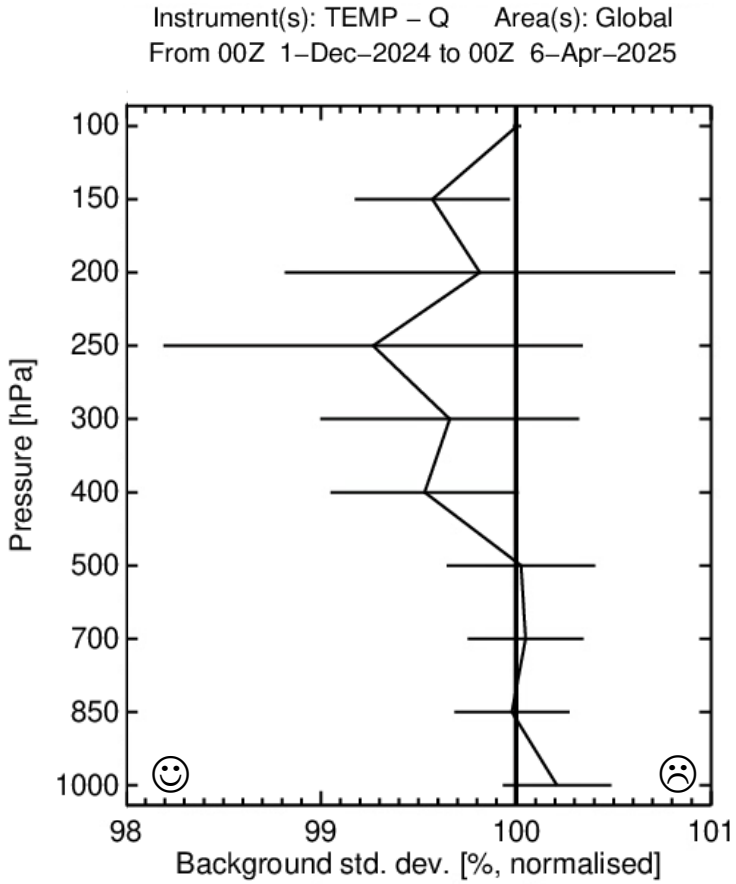

ECMWF

Assimilating EarthCARE improves fit to TOA radiation observations

Along track impact on analysis

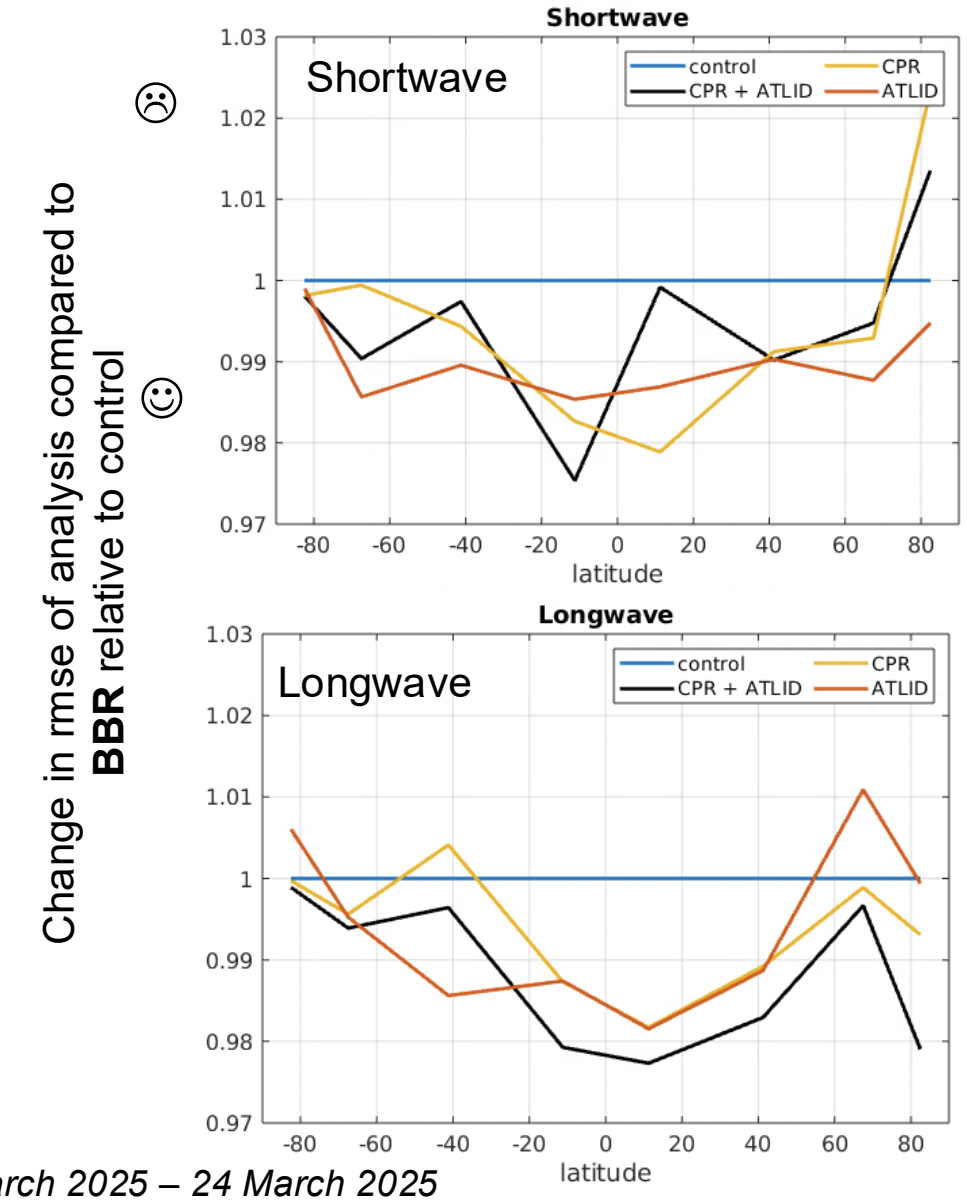

17 March 2025 – 24 March 2025

Global impact on day 1 forecast

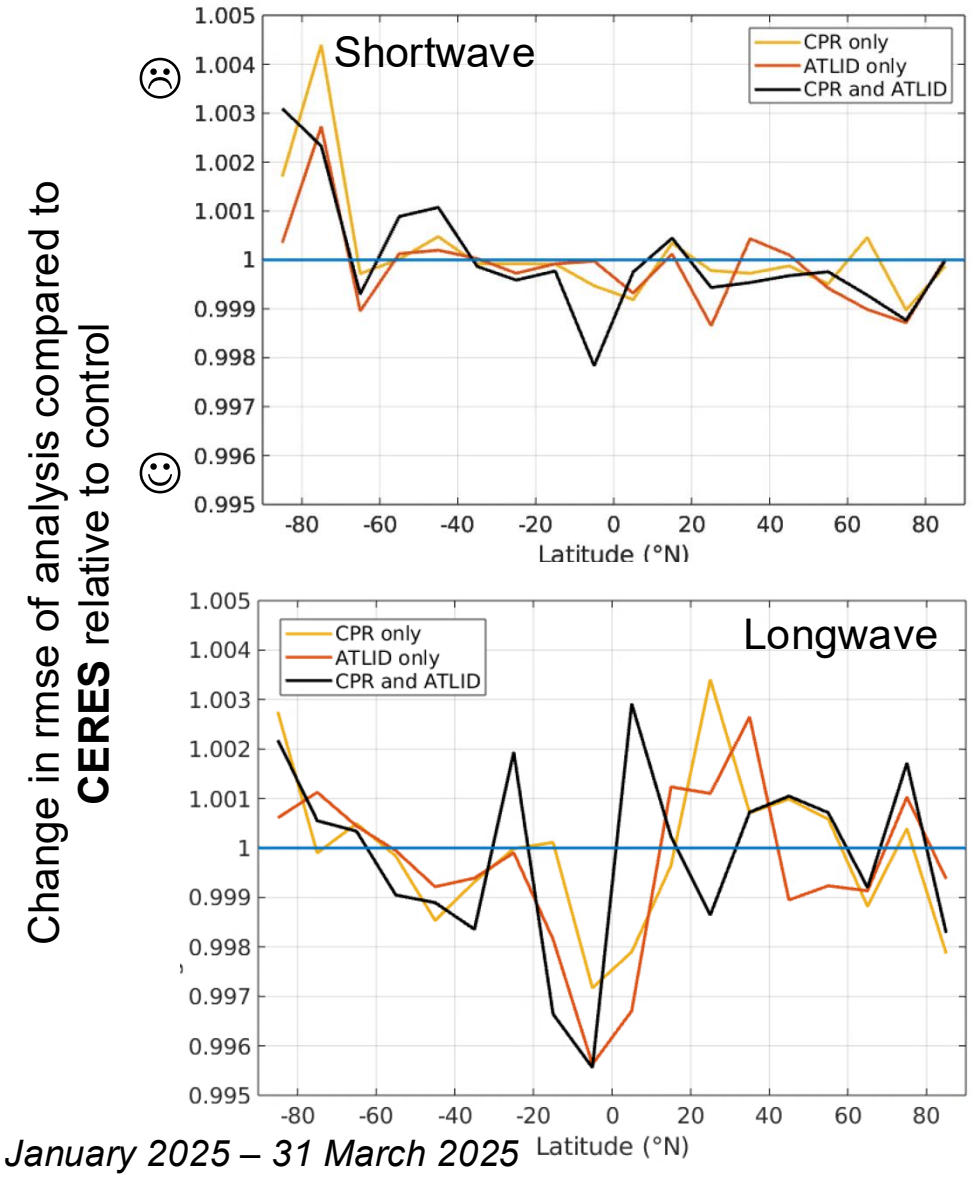

1 January 2025 – 31 March 2025

Assimilating radar reflectivity improves medium-range forecasts of winds in the extra-tropics

- Improvements of 0.5 - 1 % at day 3-4 in cloudy regions, consistent with CloudSat assimilation experiments.
- Smaller, positive impact on temperature scores.

EarthCARE hydrometeor fraction

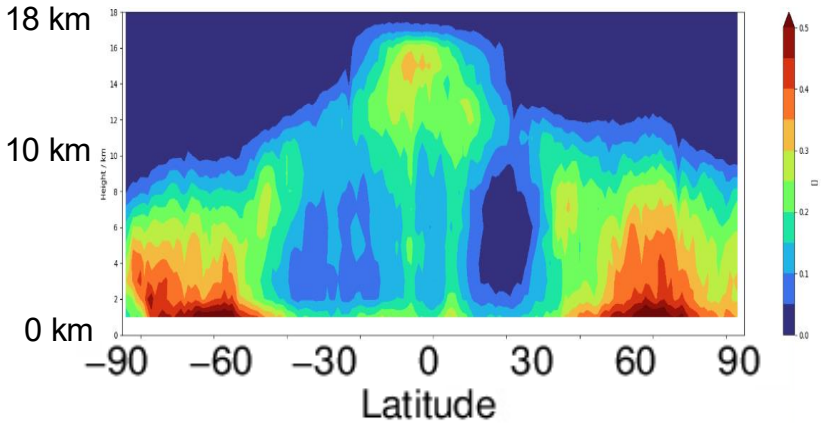

CPR-only OSE (20241201 to 20250406)

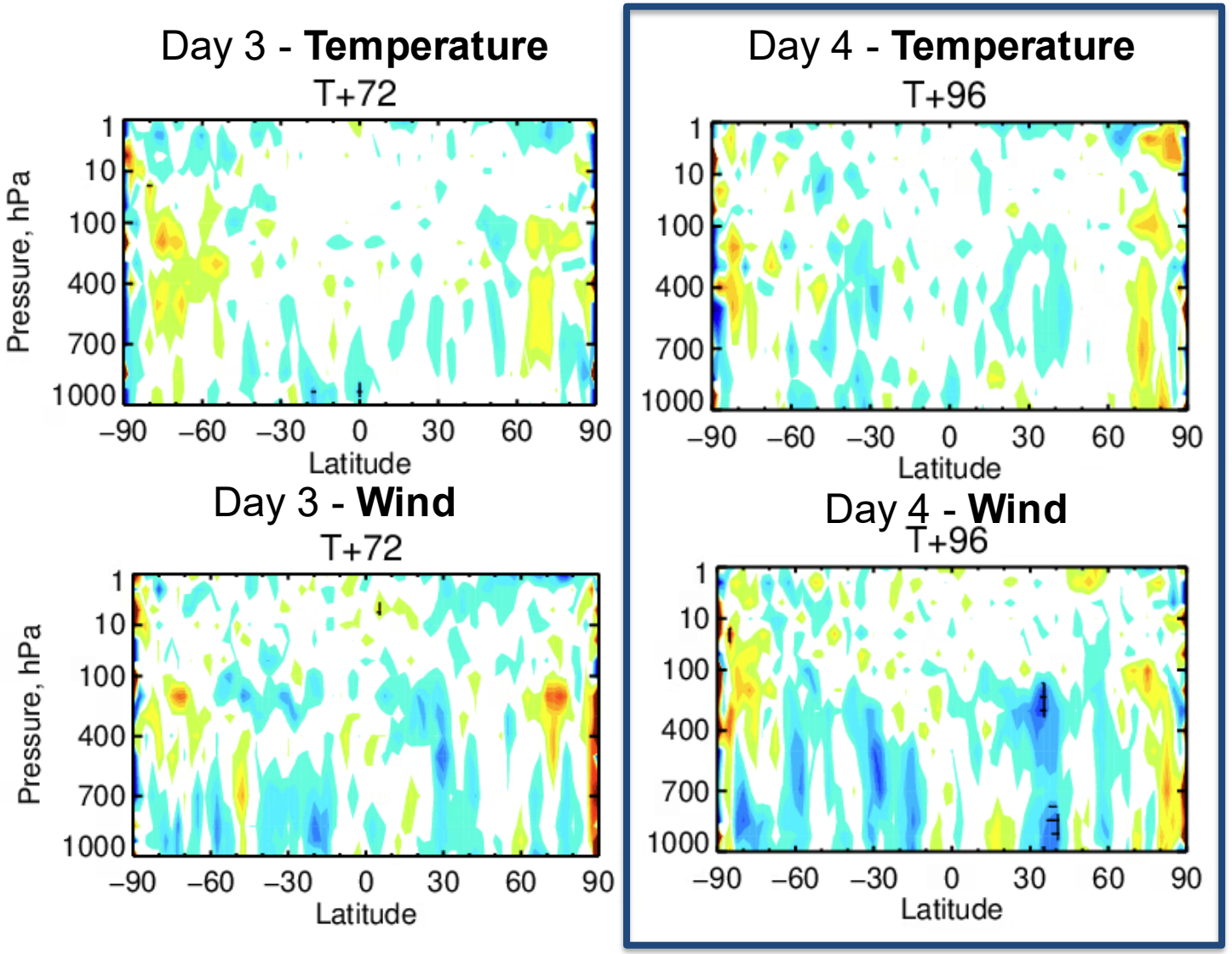

EarthCARE CPR impact relative to other observations (Kamil Mroz)

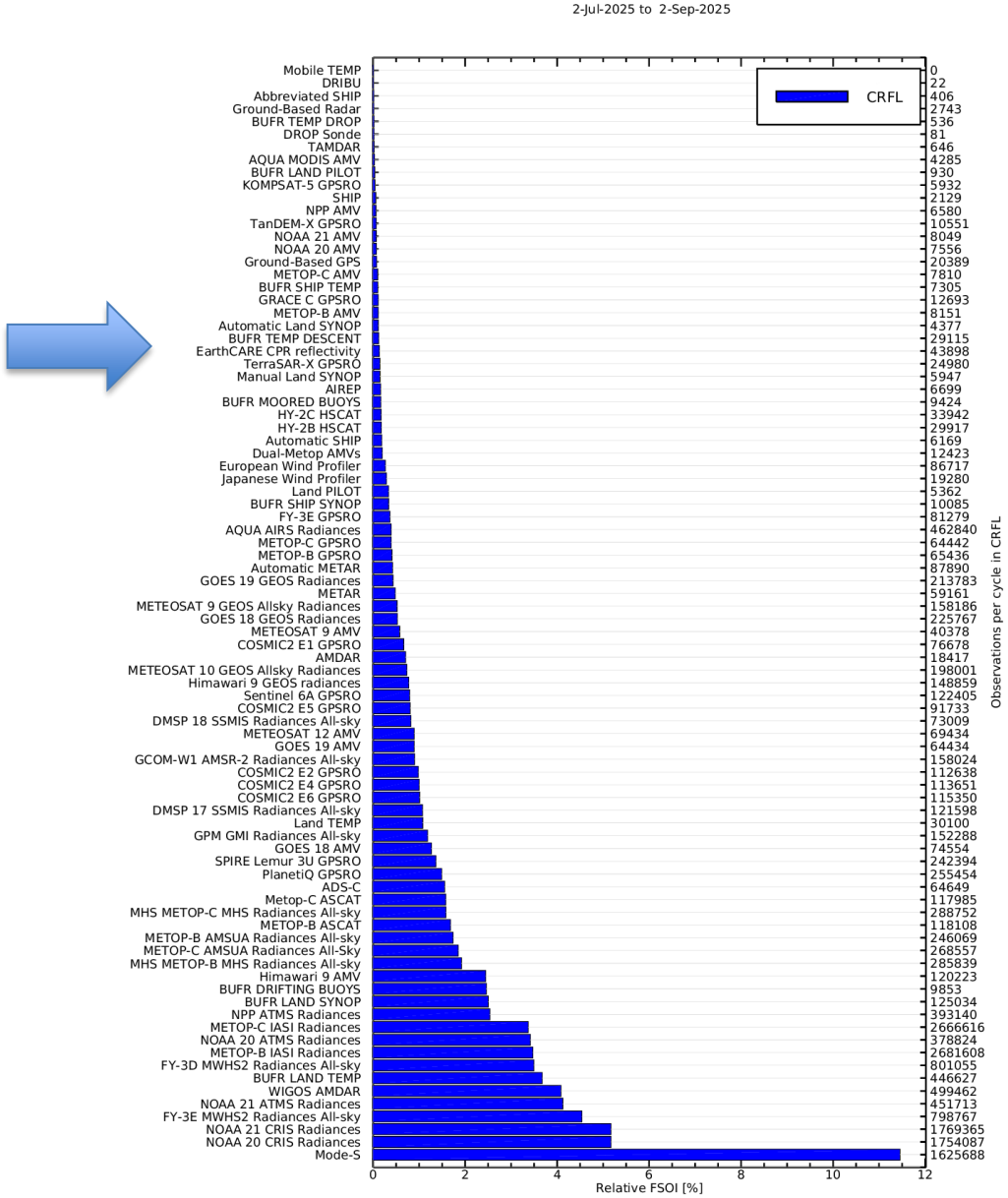

- Forecast sensitivity to observations impact (FSOI) scores use an adjoint technique to assess the impact of different observation types on forecast error.
- Analysis increments from **EarthCARE CPR observations contribute 0.15 %** to the total reduction in 24 hour forecast error for each 4D-Var cycle.
- FSOI scores can be misleading due to correlations between observation types, non-linearities and neglect humidity information (when using dry energy norm).

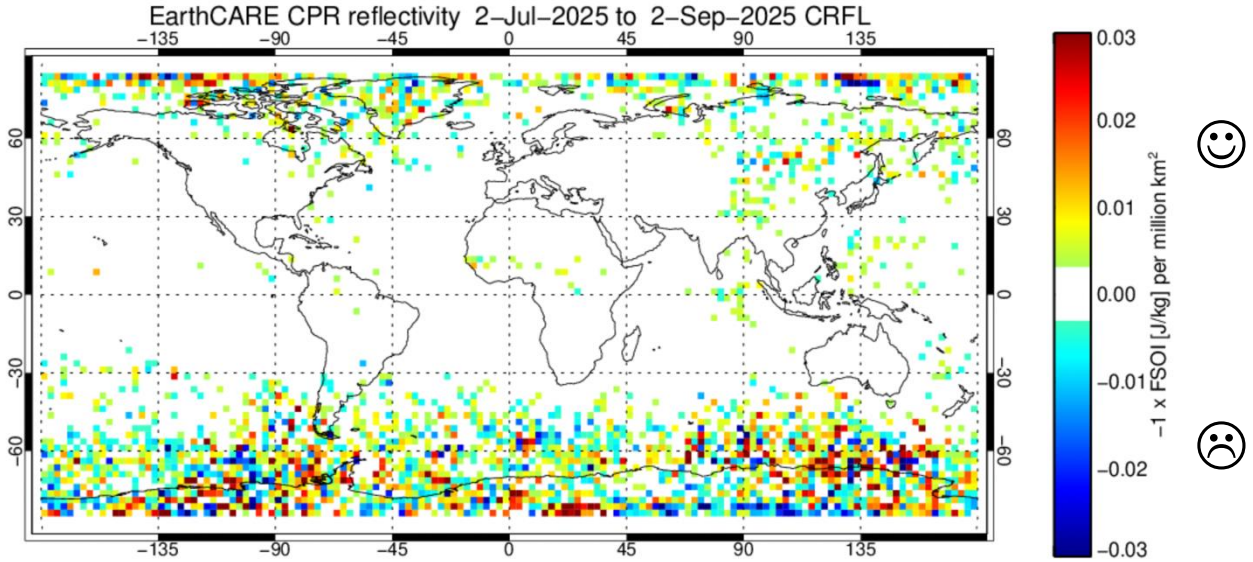

A few open questions

- What are the relative impacts of CPR and ATLID?
- Can we assimilate radar and lidar in ‘clear-sky’?
- Are we prepared for future missions?
  - What would be the impact of a conically scanning w-band radar such as WIVERN?
  - What would be the impact of assimilating GPM-DPR style observations?
- How do active observations interact with all-sky microwave observations?
- How can EarthCARE help with model evaluation as simulations and assimilation move towards convective scale resolution?

Model evaluation using EarthCARE

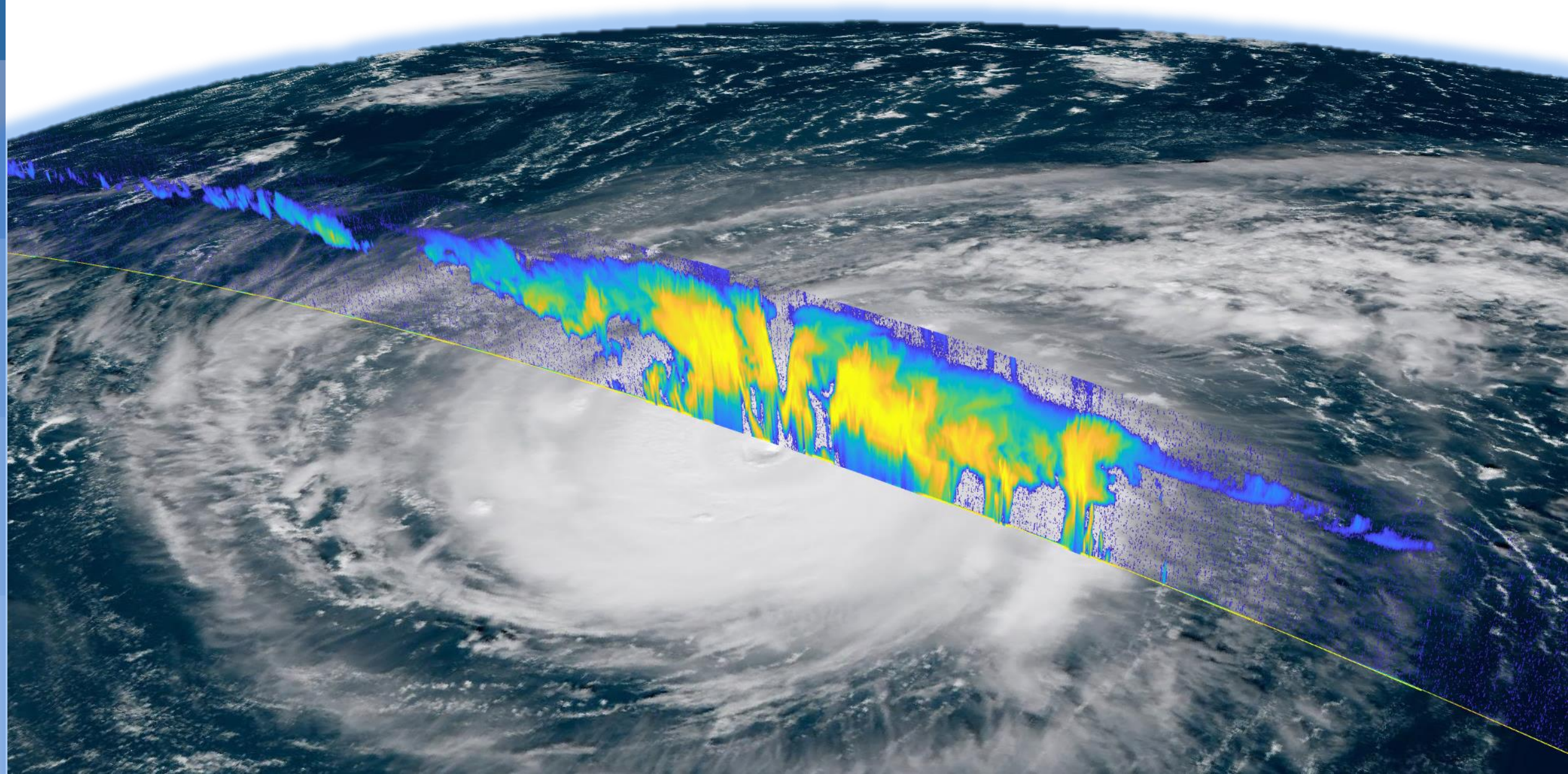

Cirrus bias in the IFS?

Hydrometeor fraction zonal cross-section

EarthCARE (ATLID + CPR detections)

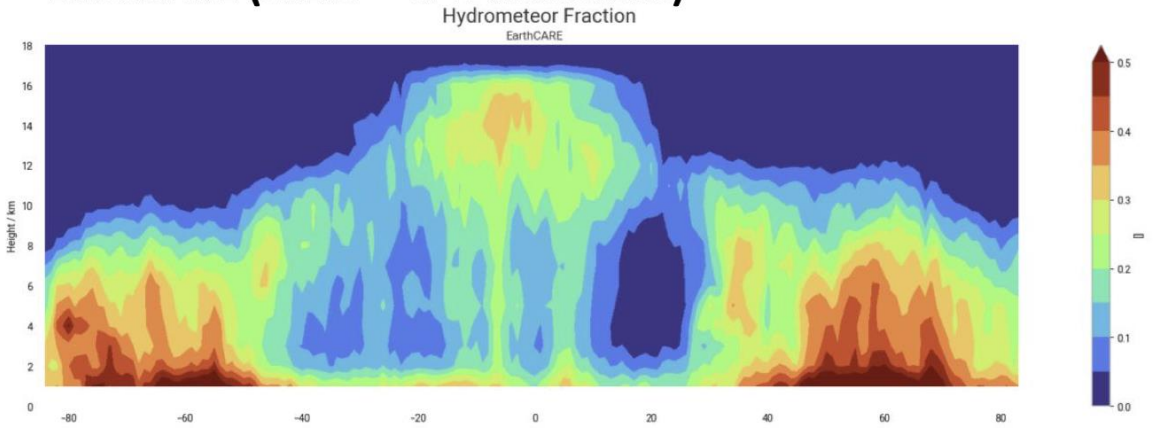

Current IFS – EarthCARE

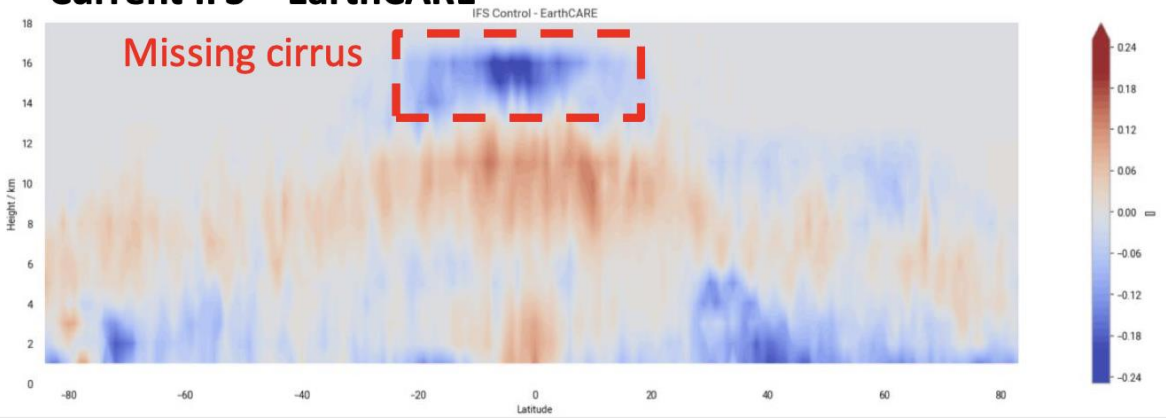

- ECMWF is missing tropical thin, high (and therefore cold) cirrus detected by EarthCARE, particularly from convective outflows
- What process is missing? What is the radiative effect?

ATLID (Tropics ocean only)

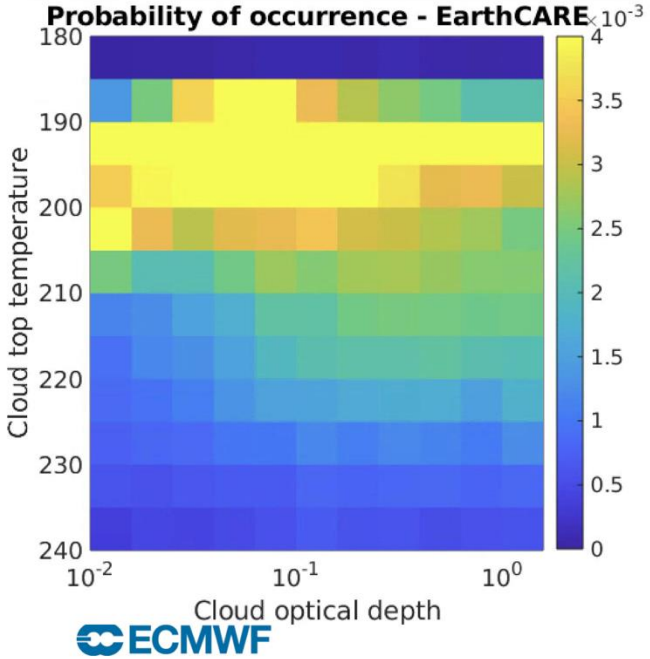

IFS (Tropics ocean only)

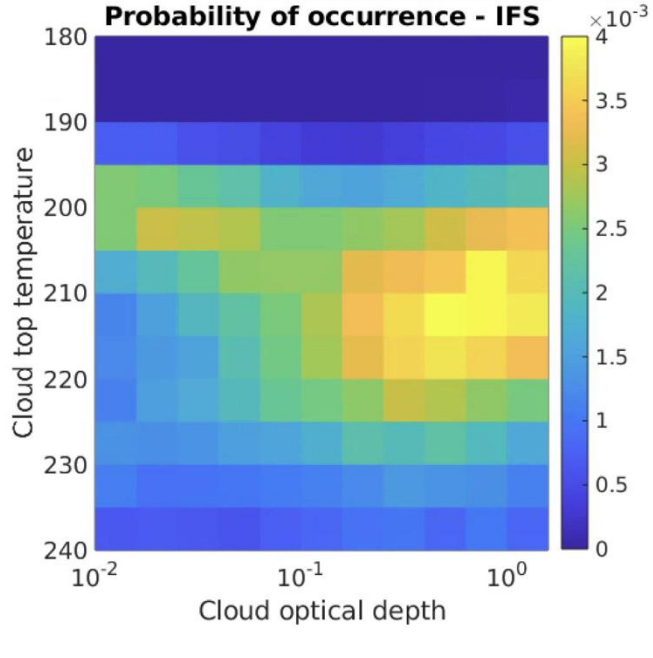

ECMWF

ATLID is a gamechanger for testing aerosols in models!

Peter Hill (ECMWF)

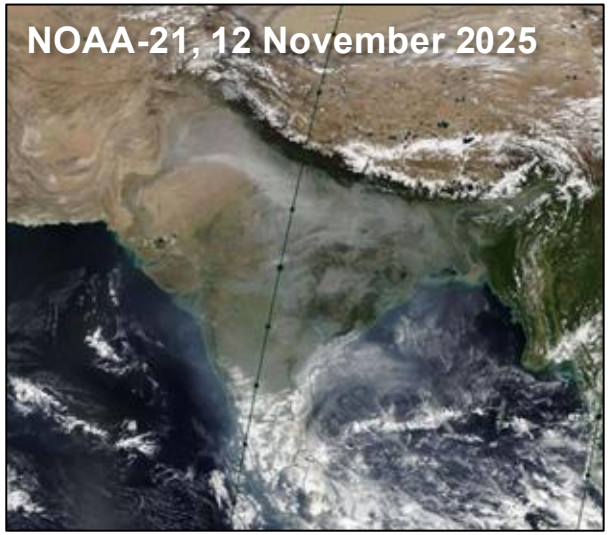

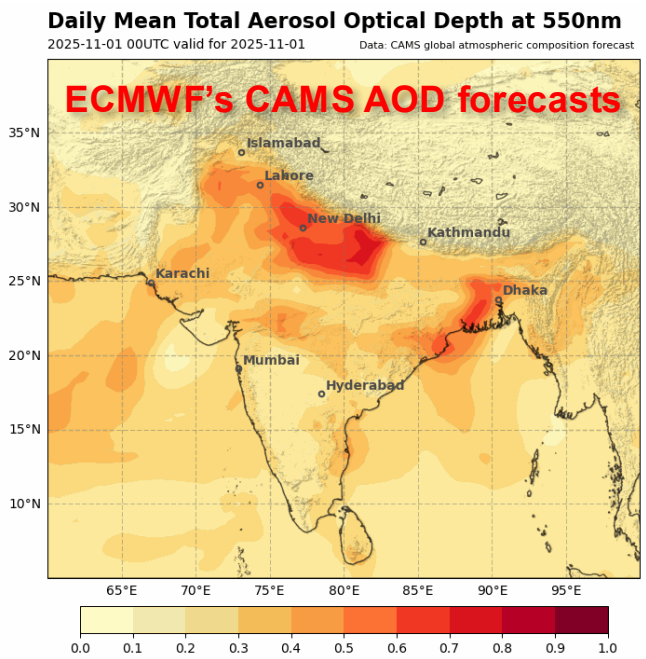

- Evaluation of CAMS aerosol 355-nm extinction profiles using EarthCARE

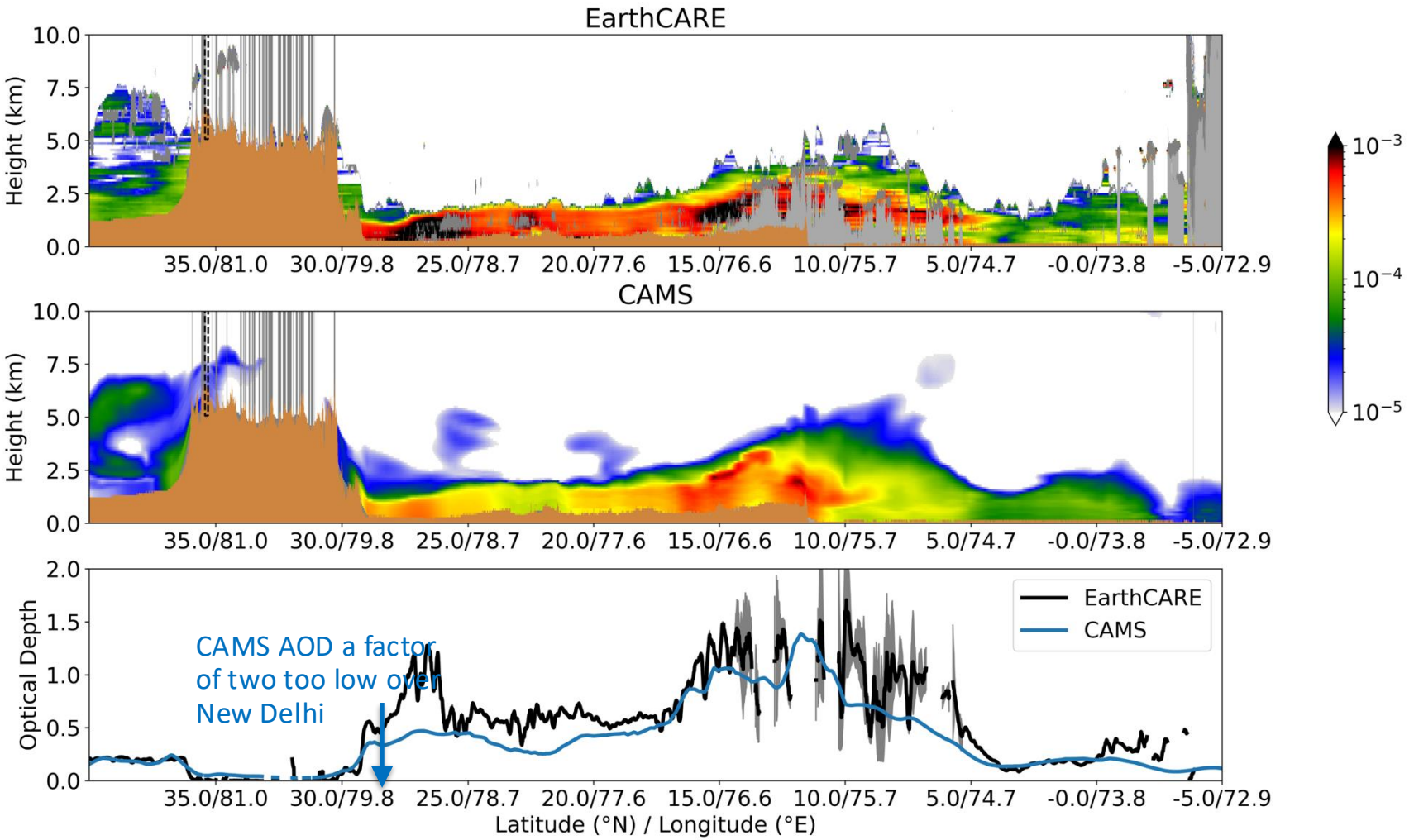

The day EarthCARE hit Hurricane Humberto

28 Sept 2025

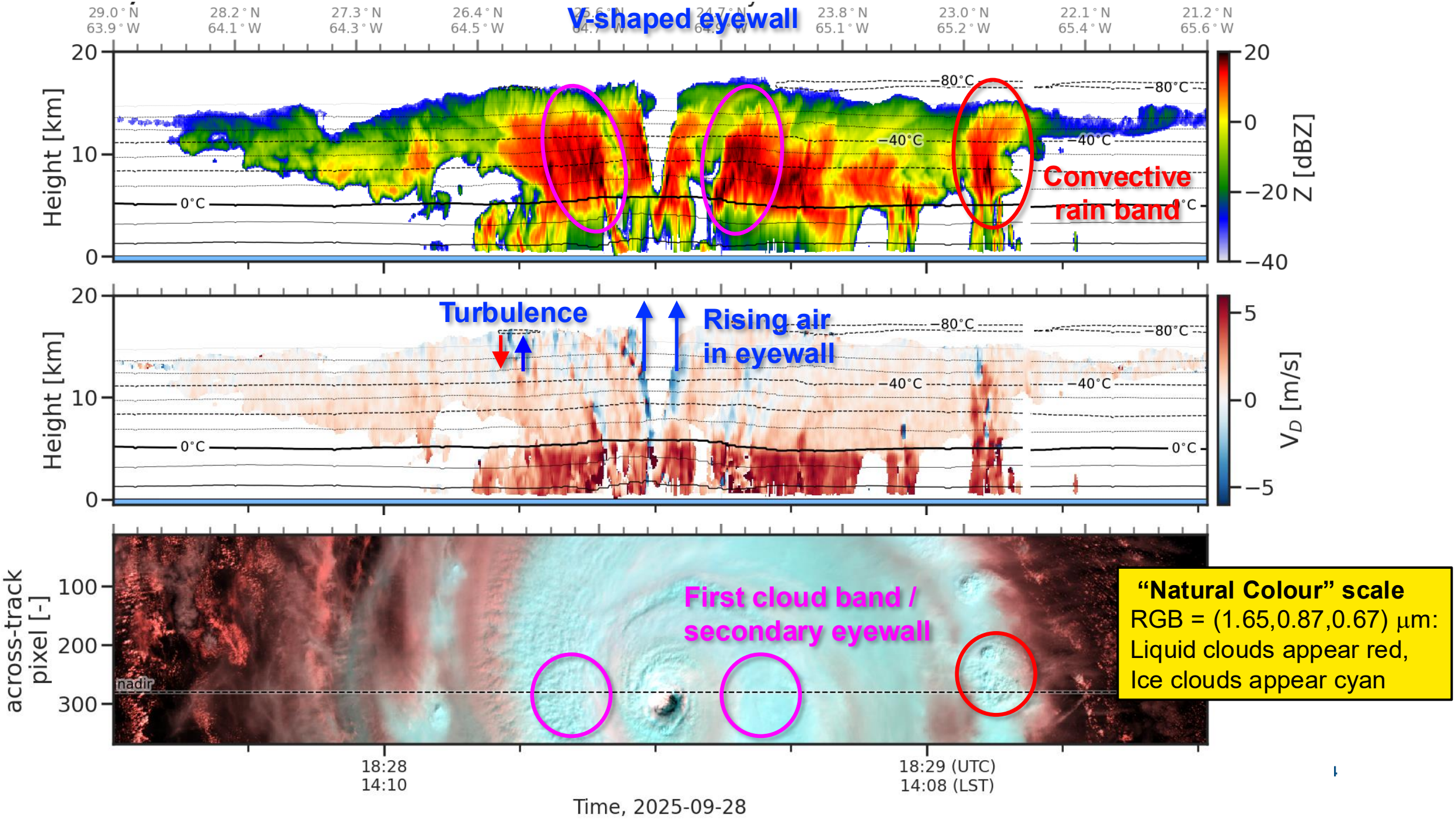
29.0 ° N
63.9 ° W
28.2 ° N
64.1 ° W
27.3 ° N
64.3 ° W
26.4 ° N
64.5 ° W
23.8 ° N
65.1 ° W
23.0 ° N
65.2 ° W
22.1 ° N
65.4 ° W
21.2 ° N
65.6 ° W
V-shaped eyewall
Height [km]
20
10
0
−80°C
−40°C
0°C
Convective rain band
Z [dBZ]
20
0
−20
−40
Turbulence
Rising air in eyewall
V_D [m/s]
5
0
−5
across-track pixel [-]
100
200
300
nadir
First cloud band / secondary eyewall
"Natural Colour" scale
RGB = (1.65,0.87,0.67) μm:
Liquid clouds appear red,
Ice clouds appear cyan
18:28
14:10
18:29 (UTC)
14:08 (LST)
Time, 2025-09-28

How does IFS perform in 5-day forecasts?

Mark Fielding
(ECMWF)

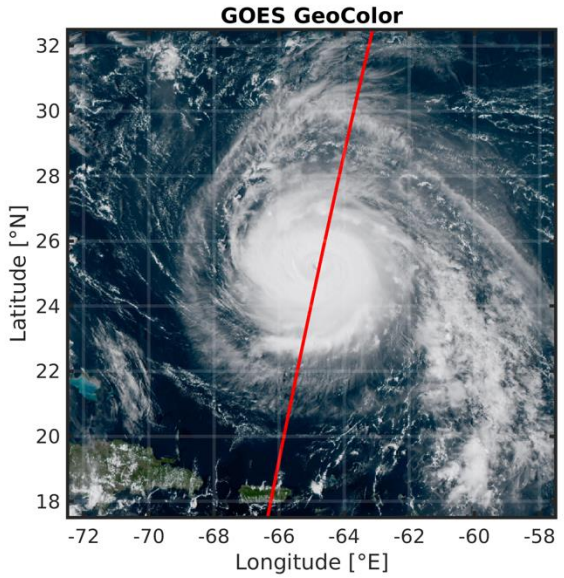

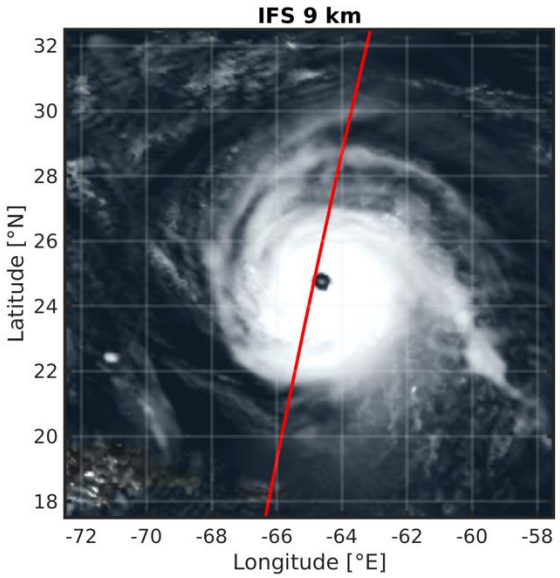

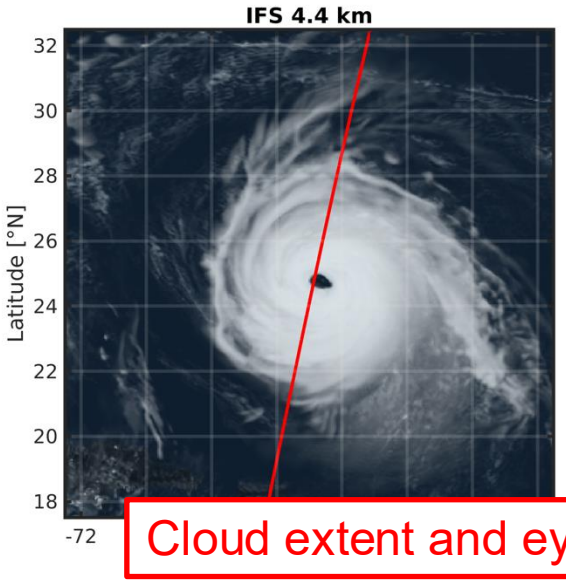

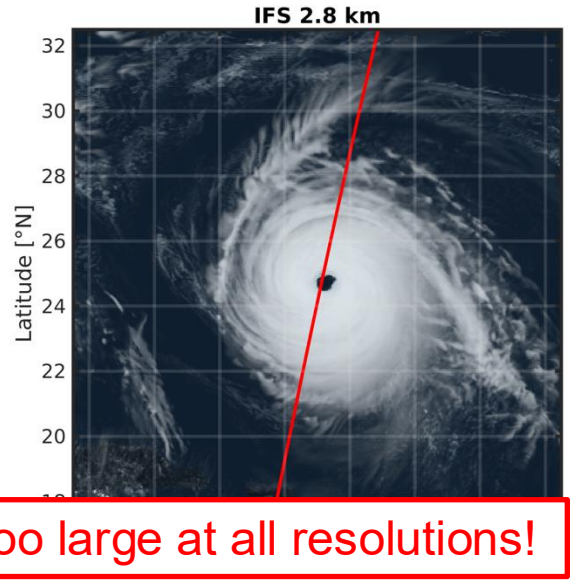

Cloud extent and eye too large at all resolutions!

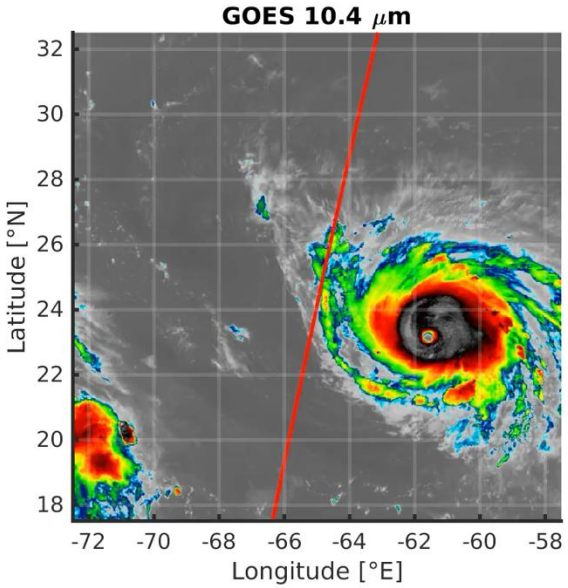

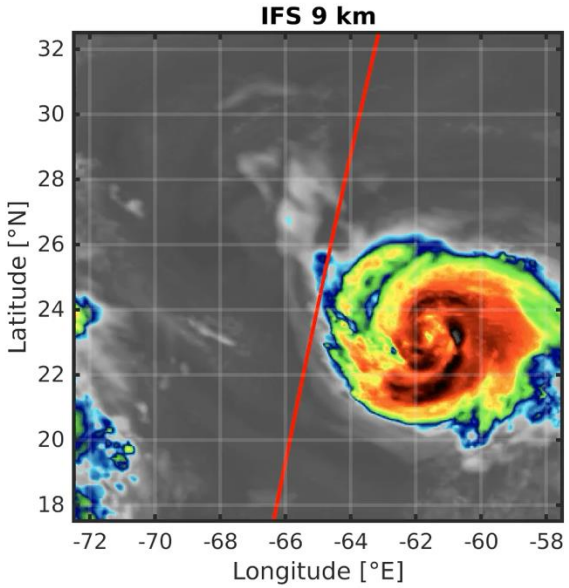

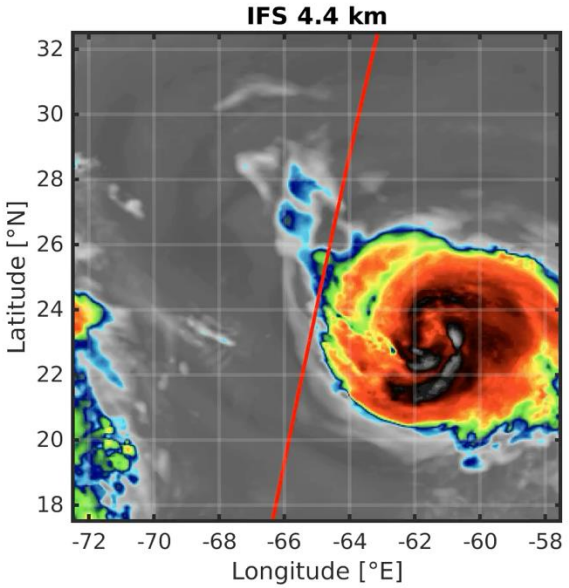

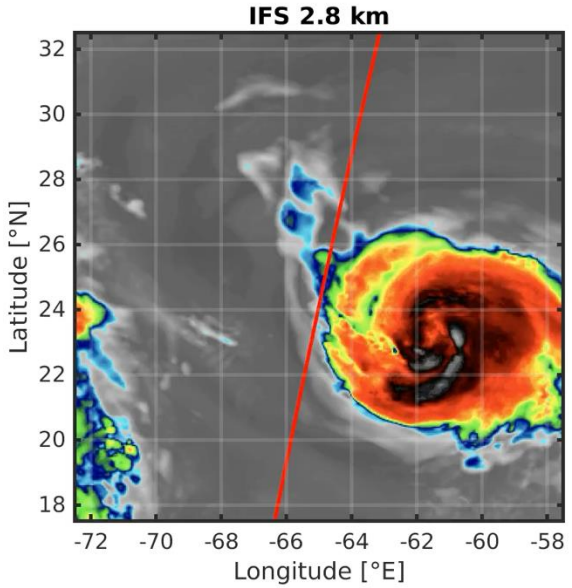

Evaluation of IFS and NICAM using CPR

Mark Fielding
Jin-de Huang, Masaki Satoh

Radar reflectivity (dBZ)

Doppler velocity (m/s)

EarthCARE CPR

IFS 9 km

IFS 4.4 km

IFS 2.8 km

NICAM 3.5 km

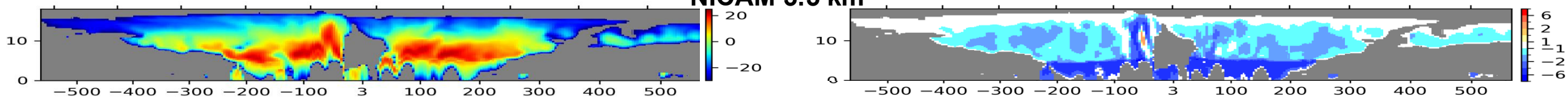

- Significant differences between models and EarthCARE, even with such high resolution
- In the ECOMIP project we are exploring how to best use these observations to improve models

Influence of gravity waves on cloud physics

Shannon Mason
(ECMWF)

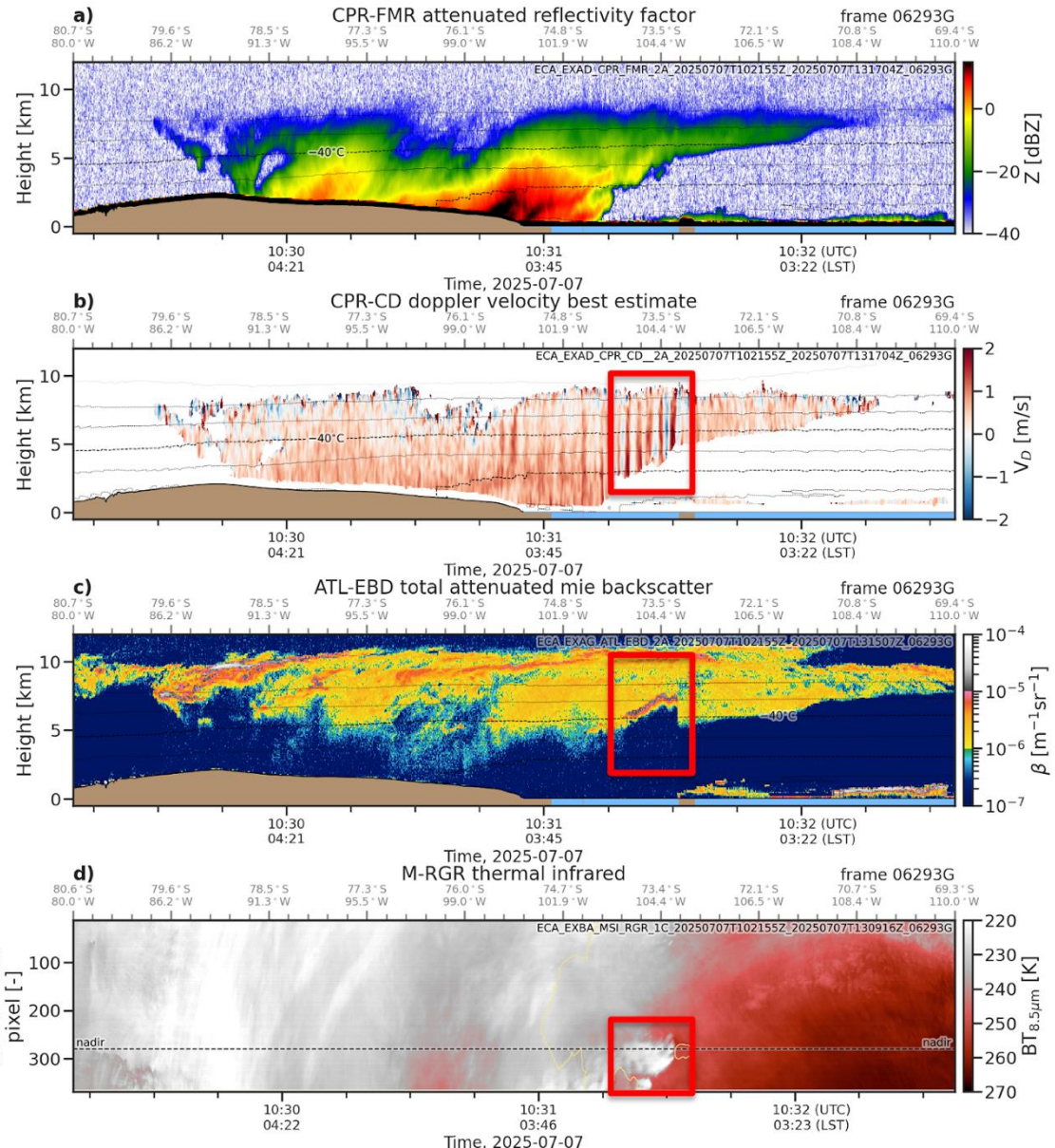

Gravity waves coincide with strong lidar backscatter at -45°C (so due to ice) and sharp drop in thermal emission

ACM-CAP: mean particle diameter drops from ~200 to ~40 μm while number concentration increases by over two orders of magnitude!

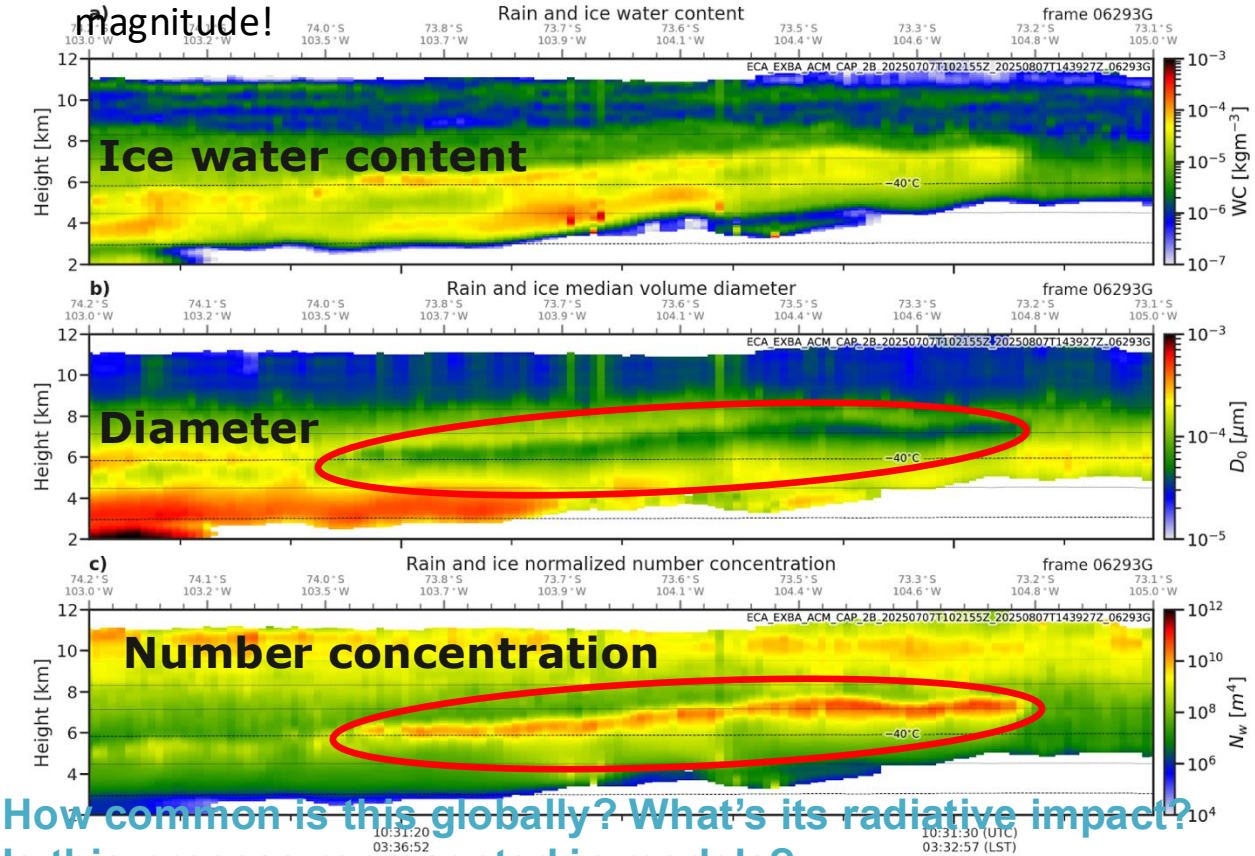

How common is this globally? What's its radiative impact?
Is this process represented in models?